LPTHE-ORSAY-91-02

ORSAY LECTURES ON LOW X DEEP INELASTIC SCATTERING

E.M. LEVIN
Laboratoire de Physique Théorique et Hautes Energies*
Université de Paris XI, bâtiment 211, 91405 Orsay Cedex, France

and
Leningrad Nuclear Physics Institute
188350 Gatchina, U.S.S.R.

Abstract

These lectures are some theoretical introduction to low x physics. They cover the following topics : evolution equations for deep inelastics structure function, unitarity constraints and modified evolution equation, taking into account shadowing correction and connected basical phenomenology.

Rykov 363
WOLBERS 234
Groshun 352
Zielinski 221
N K MONDAL 357

LPTHE Orsay 91/02
January 1991

* Laboratoire associé au Centre National de la Recherche Scientifique

Contents

Lecture 1 : Two examples from QED.

Lecture 2 : Deep Inelastic Structure Function in the region of low x (Double Log Approximation).

Lecture 3 : Double Log Approximation (continuation).

Lecture 4 : Leading Log Approximation (LLA).

Lecture 5 : Main properties and solution of LL(x)A equation (the "bare" pomeron structure in perturbative QCD).

Lecture 6 : LL(x)A with running α_S.

Lecture 7 : LL(x)A with running α_S (continuation).

Lecture 8 : Evolution Equation at $x \to 0$.

Lecture 9 : Shadowing Correction in Deep Inelastic Scattering (violation of s-channel unitarity and qualitative picture of screening in DIS).

Lecture 10 : Reggeon-like Diagram Technique in QCD.

Lecture 11 : Modified Evolution Equation.

Lecture 12 : Saturation of the Parton Density at low x.

Lecture 13 : Deep Inelastic Scattering with nucleus.

Lecture 14 : Basical Phenomenology. New physics at HERA.

Lecture 15 : Problems and hopes.

These lectures were planned as some introduction to current understanding of the low x problems in framework of perturbative QCD. I hope, that I'il be lucky to elucidate you the main theoretical ideas as well as the phenomenological situation in this extremely interesting region. First of all, why this particular kinematical region, namely, $x \to 0$ is so interesting. The answer is very simple. We faced a lot of theoretical problems here, which are difficult. However we need to solve these problems since we cannot reach the understanding the structure of the typical inelastic event without this job.

I am trying to convince you that we have a chance to achieve a full and theoretically self-consistent description of the main properties of large cross section processes at high energy in QCD at the same level of understanding as is reached in QED. So my statement is very simple. I would like to emphasize, that the principal properties of soft processes are not further away from the fundamental features of our microscopic theory - QCD - than the popular study of hard processes at high energy.

The theoretical background for the above statement is based of the consideration of the deep inelastic structure function in the region of small x. I hope, that these lectures can help the readers to understand better our two reviews[1, 2] which are really too difficult for reading in spite of our efforts to write them as simple as possible or to be absorbed in current situation of the problem, that was perfectly reviewed in two meeting last spring, namely, "Hadron Structure Function and Parton Distributions" (April, 1990, Fermilab) and Low x Workshop (May, 1990, DESY).

Lecture 1 : Two examples from QED

I would like to start my first lecture from two very simple examples in electrodynamics to clear up for your several physical points, which will be very important for understanding of the evolution equation at low x.

Let us consider the interaction of two neutral systems in Born approximation in QED. Let us assume that each of them consists of two charge spinless particles, which are heavy enough to be discussed in non relativistic way. In this case we can easily to express the inelastic cross section of such interaction or the amplitude of this interaction at transferred momentum t = 0 through the wave function of our systems (see fig. 1a). Indeed the diagram of fig. 1a can be written in the form

$$e^4 \int \psi_A^*(p)\, \psi_B^*(q) \left[\frac{(p_2 + p_2 - K)_\mu \, (q_1 + q_2 + K)}{K^2} \right]^2 .$$

$$\psi_B(p)\, \psi_B(q) \frac{d^4K}{(2\pi)^4} 2\pi\, \delta\left((p_2 - K)^2 - m_2^2 \right)$$
$$dq\, dp\, 2\pi\, \delta\left((q_1 + K)^2 - m_1^2 \right) . \qquad (1)$$

Here ψ_A and ψ_B are wave function (1) of our systems. $(2p_2 - K)_\mu$ and $(2p_1 + K)_\mu$ are the expression for electric current of spinless particles. To produce the integration let us use the Sudakov variables, namely, let us rewrite the momentum K as

$$K = \alpha\, p_A + \beta\, p_B + K_\perp$$

where $p_A = p_1 + p_2$ and $p_B = q_1 + q_2$. It is obvious that $d^4K = \frac{|S|}{2}\, d\alpha\, d\beta\, d^2K_\perp$ where $S = (p_A + p_B)^2$ if S is large enough, e.g. $S \gg m_A^2, m_B^2$.

For non relativistic particles $p_2 = \frac{p_A}{2}$, $p_1 = \frac{p_B}{2}$ and we can use the δ-function in eq. (1) to produce the integration over α and β. Indeed

$$(p_2 - K)^2 = -\beta\, S/2 + K_\perp^2$$
$$(q_1 + K)^2 = \alpha\, S/2 + K_\perp^2 . \qquad (2)$$

Taking into account the fact that our nominator can be rewritten in very simple way if we try to calculate the contribution which is the most important for high S. Indeed

$$(2p_2 - K,\, 2q_1 + K) = \frac{1}{2} S - (p_B\, K) + (p_A\, K) -$$
$$- K^2 = \frac{1}{2} S - \frac{\alpha S}{2} + \frac{\beta S}{2} - \alpha\beta S - K_\perp^2 \qquad (3)$$

since $(p_2 - K)^2 = m_2^2$ and $(q_1 + K)^2 = m_1^2$ we see that $\alpha = \frac{m_1^2 - K_\perp^2}{S}$ and $\beta = \frac{m_2^2 + K_\perp^2}{S}$. So at high S, we can neglect the contributions of αS, βS, αβS and $K_\perp^2$ terms in eq. (3) within accuracy $\frac{m_1^2}{S}$ or $\frac{K_\perp^2}{S}$.

So for high energy, finally the diagram of fig. 1a can be reduced to the form

$$\alpha_{em}^2 \cdot S \cdot 2 \cdot \int \frac{d^2K_\perp}{K_\perp^4} \cdot G_A(0)\, G_B(0) \qquad (4)$$

where $G_A(0) = \int \psi_A^*(p)\, \psi_A(p)\, dp = 1$

$$G_B(0) = \int \psi_B^*(q)\, \psi_B(q)\, dq = 1$$

is the form factors of the composite particles A and B at zero momentum transferred.

Of course to get the full answer we should sum all diagrams of the fig. 1a type. Such diagrams are shown in fig. 1b. Finally, we can express the cross section for this interaction as follows (Im A = S - σ_+ - this is the form of our optical theorem)

$$\sigma_+ = 2\,\alpha_{em}^2\, 2 \times 2 \int \left[G_A(0) - G_A\left(4\,K_\perp^2\right)\right]\left[G_B(0) - G_B\left(4\,K_\perp^2\right)\right] \frac{d^2K_\perp}{K_\perp^4} \qquad (5)$$

where

$$G_A(0) - G_A\left(4\,K_\perp^2\right) = \int \psi^*(p)\, \psi(p^*)\, dp - \int \psi^*(p + K)\, \psi(p - K)\, dp \quad .$$

Now let us look more carefully on the formula (5). We see that we have no infrared divergency since at $K_\perp \to 0$ $G_A(0) - G_A(4K_\perp^2) = 4\,\frac{\langle R_A^2\rangle K_\perp^2}{6}$ and $G_B(0) - G_B(4\,K_\perp^2) = 4\,\frac{\langle R_B^2\rangle}{6} K_\perp^2$. Of course the above

expressions reflect the fact, that our neutral system can emit photon with large wave length $\lambda = 1/K_\perp > R$ where R is the size of the system. Only if it has dipole moments which is proportional of course R. So, we face here with dipole radiation. However, I would like to draw your attention to the very interesting property of this interaction. Indeed, if we assume, that the sizes of our interacting system are quite different, for example $R_A >> R_B$, we can easily to see that there is specific region of integration, namely

$$R_A >> \lambda_\gamma >> R_B \quad . \qquad (6)$$

In this region $G_B(0) - G_B(4K_\perp^2)$ is still equal $\frac{4\,\langle R_B^2\rangle}{6} K_\perp^2$, but $G_A(0) - G_A(4\,K_\perp^2)$ tends to 1. Indeed $G_A(0) = 1$ and $G_A(4\,K_\perp^2) \to 0$ since $K_\perp^2 >> 1/R_A^2$. So, in the kinematical region (6) we can reduce our integral (5) to the form

$$\sigma_t = 8\,\alpha_{em}^2 \int_{1/R_A^2}^{1/R_B^2} \frac{4\,\langle R_B^2\rangle}{6} \cdot \frac{\pi\, d\, K_\perp^2}{K_\perp^2} =$$

$$= 8\,\alpha_{em}^2 \frac{4\,\langle R_B^2\rangle}{6}\, \pi\, \ell n \frac{R_A^2}{R_B^2} \quad . \qquad (7)$$

Thus we get some log contribution which can compensate the smallness of the coupling constant α_{em} if $\frac{R_A}{R_B} >> 1$.

Let me sum up the lessons that we have learned from this simple example.

1. If two neutral systems of particles interact with each other through exchange of photon or any massless vector particle, we have large contribution to the total cross section from the region $1/R_B^2 > K_\perp^2 > 1/R_A^2$ which is proportional $\alpha\, \ell n \frac{R_A^2}{R_B^2}$.

2. At high energy, the main contribution comes from polarizations of photon (or any massless vector particle) which are longitudinal.

2. Now let me consider the second example, namely the radiation of photon by electron-positron pair which was created with the angle θ between electron and positron as shown in fig. 2a. Let us denote θ' the angle of the emitted photon and Z the fraction of its energy (see fig. 2a). The difference of energies between the $(e^-\gamma)$ state and the e^- before emission is equal to

$$\Delta E^2 = \sqrt{Z^2p^2 + K_t^2} + \sqrt{(1-Z)^2\, p^2 + K_t^2} - p =$$
$$= \frac{K_t^2}{2Zp} + \frac{K_t^2}{2(1-Z)p} = \frac{K_t^2}{2Z(1-Z)p} \quad , \qquad (8)$$

since $\theta' = \frac{K_t}{Zp} + \frac{K_t}{(1-Z)p} = \frac{K_t}{Z(1-Z)p}$ (see fig. 2a, we take into account the fact that all angles are small here). We can see that

$$\Delta E = \frac{1}{2}\theta'^2\, Z(1-Z)p \quad . \qquad (9)$$

Due to uncertainty principles, the time of emission

$$\Delta t \approx 1/\frac{1}{2}\theta'^2\, Z(1-Z)p \quad . \qquad (10)$$

During this time the e^+ and e^- can fly away from each other on the distance

$$\Delta b_{e^+e^-} \sim \theta\Delta t = \frac{\theta}{\frac{1}{2}\theta'^2\, Z(1-Z)p} \quad . \qquad (11)$$

If we want to emit a γ, we should demand that the distance between the e^+ and e^- will be larger than the photon wave length $\Lambda_\gamma \sim 1/K_t$. If it is not so, our photon will feel the total charge of e^+ and e^- which is equal to zero. Thus we have some evident constraint

$$\Delta b_{e^+e^-} > \lambda_\gamma = 1/K_t \quad . \qquad (12)$$

Eq. (12) means that

$$\frac{\theta}{\frac{1}{2}\theta'^2\, Z(1-Z)p} >> \lambda_\gamma = 1/K_t \quad . \qquad (13)$$

So eq. (13) we can reduce to restriction

$$\theta > \theta' \qquad (14)$$

if we take into account that $K_t = \theta'\, 2\, Z(1-Z)p$.

For angles $\theta' > \theta$, photon is emitted coherently by e^+e^- pair and feels only their global charge, which is zero. Of course, the constraint (14) can be proved more accurately, but I hope, that the physical meaning of this condition have become clear. I would like only to recommend the review[3] for all details and the generalization on QCD[3].

The straight hold generalization leads to the ordering of the angles in any subsequent decay. Namely, for the case of fig. 2b we have

$$\theta_1 > \theta_2 \ldots > \theta_{i-1} > \theta_i \ldots \quad . \tag{15}$$

The main lesson from this example is very simple. For the process of the jet decay (e^+e^- annihilation for example) we have constraint (15) for dominant contribution in the cross section instead of eq. (6) which defined the essential kinematical region for scattering processes.

However I would like to stress that the physical meaning of both constraints (eqs. (6) and (15)) is really the same, namely, the wave length of the emitted gluon should be smaller than the size of radiation or

$$\Delta b_t > 1/K_t \tag{16}$$

but for scattering processes $\Delta b_t \sim R$, where K is the radius of the system of partons that emit detected gluon with momentum K, while Δb_t for decay processes should be calculated using the expression (11). Of course, this difference has very simple kinematical explanation which is seen directly from figs. 3a and b. In fig. 3a three stages of the development of a parton cascade in deep inelastic process are shown. The partons multiply in the region limited by the transverse dimension of the parent hadron.

The same three stages look quite differently for jet cascade in a e^+e^- annihilation process. Each jet lives in its own cone and decays into jet with smaller opening angles due to angular ordering condition (15).

Lecture 2 :
Deep Inelastic Structure Function in the region of small x (Double Log Approximation)

Using condition (16) we are ready now to receive the so-called evolution equation for any hard process. Let us concentrate our efforts on deep inelastic scattering in region of small x. I prefer to leave out the discussion what means the deep inelastic structure function and so on. The only thing which, I hope, everyone knows, that the cross section of virtual photon (γ^*) is equal to

$$\sigma_{\gamma^*} = \frac{\alpha_{em}}{q^2} \times F\left(x, q^2\right) \quad . \tag{17}$$

Here the first factor is the cross section of interaction of γ^* with the charged parton. $x\,F(x) = \sum e_q^2 \times q(x)$ where e_q is the charge of quark q and $x\,q(x)$ is the probability to find quark with virtuality smaller than photon virtuality (q^2).

The problem which we are going to solve can be formulated as follows. How can we calculated in QCD the probability to find parton with fixed virtuality (transverse momentum), q^2, and the fraction of energy x if we know this value at smaller q^2 (say, $q^2 = q_0^2$).

In QCD also, as in QED the probability to emit gluon "i" is proportional to

$$dW_i = \frac{\alpha_S N}{\pi^2} \frac{dx_i}{x_i} \frac{d^2K_{t_i}}{K_{it}^2} \tag{18}$$

N is the number of colours here and α_S is the coupling constant QCD

$$\alpha_S = \frac{4\pi}{b\,\ell n\, K^2/\Lambda^2} \quad \text{and} \quad b = \frac{11}{3} N - \frac{2}{3} n_f \quad ,$$

n_f is the number of flavours.

I would like to postpone the discussion why W is proportional to N others factors in eq. (18) are obvious and follows directly from dimensionless coupling constant of our microscopic theory (QCD). Using W_i we can very easily to calculate the probability to find gluon at least at $x \to 0$. Indeed, if $x'G(x', K^2)$ is probability to find gluon with fraction of energy x' and transverse momentum K, the probability $x\,G(x, q^2)$ should be equal to

$$x\,G\left(x, q^2\right) = \int d\,W_i\, x'\,G(x'\,K^2) =$$

$$= \int \frac{dx'}{x'} \frac{d\,K_t^2}{K_t^2} \frac{\alpha_S\,N}{\pi}\, x'\,G(x'\,K^2) \qquad (19)$$

(see fig. 4a). Now let us chose the essential integration region in eq. (11) using the above lesson from Born approximation. First of all $\lambda = 1/q$ should be smaller than the typical size of emitter, which is the gluon which proper size is equal to $1/K_t$. So $\lambda << \frac{1}{K_t}$ or $q_t >> K_t$. From energy conservation of course $x' > x$, but even the slight glance on the equation (19) shows you that we can get a large contribution we assume that $x' >> x$. So finally our equation can be reduced to the form

$$x\,G\left(x, q^2\right) = \int_x \frac{dx'}{x'} \int_{q_0^2}^{q^2} \frac{d\,K_t^2}{K_t^2} \frac{\alpha_S\,N}{\pi}\, x'\,G\left(x', K^2\right) \qquad (19')$$

Solution of eq. (19') is evident for fixed α_S,

$$x\,G\left(x\,q^2\right) = \int_y dy' \int_\Gamma dr' \frac{\alpha_s\,N}{\pi}\, x'\,G\left(x', K^2\right) \quad .$$

Here $\Gamma = \ell n\, q^2/q_0^2$, $y = \ell n\, 1/x$

$$\text{or} \qquad \frac{\partial}{\partial y}\frac{\partial}{\partial \Gamma}\, x\,G(x, r) = \frac{\alpha_S\,N}{\pi}\, x\,G(x\,r) \qquad (20)$$

assuming that $x\,G(x\,r) = F(\sqrt{y\,\Gamma})$ we can rewrite eq. (20) as usual differential equation, namely, $(t = \sqrt{yr})$,

$$\frac{d^2F}{dt^2} + \frac{1}{4t}\frac{dF}{dt} = \frac{\alpha_S\,N}{\pi} F(t) \quad . \qquad (21)$$

Eq. (21) has solution

$$F = I_0\left(2\sqrt{\frac{\alpha_S\,N}{\pi}\, y\Gamma}\right) \qquad (22)$$

which tends to 1 at $\Gamma \to 0$.

Now I would like to solve this equation in slightly different way. Namely, let us introduce Mellin transform of $x\,G(x, q^2) \equiv F$, namely,

$$F(\omega, \Gamma) = \int e^{y\omega}\, F(y, \Gamma)\, dy$$

$$F(y, \Gamma) = \frac{1}{2\pi i} \int_{-i\infty}^{+i\infty} F(\omega, \Gamma)\, e^{-\omega y}\, d\omega \quad . \qquad (23)$$

Of course, the contour in eq. (23) should be located to the right of all singularities in $F(\omega, \Gamma)$. It is easy to see that $F(\omega, \Gamma)$ is nothing

Lecture 3 : Double Log Approximation (continuation)

In this lecture I am going to discuss the accuracy of DLA for deep inelastic scattering and show you that situation in decay processes as e^+e^- annihilation is quite different from DIS.

Let us return to the equation (19') and let us discuss what small parameters were really used to get this equation. First of all, we suggested that dW_i has the simplest form of eq. (18). Even more the answer (30) corresponds to the probability of production "n" gluons which is proportional

$$P_n \sim \prod_{i=1}^{n} dW_i \quad . \tag{31}$$

Indeed, in eq. (19') was really included the following strong ordering in x_i and K_{i_t} :

$$x_1 >> x_2 >> x_3 \ldots >> x_{i-1} >> x_i >> x \tag{32}$$

$$\frac{1}{R_h} \sim K_{1t} << K_{2t} << K_{3t} << K_{i-1,t} << K_{i,t} << q^2 \quad . \tag{1}$$

$$\tag{2}$$

Using eqs. (32) we can calculate F_n and we can see that

$$F_n = \int_{y_0}^{y} dy_R \int_{y_0}^{y_n} dy_{n-1} \cdots \int_{y_0}^{y_2} dy_1 \, .$$

$$\left(\frac{\alpha_S N}{\pi}\right)^n \int_{\Gamma_0}^{\Gamma} d\Gamma_n \int_{\Gamma_0}^{\Gamma_n} d\Gamma_{n-1} \cdots \int_{\Gamma_0}^{\Gamma_2} d\Gamma_1 =$$

$$= \frac{1}{(n\,!)^2} \left(\frac{\alpha_S N}{\pi} y\Gamma\right)^n \rightarrow \tag{33}$$

$$F(y, \Gamma)^2 \sum_{n=0}^{\infty} P_n(y\Gamma) \rightarrow \sum \frac{1}{(n\,!)^2} \left(\frac{\alpha_S N}{\pi} y\Gamma\right)^n =$$

$$= I_0\left(2\sqrt{\frac{\alpha_S N}{\pi} y\Gamma}\right) \, . \tag{34}$$

So our equation we really have received in so-called double log approximation. In this approach, we consider the parameter

$$\frac{\alpha_S N}{\pi} \ell n\, 1/x \; \ell n \frac{q^2}{q_0} \sim 1 \tag{35}$$

but all other parameters such as

$$\frac{\alpha_S N}{\pi} \ell n \frac{q^2}{q_0^2} << 1$$

$$\frac{\alpha_S N}{\pi} \ell n\, 1/x << 1$$

$$\alpha_S << 1 \tag{36}$$

were assumed to be small.

Let us try to understand in more transparent way the origin of the conditions (36). Assume for example, that we have lost one log integration over d^2K_i in dW_i. So $W_i = \frac{N\,\alpha_S}{\pi} y\Gamma + \Delta W_i$ and ΔW_i is proportional only to $\frac{N\,\alpha_S}{\pi} \ell n\, 1/x$. Putting this expression for W_i in (31) we immediately get that

$$P_n \sim \frac{1}{n\,!} \prod W_i = \frac{1}{n\,!^2} \prod \left(\frac{N\,\alpha_S}{\pi} y\Gamma + \Delta\, W_i\right)^n \text{ and so}$$

$$\Delta F = \Delta \sum P_n = \Delta W \sum n P_n = \Delta W \langle n \rangle F \times \frac{1}{\frac{N \alpha_S}{\pi} y\Gamma}$$

but $n = \sqrt{\frac{\alpha_S N}{\pi} y\Gamma}$ just from explicit form of eq. (34). Now we are ready to estimate the accuracy of our equation. Indeed

$$\frac{\Delta F}{F} = \Delta W \langle n \rangle \cdot \frac{1}{\frac{N \alpha_S}{\pi} y\Gamma} << 1$$

or $$\frac{\alpha_S N}{\pi} \ell n\, 1/x << \Gamma \quad . \qquad (37)$$

In the case when we have lost the log integration over dx, it is obviously, that ΔW is of the order of $\frac{\alpha_S N}{\pi}\Gamma$ and instead of eq. (37) we have

$$\frac{\alpha_S N}{\pi}\Gamma << \ell n\, 1/x \quad . \qquad (37')$$

Of course, the two above constraints for constant α_S can be rewritten in the form (36), but I would like to draw your attention to the fact, that if you take into account the running coupling constant α_S in QCD you can see that eqs. (37) and (37') can be reduced to ($\alpha_S = \frac{4\pi}{b\Gamma}$)

$$\ell n\, 1/x << \frac{B}{4}\Gamma^2 \qquad (37'')$$

and

$$\frac{4}{b} << \ell n\, 1/x \quad .$$

Eqs. (37") can give us very interesting information. Indeed, for running α_S two above cases give quite different constraints. We should be very careful with summing all $(\ell n\, 1/x)^n$ contribution with better accuracy than in DLA equation, because only log integration over K leads the strong restriction of the region of x (the first one from eq. (37")). However, more careful integration over x when we collecting $(\ell n\, q^2)^n$ contribution lead to more precise answer only in limited region of x, which defines by the second inequality in eq. (37").

You can see the picture in figs. 4c and 4d, which show the kinematical regions where DLA gives the correct answer. You see the obvious difference between two cases : running α_S and α_S = const. The full presentation of the DLA selection is the following

$$F(y,\Gamma) = \left(1 + O\left(\sqrt{\frac{N \alpha_S y}{\pi \Gamma}}\right) + O\left(\sqrt{\frac{\pi \alpha_S \Gamma}{\pi y}}\right)\right) \cdot F_{DLA}(y,\Gamma) \quad . \qquad (38a)$$

It should be stressed that eq. (38a) gives you new way, how we try to understand the accuracy of our solution. We estimate the relative precision of our solution $\frac{\Delta F}{F}$. The answer in the form (38a) is valid even when $\alpha_S\, \ell n\, q^2\ 1/x >> 1$. This fact is the most important for future. And the main our goal now is to improve double log approach in such way, that we would like to get the solution of the problem within accuracy ($F_{LLA}(y\Gamma)$)

$$F(y,\Gamma)^2 = \left(1 + O\left(\sqrt{\alpha_S}\right)\right) F_{LLA}(y\Gamma) \quad . \qquad (38b)$$

Double Log Approximation for e^+e^- annihilation

For decay processes it turns to be more convenient to rewrite dW_i of eq. (18) in slightly different way, using θ_i instead of K_{it}, since for these processes we have the strong ordering in angles (see eq. (15)). After that we can use expression (31) for p_n if we take

$$dW_i = \frac{\alpha_S N}{\pi} \frac{d\theta_i^2}{\theta_i^2} \frac{dx_i}{x_i} . \qquad (39)$$

So

$$p_n = \int_{y_0}^{y} dy_n \int_{y_0}^{y_n} dy_{n-1} \cdots \int_{y_0}^{y_2} dy_1 . \qquad (40)$$

$$\left(\frac{\alpha_S N}{\pi}\right)^n \int_{\theta_{min}}^{1} \frac{d\theta_n^2}{\theta_n^2} \int_{\theta_n}^{1} \frac{d\theta_{n-1}^2}{\theta_{n-1}^2} \cdots \int_{\theta_2}^{1} \frac{d\theta_1^2}{\theta_1^2} .$$

Thus the answer for structure function in this annihilation process is the same as for deep inelastic scattering, namely

$$F(x, \theta^2, \theta_{min}) = \sum p_n = I_0\left(\sqrt{\frac{4 N \alpha_S}{\pi} \ln \frac{1}{\theta_{min}^2} \ln 1/x}\right) \qquad (41)$$

and the only problem to understand the value of θ_{min}. Of course, this value depends on our point of view on the hadronization since the decay of jet comes to the end namely, the hadronization stage. Perturbative QCD can be applied only at the stages when $K_{it} > \mu > (K_t)_{hadron}$ and $\alpha(\mu^2) << 1$. It means that

$$\theta_{min} = 2\mu/xQ . \qquad (42)$$

So the result can be described by expression

$$\bar{F}(x, \theta_{min}) = I_0\left(\sqrt{\frac{4N \alpha_S}{\pi} \ln \frac{1}{x} \ln \frac{4\mu^2}{x^2Q^2}}\right) =$$

$$= I_0\left(\sqrt{\frac{8N \alpha_S}{\pi} \ln \frac{1}{x} \left(\ln \frac{Q}{2\mu} - \ln \frac{1}{x}\right)}\right) . \qquad (43)$$

Comparing eqs. (43) and (39) we immediately see that in the region of $x \sim 1$ when $\ln \frac{Q}{2\mu} >> \ln 1/x$, the structure functions are coincided for both processes, but for small x the behaviour of structure functions looks absolutely different. $\bar{F}$ goes to zero and we have maximum in inclusive spectrum of hadrons in e^+e^--annihilation, just as F for deep inelastic scattering grows very rapidly, namely, at small x.

We could see this property just from condition (15) : indeed, the angular ordering means that

$$\frac{K_{i-1t}}{x_{i-1}} > \frac{K_{it}}{x_i} . \qquad (44)$$

If $x_{i-1} \approx x_i - 1$ from the above expression follows the ordering in K_t as for deep inelastic scattering, but in the region of small x, situation changes crucially and we have to use only angular ordering.

Lecture 4 : Leading Log Approximation

Double Log Approximation gives us the understanding of the main qualitative properties of QCD solution in the region of small x and large (really very large) virtualities. But for DIS the constraint (16) does not depend on x and leads to ordering in transverse momentum (virtuality). We can use this property and develop two different approaches. In the first one we refuse to get large log 1/x contribution. So the smallness of α_S is compensated by large log q^2 in this approach. The second on the contrary uses only large log 1/x contribution and could be applied to small virtualities.

Gribov-Lipatov-Altarelli-Parisi equation

We shall start from the first, which is so-called Leading Log (q^2) Approximation. We use here the following set of parameters

$$\alpha_S \ln q^2/q_0^2 \sim 1$$

$$\alpha_S \ln 1/x << 1$$

$$\alpha_S << 1 \quad . \qquad (45)$$

This approach was firstly suggested by Gribov and Lipatov[4] for all field theories with dimensionless coupling constant. Lipatov even gave the partonic interpretation of LL(q^2)A equations. Then the case of QCD was specially reconsidered by Altarelli and Parisi in the West[6] and by Dokshitzer in my country. Altarelli and Parisi used quite different technique to prove the LL(q^2)A in comparison with Gribov and Lipatov and formulated the equation and the problem as a whole in the way which allowed to develop the systematic approach the deep inelastic scattering processes. Here, I do not want to discuss this approach in any details, because it was excellently reviewed by DDT[6]. I would like only to tell you a little bit about space-time picture of the parton cascade in this

case. To illustrate this picture let us consider the decay of a parton in the parton cascade (see fig. 5a). If we would like to have large log of K_t, we really consider the case that is shown in fig. 5a. One large parton which radius is of the order of $1/K_{i-1t}$ decay into two small partons. Their proper sizes are of the order of $1/K_{it}$. ($r_i \sim 1/K_t$). So our log $K^2_{r_{i-1}}$ here, is the result of integration $\int^{r_{i-1}} \frac{d\, r_i}{r_i}$. Since the distance between two parton after decay is large enough and much larger than their proper sizes. We can neglect interaction between partons. It means, that the structure of equation here remains to be the same as in DLA (see eq. (19)).

The only change is the fact that dW_i now has more complicated dependence on x_i. So the equation has the form

$$x\, G\left(x, q^2\right) = \int_{q_0}^{q^2} \frac{\alpha_S\, N}{\pi} P\left(\frac{x}{x'}\right) dx'\, x\, G\left(x', q^2\right) \frac{dq'^2}{q^2} \quad . \qquad (46)$$

The second modification is also trivial, we should take into account not only gluon structure function but quark and antiquarks one. The third modification looks more complicated from the first sight. Namely we should subtract in the right hand side of eq. (46) the terms $2 \int_{q_0}^{q^2} \frac{dq'^2}{q'^2} \int \frac{\alpha_S\, N}{\pi} P(Z)\, dZ \,.\, xG(xq^2)$. So the final structure of the GLAP equation is shown in fig. 6b. The first term describes the change of the transverse momentum of quark (gluon) results from quark (gluon) decay on quark (gluon) and gluon. The second one accounts for the fact that the parent parton that decays into softer ones ceases to exist. The solution of GLAP equation can be found in the form eq. (28) and the only difference that γ_n becomes more complicated function on "n".

At the moment we have large practice in numerical solution of this equation. So we understand all values which are important in this case. However, I would like to emphasize once more, that this equation has, theoretically speaking, very restricted kinematical region where it was proved, namely large $q^2 > q_0^2$ but $x \sim 1$. I am going to return to discussion of GLAP-equation in the next lecture. I would like to draw your attention to the fact that the second term in evolution equation violates the probabilistic interpretation of the deep inelastic process or may be better to say, the probabilistic interpretation demands reformulation what is the parton in our parton cascade. The situation is very simple. Each produced parton is accompanied by a lot of sufficiently soft gluon and we should redefine how many from such gluons our trigger measures as one parton. After such the redefinition, of course, the gluon in our Feynman diagrams should also to be reconsidered, and its propagator should contain some factor that renormalizes its propagator. But unfortunately, such redefinition inside the parton approach depends crucially in the value which we would like to calculate and on the process which we are considering (or on the kinematical region).

Kuraev-Lipatov-Fadin equation[7]

The second generalization of DLA is also now understandable. We would like to preserve the $\ell n\ 1/x$ contribution and neglect $\alpha_S \log q^2/q_0^2$ corrections. So the set of parameters for such so-called Leading Log 1/x Approach is evident

$$\left.\begin{array}{c} \alpha_S\ \ell n\ 1/x \sim 1 \\ \alpha_S\ \ell n\ q^2/q_0^2 << 1 \\ \alpha_S << 1 \end{array}\right\} . \qquad (47)$$

In kinematical region (47) the space-time picture for the parton decay looks as shown in fig. 6a. So here we cannot avoid the interaction between partons in the final state. Our large contribution comes in this approach from the ordering in x. To clarify the problem let us consider the simplest diagrams of fig. 6b for high energy quark-quark scattering. The Born Approximation for this process is the diagram of fig. 6b and using the experience in calculating the Born Approximation diagram in QED it is easy to understand that this diagram is equal to

$$A(6b) = S\,\frac{C_2^2\,\alpha_S^2}{N^2 - 1}\int \frac{d^2 K_t}{K_t^4} \qquad (48)$$

where $C_2 = \frac{N^2 - 1}{2N}$ if N is the number of colours. Let us consider now the emission of one extra gluon (see diagrams in fig. 6c). It is easier to consider the diagram for emission of gluon with momentum q and after that calculate the amplitude which is equal to square of the emission amplitudes. Thus the contribution of the diagrams of fig. 6c is equal to

$$\int M_{2\to 3}^2\,\delta\left(q^2\right)\frac{d^4 q}{(2\pi)^4} . \qquad (49)$$

Let us consider this integration assuming that all transverse momenta are restricted. Introducing Sudakov variables, we can express q through $\alpha\beta$ and q_t. Indeed

$$q = \alpha\, p_A + \beta\, p_B + q_t$$

so $\quad q^2 = \alpha\beta S + q_t^2 \ ; \ S = 2\left(p_A\, p_B\right)$

$$d^4q = d^2q_t \, d\alpha \, d\beta \, \frac{S}{2} \quad .$$

Integrating over $d\beta$ we see that exp (49) can be rewritten as

$$\int_{\frac{K'^2_t}{S}}^{1} M^2_{2\to 3} \, \frac{d^2q_t \, d\alpha}{2\alpha} \quad . \qquad (50)$$

The lower limit of integration we can calculate from the condition $(q + p_B)^2 > K'^2_t$ or $\alpha S >> K'^2_t$. From eq. (50) it is obvious that log 1/x contribution (or $\ell n \, \alpha$) appears only if the amplitude for the production of new gluon q does not depend on α. This is so for diagram of fig. 6c (1). First of all, let us note that K^2 and K'^2 are equal to K^2_t and K'^2_t. Indeed $(p_A + K)^2 = 0$ and $(p_B - K')^2 = 0$.

So $\quad \beta_K S + K^2_t = 0 \quad - \alpha_K S + K'^2_t = 0 \quad . \qquad (51)$

$$\alpha = - \alpha_K + \alpha_{K'} \quad \text{since } \alpha_{K'} << \alpha \quad .$$

$$- \alpha_K = \alpha \qquad \beta_K = - \frac{K^2_t}{S} << \beta_{K'}$$

so $\quad \beta_{K'} = \beta \quad .$

Thus from eqs. (51) we have

$$K^2 = \alpha_K \, \beta_K \, S + K^2_t = \alpha \, \beta_K \, S + K^2_t =$$

$$= - \alpha \, K^2_t + K^2_t = K^2_t \, (1 - \alpha) = K^2_t$$

since $\quad \alpha << 1$

$$K'^2 = \alpha_{K'} \, \beta_{K'} \, S + K'^2_t = \beta \, K'^2_\perp + K'^2_t =$$

$$= K'^2_t (1 + \beta) = K'^2_t \left(1 - \frac{q^2_\perp}{S} \right) = K'^2_t \quad .$$

Let us calculate now the vertex for gluon emission in diagram of fig. 6c (1). Using the usual Feynman rules for QCD we can calculate the vertex for gluon emission.

$$\Gamma_\sigma = i \, g \, f_{abc} \, p_{A\mu} \, p_{B\nu} \, \Gamma_{\mu\nu\sigma} \qquad (51')$$

where $\quad \Gamma_{\mu\nu\sigma} = g_{\mu\nu} \, (K + K')_\sigma + g_{\mu\sigma} \, (- K' - q)_\mu + g_{\sigma\mu} \, (q - K)_\nu$

we need Γ_σ only for σ which is perpendicular to p_A and p_B since gluon q is real ($q^2 = 0$). So it is very easy to get

$$\Gamma_\sigma = i \, \delta \, f_{abc} \, \frac{S}{2} \, (K + K')_{t\sigma} \quad . \qquad (52)$$

Thus finally the diagram of fig. 6c (1) gives the contribution

$$g^2 \, t^a_{iK} \, i \, g \, f_{abc} \, T^C_{i'K'} \, \frac{S}{2} \, (K + K')_{\perp\sigma} \, \frac{1}{K'^2_t \, K^2_t} \qquad (53)$$

as you see in eq. (53) there is not any dependence on α, so if we put this expression in eq. (50) we will get the log contribution.

Let us now consider the diagram of fig. 6c (2). At first sight this diagram cannot give log integration, since the propagator (p_A +

$K')^2 = \beta_{K'} S + K'^2_t = \beta S + K'^2_t = -\frac{q^2_t}{\alpha} + K'^2_t = -\frac{q^2_t}{\alpha}$. Thus we have

integral $\int \frac{d\alpha}{\alpha}\alpha \to O(1)$. But the above statement is not correct. Let us look more carefully on the nominator. The vertex of emission of gluon from quark $\gamma_{\sigma'}$ is equal to $(2p_A + K + K')_\sigma$. The vertex Γ_σ in diagram of fig. 6c (1) also contains the longitudinal part namely $\Gamma_\sigma = i\delta f_{abc} \frac{S}{2} (K + K')\sigma$. In $M^2_{2\to 3}$ we have the convolution $\gamma_{\sigma'} g_{\sigma'\sigma} \Gamma_\sigma$.

$g_{\sigma'\sigma} = \frac{p_{A\sigma} p_{B\sigma'} + p_{B\sigma} p_{A\sigma'}}{(p_A p_B)} + g^{\perp}_{\sigma'\sigma} = g^{L}_{\sigma'\sigma} + g^{\perp}_{\sigma'\sigma}$. Only $g^{L}_{\sigma'\sigma}$ can give the log contribution to our integral. It is easy to see that

$$\gamma_{\sigma'} g^{L}_{\sigma'\sigma} \Gamma_\sigma = \frac{(K + K', p_A)(p_B, K + K')}{(p_A p_B)} + \frac{(2p_A + K + K', p_B)(p_A, K + K')}{(p_A p_B)} = \frac{(p_A p_B) - (\beta_K + \beta_{K'})(p_A p_B)(\alpha_K + \alpha_{K'})}{(p_A p_B)} + \frac{(p_A + p_K)(2 + \alpha'_K - \alpha_{K'})(p_A p_K)(\beta_K + \beta_{K'})}{(p_A p_B)} . \tag{54}$$

From eq. (54) only the term $2\langle p_A p_B\rangle (\beta_K + \beta_{K'})$ gives the contribution that can compensate the smallness of the order of α which appears due to the factor $(p + K')^2$ in the dominator. But $2(p_A$

$p_B)(\beta_K + \beta_{K'}) = S\beta$ and cancels the propagator $(p_A + K')^2$. Thus to get the answer we should calculate the whole sum of diagram in fig. 6c. Instead of this procedure let us use some trick, taking into account the gauge invariance in explicit form. Let us look on the sum of diagrams 6c (1), 6c (2), 6c (3) as on the amplitude of interaction gluon K' with the quark p_A (see fig. 6d (1)). Due to gauge invariance $K'_\mu M_\mu = 0$ or

$$\left(\alpha_{K'} p_{A\mu} + \beta_{K'} p_{B\mu} + K'_{t\mu}\right) M^2_\mu = 0 . \tag{55}$$

But let us note, that all particles inside M_μ have a large projection of their momenta only on p_A. However $p_{A\mu} M_\mu$ can be large only if M_μ has a large component along p_B. It means that we can neglect $p_A M_\mu$ in eq. (55). So eq. (55) gives as the relation

$$p_{B\mu} M_\mu = -\frac{K'_{t\mu}}{\beta_{K'}} M_\mu . \tag{56}$$

Of course we can consider the sum of the diagrams 6c (1), 6c (4) and 6c (5) as the diagram of fig. 6d (2) and apply the same trick to the amplitude M'_ν. It gives us

$$p_{A\nu} M'_\nu = -\frac{K_{t\nu} M'_\nu}{\alpha_K} . \tag{57}$$

Using eqs. (56) and (57) we see immediately that in the amplitude M_μ survives only the first diagram since others have no longitudinal polarization and to this reason we cannot compensate the smallness in the integral (50) coming from the propagator $(p_A + K)^2$. The same happens also in the amplitude M'_ν. So the resulting answer for the whole sum of diagrams looks very simple - the only one diagram of fig. 6c but with the specific vertex for gluon emission, that is equal

$$\Gamma_\sigma = ig\, f_{abc} \frac{2K_{t\mu}\, K'_{t\nu}}{\alpha\beta S}\, \Gamma_{\mu\nu\sigma} \qquad (58)$$

where $\Gamma_{\mu\nu\sigma}$ is given by usual Feynman rules for QCD. Γ_σ looks very simple if we take into account the fact that $\alpha\beta S = q_t^2$. I would like to miss here sufficiently long but simple algebra and rush out to the answer.

$$\Gamma_\sigma = ig\, f_{abc} \frac{2}{q^2}\left(q^2\, K_\sigma - K^2\, q_\sigma\right) \qquad (59)$$

using this expression we can calculate the integral (50) and the final answer is

$$A(6c) = S\, \frac{\alpha_S^2\, C_2^2}{N^2 - 1} \int_0^y dy' \int \frac{d^2 K_t}{K_t^4} \cdot K(K, K') \frac{d^2 K'_t}{K'^4_t} \cdot \frac{N\, \alpha_S}{\pi^2} \qquad (60)$$

Here K(K, K') is equal to

$$K(K, K') = \frac{K_t^2\, K'^2_t}{q^2} \quad . \qquad (61)$$

So eq. (60) gives us the very elegant answer for contribution when we have three particle in the intermediate state or in the other words for emission of extra gluon, but in the same order of α_S there are diagrams in which no secondary gluons produces (see fig. 6f). These diagrams describe the α_S corrections to Born amplitude (M^2) and we can calculate the contribution to full elastic amplitude as

$$\int M^{(2)}_{2\to 2}\, M^{(1)}_{2\to 2} \frac{d^2 K_t}{(2\pi)^2} \quad . \qquad (62)$$

The extra log contribution should be hidden in $M^{(2)}_{2\to 2}$ amplitude, namely, in its real part. To extract this log we use once more one trick, namely, we prefer to calculate the real part of $M^{(2)}$ using the dispersion relation

$$\mathrm{Re}\, M^{(2)}_{2\to 2} = \int \frac{\mathrm{Im}_S\, M^{(2)}}{S' - S} dS' + \int \frac{\mathrm{Im}_K\, M^{(2)}}{u' - u} dK' \qquad (63)$$

and we can express $\mathrm{Im}_S\, M^{(2)}$ and $\mathrm{Im}_u\, M^{(2)}$ as integral of

$$\mathrm{Im}_S\, M^{(2)} = \int |M^{(1)}|^2 \frac{d^2 K'_t}{(2\pi)^2} \quad . \qquad (64)$$

Of course the integral (6a) or $\mathrm{Im}_S\, M^{(2)}$ and $\mathrm{Im}_u\, M^{(2)}$ is nothing more than our Born amplitude or in the other words the diagrams of figs. 6f (1) and (2) but for transferred momentum K_t^2. (In eq. (48) we put this momentum is equal to zero). The expression (64) is the function of transferred momentum K_t, which can be easily calculated. This function

$$\Sigma_S(K^2) = \frac{\alpha_S}{2\pi} \int \frac{d^2 K'_t}{(K - K')_t^2\, K'^2_t} \times C_S \qquad (65)$$

where C_S is colour factor which corresponds to diagram 6f (1). Σ_u differs from Σ_S only by coefficient C_K. Thus, the full answer for $M^{(2)}$ we can easily to get just from eq. (63).

Lecture 5 :
Main properties and solution of LL(x)A equation (the "bare" pomeron structure in perturbative QCD)

1. Main properties of LL(x)A equation

Here I would like to discuss the main properties of KLF equation (see eqs. (75) and (74)).

1) DLA

It is easy to see directly from eq. (75) that if we would like to find solution for sufficiently large virtuality q^2, we can restrict ourselves only oversimplified form of the kernel K(qq') namely $K(q, q') = \frac{1}{q^2}$, since q' << q. In this case eq. (75) can be reduced to the form

$$\frac{d\varphi(y, q)}{dy} = \frac{1}{q^2} \frac{\alpha_S N}{\pi} \int_{q_0}^{q} dq'^2 \, \varphi\left(q'^2\right) . \qquad (77)$$

Due to eq. (76) $\int_{q_0}^{q} dq'^2 \, \varphi\left(q'^2\right) = 4\sqrt{2}\,\pi^3 \times G\left(x, q^2\right)$ so eq. (77) can be written just for x G(x, y') namely

$$\frac{d}{dy} \cdot \frac{d\, x\, G\left(x\, q^2\right)}{d\, q^2} = \frac{1}{q^2} \frac{\alpha_S N}{\pi} x\, G\left(x\, q^2\right) \qquad (78)$$

or

$$\frac{d}{dy} \frac{d}{d\Gamma} F(y, \Gamma) = \frac{\alpha_S N}{\pi} F(y, \Gamma) \qquad (79)$$

where $F(y, \Gamma) = x\, G(x, q^2)$, $y = \ell n\, 1/x$, $\Gamma = \ell n \frac{q^2}{q_0^2}$. Eq. (79) coincides with eq. (20) which gave us DLA.

2) Qualitative difference between LL(q^2)A and LL(x)A

As I discussed before the main qualitative difference between LL(q^2)A and LL(x)A really is reflected to different situation with interaction in the final state. If in LL(q^2)A we can neglect this interaction (see fig. 5'a), in LL(x)A we have to take into account such an interaction (see fig. 6a). However, KLF were very lucky, since they rewrote this interaction in the final state in LLA only through the reggeization of gluon. Indeed, the equation (75) looks as summation of ladder diagrams, but really it is not so, as I tried to convince you calculating the diagrams of α_S^3 order. Indeed, if the emission of gluon could be written as new ladder diagram with the vertex which completely different from the vertex in usual ladder diagram, the new set of diagrams should be taken into account which was reduced to reggeization of gluon. Qualitatively new kernel K(q q') differs from the kernel in GLAP equation, and has two new properties :

1. There is no ordering in q. It means that if in GLAP q >> q', here q' is of the order of q. Of course such enlargement of the integration region in q' leads to increase of the structure function of gluons in the region of small x.

2. Reggeization of gluons leads to new gluon propagator which is smaller than the propagator of the perturbative gluon. So reggeization as any interaction in the final state reveals itself in some shadowing (screening) effect.

These two effects have the same order of magnitude, even more they compensate each other strictly at the point q = q'. The above discussion we can summarize as some table which gives as the comparison between LL(q)A (GLAP) and LL(x)A (KLF) approaches.

Table I
The comparison between $LL(q^2)A$ and $LL(x)A$

$LL(q^2)A$	$LL(x)A$
$y_1 \approx y_2 \approx y_3 \approx \dots \approx y_n$	$y_1 >> y_2 >> y_3 \dots >> y_n$
$q_1^2 >> q_2^2 >> q_3^2 >> >> q_0^2$	$q_1^2 \approx q_2^2 \approx q_3^2 \approx \quad \approx q_0^2$
No interaction in the final state	Final state interactions leads to gluon reggeization

Even the slight glance on the above table shows you that kinematics of LL(x)A is very close to the multiperipheral kinematical region. This question as well as detail structure of LL(x)A solution will be discussed in the next sections of this lecture.

2. Solution of LL(x)A equation

Before discussing some new qualitative figures of LL(x)A let us find the exact solution of this equation (see [8]). Anyone can check that $\varphi_f = (q^2)^{f-1}$ is the eigenfunction of our kernel. Indeed, after sufficiently long algebra we can see that

$$\frac{1}{\pi} \int K(q\, q')\, \varphi_f(q')\, d^2q' = \chi(f)\, \varphi(q) \qquad (80)$$

where

$$\chi(f) = 2\psi(1) - \psi(f) - \psi(1 - f) \qquad (81)$$

and

$$\psi(f) = \frac{d\, \ell n\, \Gamma(f)}{dt}$$, $\Gamma(t)$ is the Euler gamma function here.

Of course, the fact, that φ_f is the eigenfunction is clear just from dimension estimates. Indeed, $K(q\, q')$ is the homogeneous function of q'^2/q^2. So we have some integral $\int K(q'\, q)\, d^2q' \left(\frac{q'^2}{q^2}\right)^{f-1}$ which depends only on f. Eq. (81) is the result of the calculation of such an integral. I refer to original papers of Kuraev, Lipatov and Fadin and Balitsky and Lipatov[7, 8] for all details. From the equation (80) we can easily find the general solution of KLF equation. Using double Mellin transform we can reduce the equation (72) to the algebric form. Indeed

$$\varphi\left(q^2, y\right) = \int \frac{d\omega\, df}{(2\pi i)^2} e^{\omega y}\, \varphi_f(\Gamma)\, C(\omega, f) \qquad (82)$$

where $\Gamma = \ell n\, q^2/q_0^2$ and the contours integration in respect to ω and f are situated to the right of singularities of φ_f and $C(\omega, f)$. For $C(\omega, f)$ our equation has the form

$$\omega\, C(\omega, f) = \frac{\alpha_S N}{\pi} \left(\int K(q, q') \frac{\varphi_f\left(q'^2\right)}{\varphi_f\left(q^2\right)} dq'^2 \right) C(f, \omega) \qquad (83)$$

or taking into account the fact that $\varphi_f(q^2) = e^{(f-1)\Gamma}$ we have

$$\omega\, C(\omega, f) = \frac{\alpha_S N}{\pi} \chi(f)\, C(\omega, f) \quad . \qquad (84)$$

Finally, the general solution of KLF equation is

$$\mathrm{Re}\, M^{(2)}_{2\to 2} = S\left(C_S - C_K\right) \ln S\, \Sigma\left(K^2\right) \quad . \tag{66}$$

The colour coefficient has a very famous relation between them, which is shown in fig. 6d (1). Using this relation we can easily calculate C_S-C_K. Really this calculation is given in fig. 6d (2). Thus $\mathrm{Re}\, M^{(2)}_{2\to 3}$ has the same colour structure as one gluon exchange in Born diagram. So we can rewrite the result (66) as the correction to the trajectory of gluon, e.g. instead of gluon with propagator $1/K^2.S$ we can write the new propagator $\frac{1}{K^2} S^{\alpha^G}(K^2)$, where $\alpha(K)$ is equal to

$$\alpha^G\left(K^2\right) = 1 - \frac{\alpha_S N_c}{\pi^2} \int \frac{K^2\, d^2K'}{(K - K')^2\, K'^2} \quad . \tag{67}$$

It is interesting also to mention than we can use another form for $\alpha^G(K^2)$, namely

$$\alpha^G\left(K^2\right) = 1 - \frac{\alpha_S N_c}{2\pi^2} \int \frac{K_t^2\, d^2K'}{(K - K')_t^2 \left[K'^2 + (K - K')^2\right]} \quad . \tag{68}$$

Thus the answer for whole sum of diagrams 6f is equal

$$A(6f) = S \frac{\alpha_S^2\, C_2^2}{N^2 - 1} \int \left(\alpha^G\left(K^2\right) - 1\right) . 2 . \frac{d^2K}{K_t^4} \quad . \tag{69}$$

The full answer for A in α_S^3 order we can get summing eqs. (61) and (69). It can be represented in the form

$$A(2) = S \frac{\alpha_S^2\, C_2^2}{N^2 - 1} \int_0^y dy' \int \frac{d^2K_t}{K_t^2} K(KK') \frac{d^2K'_t}{K'^2_t} \frac{N\, \alpha_S}{\pi^2}$$

$$y = \ln S \tag{70}$$

where

$$K(K',K') - \frac{1}{K'^2} = \frac{1}{(K - K')^2} \frac{1}{K'^2} - \frac{K^2}{(K - K')^2 \left[K'^2 + (K - K')^2\right]} \frac{1}{K^2} \tag{71}$$

Using eqs. (70) and (71) we can introduce function $\varphi(K)$ and rewrite the total cross section for quark-quark interaction through this function

$$\sigma_{qq} = \frac{C_2\, \alpha_S}{4\pi \sqrt{N^2 - 1}} \int \varphi\left(y, q'^2\right) / q'^2_t\, dq'^2 \quad . \tag{72}$$

For φ eq. (70) gives the equation

$$\varphi^{(2)}(q, y) = \frac{\alpha_S N}{\pi^2} \int_0^y dy' \int d^2q'\, K(q, q')\, \varphi^{(1)}(y', q') \tag{73}$$

where

$$K(q, q')\, \varphi(q') = \frac{1}{(q - q')^2} \varphi(q') - \frac{1}{\left(q'^2 + (q - q')^2\right)} \frac{q^2}{(q - q')^2} \varphi(q) \tag{74}$$

and $\quad \varphi^{(1)} = \frac{\alpha_S\, C_2}{4\pi \sqrt{N^2 - 1}} . \frac{1}{q^2} .$

Really eqs. (73) and (74) give us the resulting answer and define the equation which is correctly sum the $(\alpha_S \ln 1/x)^n$ contributions. We would like only to rewrite this equation in more convenient form, namely

$$\frac{d\varphi\left(y = \ln 1/x,\ q^2\right)}{dy} = \frac{N\,\alpha_S}{\pi^2} \int K(q,\ q')\ \varphi\left(y,\ q'^2\right)\ d^2q' \qquad (75)$$

where K(q, q') is defined by eq. (79). The gluon structure function can be rewritten through φ in the following way (N = 3)

$$x\,G\left(x,\ q^2\right) = \int_{q_0^2}^{q^2} \varphi\left(y = \ln 1/x,\ q'^2\right)\ dq'^2/4\sqrt{2}\,\pi^3 \ . \qquad (76)$$

Thus, eqs. (72) (74) (75) and (76) give the full answer on the question what is the equation in LL(x)A. This equation was firstly received by Fadin, Kuraev and Lipatov[7] and then discussed in details in QCD by Balitsky and Lipatov[8]. This equation can describe the amplitude in the region when virtuality q^2 is not much larger than initial virtuality q_0^2. So, speaking in physical termines, this equation defines the structure of the pomeron exchange in QCD. The resulting structure of the equation (75) looks as the summation of ladder diagrams (see fig. 7). However, such ladder diagrams are only effective representation the whole huge set of diagrams which were really summed. I hope that I convinced you that it is so in our the simplest example of the diagrams of α_S^3 order. In this effective ladder the first part of our kernel K(q, q') describes the emission new gluon with the vertex which differs from the vertex of the Feynman diagram and which is defined by eq. (59). The second term in the kernel K(q, q') (see eq. (74)) describes the reggeization of gluon, which are vertical in t-channel.

In next lecture I'll try to convince you that the simplicity of the equation (75) is only at the first sight and it contains a lot of new physical phenomena.

$$\varphi(q, y) = \frac{1}{(2\pi i)^2} \int e^{\frac{\alpha_S N}{\pi}\chi(f)y+(f-1)\Gamma} \bar{\varphi}(f)\, df \qquad (85)$$

where $\bar{\varphi}(f)$ should be calculated just from initial condition namely from the value $\varphi(q^2, y)$ at $y = y_0$. Now, let us reproduce the DLA solution using the general answer of eq. (85). Let us note, that the kernel $\chi(f)$ has some special behaviour at $f \to 0$ (or $f \to 1$). For $f \to 0$ $\chi(f) \to \frac{1}{f}$

$$\text{so} \quad \varphi\left(q^2, y\right) = \frac{1}{(2\pi i)^2} \int e^{\frac{\alpha_S N}{\pi f}y+(\sigma - p)\Gamma} \bar{\varphi}(\sigma)\, df \quad . \qquad (86)$$

For large y and Γ we can use the steepest descent method to calculate the integral.

The saddle point can be found from the condition

$$-\frac{\alpha_S N}{\pi f_0^2} y + G = 0 \quad .$$

$$\text{so} \qquad f_0 = \sqrt{\frac{\alpha_S N y}{\pi \Gamma}} \quad . \qquad (87)$$

Putting eq. (87) in the integral (86) we see that

$$\varphi\left(q^2, y\right) = \frac{1}{(2\pi)^2} e^{-\Gamma} e^{2\sqrt{\frac{\alpha_S N}{\pi}\Gamma y}} \bar{\varphi}(f_0) \sqrt{\frac{\pi f_0^3}{\alpha_S N y}} \qquad (88)$$

So we reproduce the DLA solution. Of course, we can now find the function $\bar{\varphi}(f_0)$ from initial condition, for example $\bar{\varphi} = 1$ for $\varphi(q^2$

$y=0) = 1\ \delta(\Gamma - \Gamma_0)$. Really solution (88) can be valid only in the kinematical region when $f_0 << 1$ or $\sqrt{\frac{\alpha_S N y}{\pi G}} << 1$, or

$$\frac{\alpha_S N}{\pi} y << \Gamma^2 \quad . \qquad (89)$$

Now let us try to look for the solution which could describe the so-called reggeon region, which corresponds $\Gamma - \Gamma_0 << \Gamma_0$, and $y >> y_0$. Our guess in this kinematical region, is that important role in our integral (85) will play $f = 1/2 + iv$ and v will be small.

At $f \to 1/2$, the kernel χ has the following expansion

$$\chi(f) = 4\,\ell n\,\tau - v^2\, 14\,\xi(3) + O\left(v^3\right) \quad . \qquad (90)$$

Here, $\xi(3)$ is the Riemann zeta function [$\xi(3) = 1.202$]. Substituting formula (90) in eq. (85) we have

$$\varphi\left(q^2, y\right) = \frac{1}{4\pi^2} \int \bar{\varphi}(v)\, e^{\frac{\alpha_S N}{\pi}(4\ell nZ - 14\xi(3)v^2)y - \frac{1}{2}\Gamma + iv\Gamma} dv \qquad (91)$$

we can easily calculate this integral once more using the steepest descent method. The saddle point in the above integration is at $v = v_0 = \frac{i\,\Gamma}{2\Delta\omega_0 y}$, where $\omega_0 = \frac{\alpha_S N}{\pi} 4\,\ell n\, 2$

$$\Delta = \frac{14\,\xi(3)}{4\,\ell n\, 2} \quad . \qquad (92)$$

So $v_0 << 1$ for all $\omega_0 y >> \Gamma$ or for all Γ up to $\omega_0 y$. The main region, is, of course, $\Gamma \sim \sqrt{\omega_0 y}$. The result of integration is evident, namely

$$\varphi\left(q^2, y\right) = \frac{\sqrt{q_0^2}}{\sqrt{q^2}} \frac{2}{\sqrt{4\pi\ \omega_0 y\ \Delta}} e^{\omega_0 y - \frac{\Gamma^2}{4\ \omega_0\ y\Delta}} . \qquad (93)$$

Let me recall that $\Gamma = \ell n\ q^2/q_0^2$. The answer (93) is normalized by the condition that $\varphi(q^2, y) = \delta(\Gamma)$ at $y \to 0$. So $\varphi(q^2, y)$ in eq. (93) is the Green function of our equation for $\Gamma << \frac{2\alpha_S N}{\pi} 14\ \xi(3)\ y$.

Now let us discuss the main qualitative feature of this new solution which we can apply for reggeon kinematical region, namely, for fixed virtualities and large y (high energy or low x).

3. Main properties of LL(x)A equation (continuation)

3) Rapid increase of the total cross section

Directly from eq. (93) one can see that $\varphi \sim e^{\omega_0 y}$ at fixed Γ. It means that the cross section φ grows at high energies (small x) as

$$\varphi \sim \left(\frac{S}{q^2}\right)^{\omega_0} \text{ where } \omega_0 = \frac{N_c\ \alpha_S\ \chi(\sigma=1/2)}{\pi} = \frac{\alpha_S}{\pi} 12\ \ell n\ 2 \qquad (94)$$

if $N_c = 3$.

It is very important to mention that in QCD the cross section grows rapidly with energy ($\sigma_t \sim S^{\omega_0}$) even for small coupling constant, $\alpha_S << 1$. Of course, this is the direct consequence of the fact that the gluon spin is equal to 1 and we have so-called long range (in rapidity) interaction between partons in the parton cascade. Such an interaction is one of the main differences

between QCD and old naive parton approach. The increase of the total cross section can be easily explained as a result of the increasing wee parton (gluon) multiplicity. Indeed, the effective ladder diagram of fig. 7 describes not only one chain of partons but also the whole parton cascade, in which each parton can produce its own branch of partons (see fig. 8). In such a cascade each gluon is able to emit one more gluon with probability $\int \frac{\alpha_S\ N}{\pi} K(q'_i\ q)\ dq'^2)dy$ in the rapidity interval Δy. So

$$dN = N\ \omega_0\ dy \qquad (95)$$

where $\omega_0 = \frac{\alpha_S N}{\pi} \int K(q'\ q)\ dq'^2$ and so the total number of wee partons (N) grows as $N = N_0\ e^{\omega_0 y}$. In other words the total cross section is proportional to elementary one

$$\sigma_0 \sim \alpha_S^2 <r^2> \qquad (96)$$

(where $<r^2>$ is the mean radius of the target) times the multiplicity of the wee partons

$$\sigma_t = \sigma_0 \exp \omega_0\ \ell n\ S\ . \qquad (97)$$

Of course, directly from eq. (97) we can estimate the mean number of cells in our "ladder", ($\bar{n}$), namely

$$\sigma_t = \sigma_0 \sum e^{\omega_0\ \ell n\ S} = \sigma_0 \sum \frac{\left(\omega_0\ \ell n\ S\right)^n}{n\ !}$$

and $\qquad \bar{n} = \omega_0\ \ell n\ S\ . \qquad (98)$

It is worth mentioning that $\bar{n}$ is proportional to the multiplicity of wee partons in a single particular branch of the parton cascade only (for example that one which is shown by double line in fig. 8e) since the total "wee" parton multiplicity is about $N \sim e^{\bar{n}}$, as seen from fig. 8.

4) Random walk in the $\ell n\, q_t^2$ plane

Another important property of the solution (93) is the fact that it describes the diffusion motion of partons in the $\ell n\, q_t^2$ plane. Such motion reflects the convergence of the kernel $K(q', q)$ in eq. (75) in respect to integration over q'^2 both for small ($q' < q$) and large ($q' > q$) q'^2 for any function φ_f with $0 < \mathrm{Re}f < 1$. This means that the essential q'^2 in the integral is of the order of q ; being a direct consequence of the fact that the QCD coupling α_S is dimensionless. Thus, we have no dimension parameters except q_t in our equation. Therefore $q' \sim q$ or the emission of each successive gluon changes $\ell n\, q_t$ by a value of the order of unity, i.e. $\ell n\, q_t - \ell n\, q'_t \approx 1$. For high energy ($y = \ell n\, 1/x >> 1$). $\ell n\, q_t$ can increase or decrease with equal probability ($\Delta\, \ell n\, q_t \approx 1$). It means that after emission of n gluon the $\ell n\, q_t$ of our particular parton changes in the value

$$\langle \ell n\, q_t^2 \rangle_n = n \langle \Delta\, \ell n\, q_t^2 \rangle = n\Delta \qquad (99)$$

where $\Delta = \langle |\Delta\, \ell n\, q_t|^2 \rangle$ for one gluon emission.

Of course eq. (99) leads to typical diffusion distribution

$$N = N(\Gamma=0)\, e^{-\Gamma^2/n\Delta} \frac{2}{\sqrt{\pi n \Delta}} \; . \qquad (100)$$

The solution (100) coincides with the general solution (93) if we take $N(\Gamma=0) = e^n$ and remember that $n = \omega_0 y$. The equation (99) leads us directly to the conclusion that the average $\ell n\, q_t$ of the parton in our parton cascade depends crucially on energy (or x_B) in our process, namely,

$$\langle \ell n^2\, q^2 \rangle = \Delta . \omega_0\, \ell n\, S \; . \qquad (101)$$

Such a diffusion is the quite new phenomena which we face in QCD in comparison with the ordinary naive parton approach. Indeed, in the naive parton model, $\langle q_t^2 \rangle$ is constant and cannot depend on the initial energy. In QCD we see that mean q_t grows remarkably with the energy (see eq. (101)). This fact changes crucially our intuition for so-called typical inelastic processes at high energy or small x_B (in DIS).

5) Parton walk in impact parameter plane

As illustration the above statement let us consider the impact parameter distribution of the parton inside of the parton cascade. Here, I would like to discuss only qualitative picture of this distribution and refer the reader to paper [2] for details.

It is well known, just from uncertainty principle, that the typical shift in impact parameter plane Δb_t is proportional to $1/q'_t$ where q'_t is the transverse momentum of the "n"th cell of the LLA ladder. It changes significantly at each diffusion step. As mentioned above the parton momentum q_t can be changed in several times from one cell to another, since $\ell n\, q'/q \sim 1$. In momentum space such variation of q'_t leads to diffusion in $\ell n\, q_t$, but in the b_t plane this increase of $\ell n\, q_t$ results in a rapid decrease of the typical shift in b_t. Indeed, directly from $\Delta b_t\, q'_t \sim 1$ follows

$$\Delta\, b_t^2 \sim \exp\left(-\, \ell n\, q'^2_t\right) = \exp\left(-\sqrt{n\Delta}\right) \to 0 \qquad (102)$$

In eq. (102) we use eq. (99).

Thus, all wee partons are frozen in b_t at sufficiently large n and q_t or in other words are located at fixed value of b_t. A wee parton shifts its position in b_t significantly only in the rare fluctuation when the parton accidently comes to the region of small $q_t \sim Q_0$ during its diffusion motion in $\ell n\, q_t$. Such propability is equal by definition to the ratios $W_0 =$

$$\frac{N(\ell n \frac{q^2}{Q_0^2} = 0)}{\int N(\ell n \frac{q'^2}{Q_0^2})\, d\, \ell n\, q'^2}$$ and equal to $1/\sqrt{n}$ ($W_{0-} = 1/\sqrt{n} = 1/\sqrt{\omega_0 y}$

accordingly to eq. (100).

Thus the characteristic displacement of the wee parton in b'_t is equal to

$$<b_t^2(n)> = \sim W_0\, n/Q_0^2 \sim \sqrt{n}/Q_0^2 = \frac{\sqrt{\omega_0\, y}}{Q_0^2} \quad . \qquad (103)$$

Thus, we receive the behaviour $<b_t^2> \sim \sqrt{n} \sim \sqrt{\ell n\, S}$ instead of $<b_t^2> \sim n \sim \ell n\, S$ which was typical for old parton approaches. The reader can find the direct calculation in ref. [2] which confirms the above qualitative arguments and reproduces expression ([10]) for $<b_t^2>$. It means that in QCD the radius of the interaction $R \sim \sqrt[4]{\ell n\, S}$ instead of $R \sim \sqrt{\ell n\, S}$ in reggeon approach.

If we look on eq. (103) we can see also some difficulty. Indeed Q_0 here is the smallnest value of the transverse momentum of parton. This value characterize the region in space that is occupied by parton inside the initial hadron, but explicit form of eq. (103) shows us that we face with infrared divergency of value of R. So

the precise answer for interaction radius depends crucially on the solution of the confinement problem, but energy dependence has so transparent physical meaning that should be the same for all solutions of this miracle problem.

6) Singularity in j-plane

Discussing the property of the high energy interaction, we used to the structure of the singularities in angular momentum plane. For simple pomeron exchange the right most singularity in j-plane was pole with trajectory $j = 1 + \Delta$ at $t = 0$. Here, we have some cut (branching point) which starts from $j = 1 + \omega_0$ and goes to the left. The character of the singularity is responsible for pre-exponent factor in our asymptotics which is equal to 1 in reggeon theory and gives additional $1/\sqrt{\ell n\, S}$ suppression in the case of QCD. This factor is not very important, but we should be very careful when we are going to generalize even trivial properties of reggeon exchange such as factorization, for example, in QCD.

7) Summary

The table II gives us the comparison between properties of QCD pomeron and old parton model approach.

Table II
Comparison of pomeron structure in QCD and old parton model

Parton (multiperipheral model)	QCD (LL(x)A)
$y_1 > y_2 > y_3 \dots > y_n$	$y_1 >> y_2 >> y_2 \dots >> y_n$
$q_1^2 \approx q_2^2 \approx q_3^2 \dots \approx q_0^2$	$q_1^2 \sim q_2^2 \approx q_3^3 \dots \approx q_0^2$
Final state interaction was taken into account in many versions of the multiperipheral models	Final state interaction leads to gluon reggeization
$\langle \ell n\, q_t^2 \rangle = \text{const}\ (S)$	$\langle \ell n\, q_t^2 \rangle \sim \sqrt{\alpha_S\, \ell n\, S}$
$\sigma_t \sim S^{\omega 0}$	$\sigma_t \sim S^{\omega 0}/\sqrt{\ell n\, S}$
$R^2 \sim \ell n\, S$	$R^2 \sim \sqrt{\ell n\, S}$
B (slope of the elastic cross section) = $2\,\alpha'\, \ell n\, S$	$B \sim \frac{1}{Q_0^2}\sqrt{\ell n\, S}$

The above table shows you that QCD gives the new impetus for your intuition at least as an example that shows what can be in the nature.

The main goal of all our further lectures is to demonstrate to you that LLA of QCD gives the description of Deep Inelastic Scattering within good theoretical accuracy. LL(x)A and LL(q^2)A give the description the full kinematical region of DIS but up to now we have considered the constant coupling α_S in QCD. As you know the main striking property of QCD is, namely, the running α_S.

So, the next point will be LL(x)A equation with running α_S.

Lecture 6 : LL(x)A with running α_S

In this lecture I am going to solve the KLF equation with running coupling constant of QCD ($\alpha_S = \frac{4\pi}{b\, \ell n\, q^2}$). This equation was firstly solved and discussed in details in ref. [1], but unfortunately only on pure theoretical level. Now we need some numerical solution of this equation and we should answer how important the difference between correct equation and GLAP numerically for accessible value of x ($x \gtrsim 10^{-5}$).

1. Equation

The form of such an equation is trivial, namely

$$\varphi\left(q^2, y\right) = \frac{N}{\pi} \int_0^y dy' \int \frac{d^2q'}{\pi} \alpha\left(q'^2\right) K(q, q')\, \varphi\left(q'^2, y'\right) . \tag{104}$$

The only question which could arise is why α_S depends on q'^2 but not q^2. Really there is no difference between such variables, since $\alpha(q'^2) - \alpha(q^2) \sim \alpha_S^2(q'^2)$ so the difference could be interpreted as next order α_S correction to the kernel K(q, q').

2. Solution

Using the explicit form for coupling constant QCD $\alpha_S = \frac{4\pi}{b\Gamma}$ (where $\Gamma = \ell n\, q^2/\Lambda^2$) and the double Mellin transform (82) we can get the following equation for $C(\omega, f)$

$$-\omega \frac{\partial}{\partial f} G(f\, \omega) = \frac{4\pi N}{\pi b} \chi(f)\, C(f\, \omega) . \tag{105}$$

Finally, the solution of equation can be written in the form

$$\varphi\left(q^2, y\right) = \int \int \frac{df\, d\omega}{(2\pi i)^2} \cdot \bar{\varphi}(\omega) \cdot e^{\omega y + (f-1)\Gamma + \frac{4N}{b\omega} \int_f^{1/2} \chi(f')\, df} \qquad (106)$$

$\bar{\varphi}$ should be found from initial condition and as we have discussed we can introduce two Green functions with different initial condition : $G_y(y, \Gamma) \to \delta(\Gamma - \Gamma_0)$ at $y = y_0$ and $G_\Gamma(y, \Gamma) \to \delta(y - y_0)$ at $\Gamma = \Gamma_0$.

3. DLA

At small x and large q^2 the integral (106) can be taken using the steepest descent method. The saddle point ω_0 and f_0 are found from the equations

$$\omega_0^2 = \frac{4N}{b\ y} \int_{f_0}^{1/2} \chi(f')\ df'$$

$$\chi\left(f_0\right) = \frac{b\ \omega_0}{4N} \Gamma \ . \qquad (107)$$

Eqs. (107) we can easily solve in the case when $f_0 \to 0$. Indeed for small f $\chi(f) = + 1/f$. So

$$\omega_0^2 = - \frac{4N}{b\ y} \ell n\ f_0$$

$$\frac{1}{f_0} = \frac{b\ \omega_0}{4N} \Gamma \qquad (108)$$

so

$$f_0 = \frac{4N}{b\ \omega_0 \Gamma} = \frac{1}{\Gamma} \sqrt{\frac{4N\ y}{b\ \ell n\ \Gamma}}$$

$$\omega_0^2 = \frac{4N\ \ell n\ 1/f_0}{b\ y} = \frac{4N\ \ell n \left(b\ \Gamma\ \omega_0/4N\right)}{b\ y} \ . \qquad (109)$$

In the region $y << \Gamma^2$ we get the leading terms in the exponent of the structure function, which is equal to

$$\varphi\left(y, q^2\right) \sim \exp\left(\sqrt{\frac{16N}{b} y\ \ell n\ \Gamma} - \Gamma\right) \ . \qquad (110)$$

Of course, if Γ is very close to Γ_0 and if $\Gamma_0 >> 1$ we can reduce eq. (110) to old form of DLA solution. Indeed $\Gamma = \Gamma_0 + \Delta\Gamma$ and $\ell n\ \Gamma = \ell n\ (\Gamma_0 + \Delta\Gamma) = \ell n\ \Gamma_0 + \frac{\Delta\Gamma}{\Gamma_0}$ and

$$\varphi\left(y\ q^2\right) \sim C \exp\left(\sqrt{\frac{16N\pi\ \Delta\Gamma}{b\ \pi\ \Gamma_0} y} - \Gamma\right) =$$

$$= C\left(\Gamma_0\right) \exp\left(\sqrt{\frac{4N}{\pi} \alpha_S\left(\Gamma_0\right) \Delta\Gamma y} - \Gamma\right) \ . \qquad (111)$$

Eq. (110) gives you the well known form of the DLA solution if we introduce new variable $\ell n\ \Gamma = \xi$ (see for example ref. [3]).

4. Numerical (Monte-Carlo) solution of the equation

Of course, I could continue to discuss the theoretical solution of eq. (106), but really such a discussion was crucially intensified by the Monte Carlo solution of the equation which was done by Marchesini and Webber[10]. They claimed that in wide region of x ($10^{-5} < x < 0.1$) and q^2 ($5\ GeV^2 < q^2 < 10\ 000\ GeV^2$) the solution of KLF equation with running α_S coincides with the solution of GLAP equation in 5-10 % accuracy.

Figure 9 is taken from the paper of Marchesini and Webber and shows you the result of Monte Carlo calculation. One loop equation means GLAP one, and multiloop equation is KLF equation with running α_S. This result was absolutely strange from point of view of our theoretical discussion. Indeed, look at table I. We see that the KLF equation takes into account larger phase space in transverse momentum so we wait for the solution of KLF which should be larger than the solution of GLAL equation. So we touch now the hot problem of LLA, which is discussing now among experts.

I hope, the first, that this puzzle, should stimulate, is the more detail theoretical investigation of the solution (106). However, even at the moment we should take in mind, that MC procedure of finding solution includes some cut-off $Q_g > \Lambda$ on the emitted transverse momenta and does not introduce the same cut-off for virtual gluons. It means that reggeization of gluons works in full strength, but the phase space for emission is restricted due to this cut-off. For example, if Q_g is equal to g_0, where q_0 is the initial virtuality from which we start to develop parton cascade using evolution equation ; the first integration (integration in the first cell of the ladder) in respect to q'_t gives twice smaller contribution than without cut-off. So such cut-off can change crucially the situation in several first cells of LLA ladder diminishing the contribution to LL(x)A equation.

However, the main problem which we should study theoretically is :

1. why the solution of LL(x)A equation is so close to solution of LL(q^2)A even for large number of cell in the ladder ?

2. is it possible that solution LL(x)A gives smaller value of deep inelastic structure function that LL(q^2)A, as shown in fig. 9 ?

5. G_Γ (y, Γ-Γ_0

Here, I am going to find the Green function $G_\Gamma(y, \Gamma-\Gamma_0)$ that gives us the development in $\Gamma = \ell n\, q^2/\Lambda^2$ if we know the initial condition, namely $\varphi(q^2=q_0^2, y)$ (or $\Gamma = \Gamma_0$, $\varphi(y, \Gamma=\Gamma_0) = \bar{\varphi}(y)$). This Green function was calculated by M. Ryskin and me many years ago, but only here I would like to publish it. So we would like to find the solution with the initial conditions

$$\varphi\left(y, \Gamma=\Gamma_0\right) = \delta\left(y - y_0\right) \quad . \tag{112}$$

The most interesting problem for us is to consider the Green function in the region of large y and sufficiently small q^2. This is the kinematical region which corresponds the $\ell n\, q_t$ diffusion in KLF equation with constant α_S, as was discussed in the previous lecture. So we restrict ourselves by simplified form of the kernel $\chi(t)$ expanding it around f = 1/2. Introducing f = 1/2 + iv, we can use the eq. (90), namely,

$$\chi(f) = \chi\left(\frac{1}{2}\right) - v^2\left(14\xi(3)\right) + O\left(v^3\right) = \chi_0\left(1 - \Delta v^2 + O\left(v^3\right)\right) \quad . \tag{113}$$

Using eq. (113) we can rewrite the solution (106) in explicit form, taking all integrals. Indeed

$$\varphi(y, q) = \int \int \frac{dv\, d\omega}{2\pi(2\pi i)} \bar{\varphi}(\omega) \,.$$

$$. \exp\left\{\omega y + iv\Gamma = \frac{1}{2}\Gamma - \frac{4N}{b\omega} i \left(v\, \chi_0 - \frac{\delta v^3}{3} \chi_0\right)\right\} \quad . \tag{114}$$

Introducing new variable

$$v' = \left(\frac{\omega_0 \Gamma_0}{\omega} \Delta\right)^{1/3} v \qquad \text{where}$$

$$\omega_0 \Gamma_0 = \frac{4N}{b} \chi(1/2) \text{ or } \omega_0 = \frac{N}{\pi} \alpha_S\left(\Gamma_0\right) \chi(1/2)$$

we can rewrite eq. (114) through Airy function (see [9] for definition and integral representation of Airy function). Resulting answer for $G_\Gamma(y, \Gamma)$ is

$$G_\Gamma(y, \Gamma) = a \frac{\Gamma}{\Gamma_0} \int e^{\omega(y-y_0)} d\omega \frac{A_i\left(\left(\frac{\omega}{\omega_0 \Gamma_0 \Delta}\right)^{1/3} \left[\Gamma - \frac{\omega_0 \Gamma_0}{\omega}\right]\right)}{A_i\left(\left(\frac{\omega}{\omega_0 \Gamma_0 \Delta}\right)^{1/3} \left[-\frac{\omega_0 \Gamma_0}{\omega} + \Gamma_0\right]\right)} \qquad (115)$$

and $a = e^{-1/2(\Gamma-\Gamma_0)}$. Anyone can check that $G_\Gamma(y, \Gamma)$ is equal to $\delta(y - y_0)$ at $\Gamma = \Gamma_0$.

First of all let us find the asymptotics of $G_\Gamma(y, \Gamma)$ in so-called diffusion region. The answer is very simple we could find the usual diffusion behaviour of G_Γ in the kinematical region where

$$1. \left(\frac{\omega - \omega_0}{\omega}\right) \Gamma_0 \left(\frac{\omega}{\omega_0 \Gamma_0 \Delta}\right)^{1/3} >> 1 \quad \text{and}$$

$$2. \frac{\omega - \omega_0}{\omega_0} > \frac{\Delta\Gamma}{\Gamma_0} \left(\Delta\Gamma = \Gamma - \Gamma_0, \Delta\omega = \omega - \omega_0\right) . \qquad (116)$$

Both above conditions (116) are needed to use the asymptotic of Airy functions in nominator and dominator of eq. (115). So G_Γ is equal to

$$G_\Gamma\left(y-y_0, \Gamma-\Gamma_0\right) = e^{-\frac{1}{2}(\Gamma-\Gamma_0)} \sqrt{\frac{\Gamma}{\Gamma_0}} \int d\omega\, e^{\omega y}\, C$$

$$\cdot \exp\left(-\frac{2}{3}\left(\frac{\omega}{\omega_0\Gamma_0\Delta}\right)^{1/2} \left[\left(-\frac{\omega_0 \Gamma_0}{\omega} + \Gamma\right)^{3/2} - \left(\frac{\omega - \omega_0}{\omega}\right)^{3/2} \Gamma_0{}^{3/2}\right]\right)$$

$$= e^{-\frac{1}{2}(\Gamma-\Gamma_0)} \sqrt{\frac{\Gamma}{\Gamma_0}} \int d\omega\, e^{\omega y}\, C \exp\left[-\frac{2}{3}\left(\frac{\omega}{\omega_0 G_0 \Delta}\right)^{1/2} \Gamma_0{}^{3/2}\right.$$

$$\left.\cdot \left\{\left(\frac{\Delta\omega}{\omega} + \frac{\Delta\Gamma}{\Gamma_0}\right)^{3/2} - \left(\frac{\Delta\omega}{\omega}\right)^{3/2}\right\}\right] = \qquad (117)$$

$$= e^{-1/2(\Gamma-\Gamma_0)} \sqrt{\frac{\Gamma}{\Gamma_0}} \int d\omega\, C\, e^{\omega y - \frac{2}{3}\left(\frac{\omega}{\omega_0\Delta}\right)^{1/2} \Gamma_0 \left(\frac{3}{2}\frac{\Delta\Gamma}{\Gamma_0}\left(\frac{\Delta\omega}{\omega_0}\right)^{1/2}\right)}$$

In eq. (117) we only interested in exponential behaviour of our Airy functions, so we include all pre-exponential factor in coefficient C.

Integration in respect to ω has a saddle point ($\Delta\omega^0$), namely

$$y - \frac{\Delta\Gamma}{2\sqrt{\omega_0\Delta}} \cdot \frac{1}{\Delta\omega_0} = 0$$

and $$\Delta\omega_0 = \frac{(\Delta\Gamma)^2}{4\Delta y^2 \omega_0} . \qquad (118)$$

So, we can use the steepest descent method to calculate the integral (117). The answer is the usual diffusion

$$G_\Gamma\left(y-y_0,\Gamma-\Gamma_0\right) = e^{-1/2\left(\Gamma-\Gamma_0\right)} \frac{1}{\sqrt{\pi\Delta\omega_0 y}} e^{\omega_0 y - \frac{(\Delta\Gamma)^2}{4\Delta\omega_0 y}} \quad (119)$$

Now let us go back to conditions (116) and specify the kinematical region in which we can give the theoretical guarantees for the answer. We put $\Delta\omega = \Delta\omega^0$ from eq. (118) in eqs. (116) and get : $(\Delta\Gamma)^0 >> \frac{y^2 4\Delta\omega_0^2}{\Gamma_0}(\Gamma_0\Delta)^{1/3}$ from the first inequality (116) and $\Delta\Gamma >> \frac{4\Delta y^2\omega_0^2}{\Gamma_0}$ from the second one. So for $4\Delta y^2\omega_0 > \Gamma_0(\Gamma_0\Delta)^{1/3}$ we can use the last restriction, if $4\Delta y^0\omega_0 < \Gamma_0(\Gamma_0\Delta)^{1/3}$ only the first one is important.

However, to apply the equation (119) to the description of the Green function we must demand that $\Delta\Gamma$ could be of the order of $\Delta\Gamma = 2\sqrt{\Delta\omega_0 y}$. It means for $4\Delta\omega_0^2 y^0 > \Gamma_0(\Gamma_0\Delta)^{1/3}$

$$\left(\frac{4\Delta y^2\omega_0^2}{\Gamma_0}\right)^2 << 4\Delta\omega_0 y$$

or $$4\Delta\left(y\omega_0\right)^3 << \Gamma_0^2$$

for large Γ_0 these two conditions cannot be satisfied simultaneously. The second case when $4\Delta\omega_0^2 y^2 < \Gamma_0(\Gamma_0\Delta)^{1/3}$ and

$$4\Delta y\omega_0 >> \frac{4\Delta\left(\omega_0 y\right)^2}{\Gamma_0}\left(\Gamma_0\Delta\right)^{1/3}$$

or

$$\Gamma_0\left(\Gamma_0\Delta\right)^{-1/3} >> \omega_0\, y$$

finally, the constraint looks as follows

$$\omega_0\, y \le \Gamma_0^{2/3}\,\Delta^{-1/3} \quad . \qquad (120)$$

Therefore we can prove the diffusion picture for LL(x)A equation but only in the restricted region of y (see eq. (120), which crucially depends on the value of the initial virtuality.

This is very important conclusion which means first of all that the running α_S is essential to understand the character of the behaviour of the deep inelastic structure function at low x. To understand what means the constraint (120), let us consider the ordinary situation in practice, namely, let us take $q_0^2 = 5\ \mathrm{GeV}^2$ and $\Lambda = 100$ MeV. Thus, $\Gamma_0 = \ell n \frac{q_0^2}{\Lambda^2} = 6.2$, $\omega_0 = \frac{N}{\pi}\alpha_S(q_0^2)\,\chi(1/2) = 0.65$, $\Delta = 6.5$. So we can apply the diffusion solution in the region of $y = \ell n\, 1/x$

$$0.65\ y \le (6.2)^{2/3}\ (6.5)^{-1/3}$$

or $$y << 3.2 \quad ; \quad \text{or } x \ge 1/20 \quad .$$

So namely in the important kinematical region of the future experiments at HERA we should be very carefull with the application of the simplest asymptotic formula for the deep inelastic structure function.

Now let us discuss in more details the structure of singularities in ω-plane for the solution (115). Let me recall you that our contour of integration is to the right of all singularities,

so our knowledge of the singularities allows us to take integral and understand the behaviour of $G_\Gamma(y, \Gamma')$. Function $Ai(\omega)$ is the analytical function of its argument. So the origin of singularities in eq. (116) is the only zeros of $Ai((\frac{\omega}{\omega_0\Gamma_0\Delta}1/3(-\frac{\omega-\omega_0}{\omega}\Gamma_0))$. Within good numerical accuracy the zeros of Ai can be calculated using the following formula

$$\left(\frac{\omega}{\omega_0\Gamma_0\Delta}\right)^{1/3}\left(\frac{\omega_0-\omega}{\omega}\Gamma_0\right)=\left(\frac{3}{2}\left(\frac{3}{4}\pi+\pi K\right)\right)^{2/3} \qquad (121)$$

for very large K ω_K tends to zero as $\omega_K \sim 1/K$. The other very interesting observation is the fact that right more singularity (pole) turns out to be considerable less than the value of ω_0. For example, for typical situation $q_0^2 = 5\ GeV^2$, $\Lambda = 100$ MeV $\omega_0 = 0.65$ and $\omega_{K=0} = 0.3$. It means that our Green function for LL(x)A equation with running α_S grows only as $\left(\frac{1}{x}\right)^{\omega_{K=0}}$ and such increase is much smoother than $(1/x)^{\omega_0}$ for LL(x)A with α_S = const. The table III shows you the value of ω_K for different $\Gamma_0 = \ell n \frac{q_0^2}{\Lambda^2}$. You can see that starting with K = 3-4 we face the 1/K behaviour of ω_K, and for larger q_0^2 $\omega_{K=0}$ tends to ω_0. The residue for the pole $\omega = \omega_K$ behaves as

$$e^{-2/3\left(\frac{\omega_K}{\omega_0\Gamma_0\Delta}\right)^{1/2}\left[\left(-\frac{\omega_0\Gamma_0}{\omega_K}+\Gamma\right)^{3/2}\right]}.$$

So the resulting answer for $G_\Gamma(y\Gamma)$ we can represent as some seria of the following type

$$G_\Gamma(y-y_0,\Gamma)=\sum_K e^{\omega_K(y-y_0)}.(-1)^K.$$
$$.\ e^{-2/3\left(\frac{\omega_K}{\omega_0\Gamma_0\Delta}\right)^{1/2}\left[\left(-\frac{\omega_0\Gamma_0}{\omega_K}+\Gamma\right)^{3/2}\right]}. \qquad (122)$$

Table III
ω_K for LL(x)A equation with running α_S

$\Gamma_0\backslash\omega$	ω_0	$\omega_{K=0}$	$\omega_{K=1}$	$\omega_{K=2}$	$\omega_{K=3}$	$\omega_{K=4}$	$\omega_{K=5}$
4	1	0,3	0,17	0,12	0,093	0,075	0,064
8	0.5	0,22	0,135	0,102	0,081	0,068	0,068
12	0,33	0,17	0,115	0,087	0,072	0,001	0,053
16	0.25	0,14	0,1	0,078	0,064	0,056	0,05
20	0.2	0,122	0,09	0,071	0,069	0,051	0,046

The factor $(-1)^K$ originates from the denominator, since Ai(x) is very similar to $x^{2/3}$. In wide region of our kinematical variable the first term in the above sum (122) dominates, and only at large Γ the contribution of the second term can be comparable with the first one. Indeed

$$G_\Gamma(y-y_0,\Gamma) = e^{\omega_{K=0}(y-y_0)-2/3\left(\frac{\omega_{K=0}}{\omega_0\Gamma_0\Delta}\right)^{1/2}\Gamma^{3/2}} - e^{\omega_{K=1}(y-y_0)-2/3\left(\frac{\omega_{K=1}}{\omega_0\Gamma_0\Delta}\right)^{1/2}\Gamma^{3/2}}.$$

The ratio of the second term ($G^{(2)}$) to the first one ($G_\Gamma^{(1)}$) is equal to

$$R = \frac{G^{\Gamma}_{(2)}}{G_\Gamma^{(1)}} = e^{\left(\omega_{K=1}-\omega_{K=0}\right)\left(y-y_0\right)} \cdot$$

$$\cdot\, e^{+2/3\,\Gamma^{3/2}\left(\omega_0\Gamma_0\Delta\right)^{-1/2}\left(\sqrt{\omega_{K=0}}-\sqrt{\omega_{K=1}}\right)} .$$

So $R \to 1$ if

$$\left(\omega_{K=1}-\omega_{K=0}\right)\left(y-y_0\right) = -\,2/3\,\Gamma^{3/2}\left(\omega_0\Gamma_0\Delta\right)^{-1/2} \cdot \left(\sqrt{\omega_{K=0}}-\sqrt{\omega_{K=1}}\right)$$

or

$$\left(\sqrt{\omega_{K=1}}+\sqrt{\omega_{K=0}}\right) y = 2/3\,\Gamma^{3/2}\left(\omega_0\,\Gamma_0\,\Delta\right)^{-1/2} .$$

It means that for fixed Γ only for

$$y \leqslant 2/3\,\Gamma^{3/2}\left(\omega_0\Gamma(0)\Delta\right)^{-1/2} \cdot \left(\sqrt{\omega_{K=0}}+\sqrt{\omega_{K=1}}\right)^{-1}$$

the second pole could be important. For typical case $q_0^2 = 5\ \mathrm{GeV}^2$ and $\Lambda = 100$ MeV ($\Gamma_0 = 6.2$), y should be smaller than

$$y \leqslant 0{,}13\,\Gamma^{3/2}$$

if you would like to take into account the second pole. It means that for $q^2 = 10^3\ \mathrm{GeV}^2$ (at $\Lambda = 100$ MeV, $y \le 5$, or $x \ge 10^{-2}$ and for $q^2 = 10^5\ \mathrm{GeV}^2$, $y < 9$ or $x > 10^{-4}$. Even this rough estimation shows

us that the most important contribution at small x is the first pole (the right most one). More detail estimation just from eq. (122) shows that restriction on y even more strong, since $y \le 0.13\ (\Gamma-\Gamma)^{3/2}$, where $F = \frac{\omega_0\Gamma}{\omega_{K=0}} \approx 2\Gamma_0$. Such an improvement gives $y \le 1$ for $q^2 = 10^5\ \mathrm{GeV}^2$. So really, for initial conditions at $q_0^2 = ,5\ \mathrm{GeV}^2$, we can restrict ourselves only the contribution of the first pole in our Green function $G_\Gamma(y\Gamma)$ at $x < 10^{-1}$.

Now let us remember that we use the expansion (113) for kernel $\chi(f)$, so we should return to discussion how small v gave the contribution in our Green function $G_\Gamma(y, \Gamma)$. Let us note that the asymptotics of Ai-function corresponds sufficiently large value of v. Indeed

$$\mathrm{Ai}(x) = \int dv'\, e^{xv'-\frac{v'^3}{3}} . \qquad (123)$$

In integral (123) you can see the saddle point

$$v'_0 = \sqrt{x}$$

which leads to asymptotics behaviour

$$\mathrm{Ai}(x) \sim e^{2/3\,x^{3/2}} .$$

In our case $x = \left(\frac{\omega}{\omega_0\Gamma_0\Delta}\right)^{1/3}\left(\Gamma - \frac{\omega_0\Gamma_0}{\omega}\right)$. Thus for large Γ the typical v is large ($v \sim \Gamma^{1/2}$). Therefore, in the case when the first (or several) pole is important, for large Γ we cannot restrict ourselves by the oversimplified expression (113) for kernel $\chi(f)$. Returning to

our old variable ν from ν' in eq. (114), we see that saddle point corresponds to the value ν^0 which is equal to

$$\nu^0 = \left(\frac{\omega_0 \Gamma_0}{\omega_{K=0}}\right)^{1/6} \left(\Gamma - \frac{\omega_0 \Gamma_0}{\omega_{K=0}}\right)^{1/2}$$

for the right most pole.

For case $q_0^2 = 5\ \mathrm{GeV}^2$ and $\Lambda = 100$ MeV at $q^2 = 10^5\ \mathrm{GeV}^2$ we have

$$\nu^0 = 1 \ .$$

It means that we cannot use our expansion for the kernel in this kinematical region.

Thus, our main conclusion from the above consideration, that for sufficiently small x (large y) namely at $y \gg 1$; we suspect that our ν cannot be small in LL(x)A equation with running α_S on the contrary of the case of constant α_S. Practically, it means that we should study the complete expression for kernel in the solution (116). I am going to discuss $G_\Gamma(y, \Gamma)$ for general expression for the kernel, but slightly later.

Lecture 7 :
LL(x)A with running α_S (continuation)

In this lecture I am going to continue the discussion of the solution of LL(x)A with running coupling constant α_S. Really, I would like to discuss only two problems : the Green function $G_y(y-y_0, \Gamma-\Gamma_0)$ and the trajectory method. After that I hope, the scale of the difference between the solutions of LL(x)A and LL(q^2)A will be absolutely clear for you.

6. $G_y(\Gamma-\Gamma_0, y-y_0)$

Here I would like to find the Green function $G_y(\Gamma-\Gamma_0, y-y_0)$, G_y is the solution of the equation (104) with the initial condition $y = y_0$ $G_y = \delta(\Gamma-\Gamma_0)$. To find G_y let us rewrite eq. (109) adding the non integral term $\delta(\Gamma-\Gamma_0)$ that is

$$\varphi\left(q^2, y\right) = \frac{N}{\pi} \int_{y_0}^{y} dy' \int \frac{d^2q'}{\pi} \alpha\left(q'^2\right) K(q, q') \varphi\left(q'^2, y'\right) + \delta\left(\Gamma - \Gamma_0\right) \theta\left(y - y_0\right) \ . \qquad (124)$$

Using the double Mellin transform we can get the following equation instead of eq. (105)

$$- \omega \frac{\partial}{\partial f} C(f, \omega) = \frac{4N}{b} \chi(f)\ C(f, \omega) + \Gamma_0\ e^{-(f-1)\Gamma_0} \ . \qquad (125)$$

The solution of homogeneous equation has been found (see eq. (106)) namely

$$C_n(f,\omega) = e^{\frac{4N}{6\omega}\int_f^{1/2}\chi(t')\,dt'}\,\bar{\varphi}(\omega) \quad . \tag{126}$$

As usually, we can find the solution of eq. (125) in the form $C(f,\omega) = x\,C_h(t\omega)$ and for x we have the equation

$$\frac{\partial x}{\partial f} = -\frac{\Gamma_0}{\omega}\,C_h^{-1} \quad .$$

So finally

$$C(f\,\omega) = \frac{\Gamma_0}{\omega}\,e^{\frac{4N}{b\omega}\int_f^{1/2}\chi(f'')\,df''+\Gamma(f-1)} \quad .$$

$$\int_f^{\infty} df'\,e^{-\frac{4N}{b\omega}\int_{f'}^{1/2}\chi(f''')\,df'''-\Gamma_0(f'-1)} \tag{127}$$

and the full answer is

$$G_y\left(\Gamma-\Gamma_0,\,y-y_0\right) = \int\int e^{\omega(y-y_0)}\,\frac{d\omega\,dt}{(2\pi i)^2}\,.\,e^{\frac{4N}{b\omega}\int_f^{1/2}\chi(f'')\,df''}\,.$$

$$.\,e^{\Gamma(f-1)}\,.\,\frac{\Gamma_0}{\omega}\int_f^{\infty}df'\,e^{-\frac{4N}{b\omega}\int_{f'}^{1/2}\chi(f''')df'''}\,.\,e^{-\Gamma_0(f'-1)} \tag{128}$$

we can take the integral over ω and reduce the eq. (128) to the form

$$G_y\left(\Gamma-\Gamma_0,\,y-y_0\right) = \int\int e^{(f-1)\Gamma-(f'-1)\Gamma_0}\,\Gamma_0\,\frac{df\,df'}{(2\pi i)}\,\nu(f'-f)$$

$$I_0\left(2\sqrt{(y-y_0)\,\frac{4N}{b}\int_f^{f'}\chi(f'')\,df''}\right) \quad . \tag{129}$$

First of all we can check, that at $y = y_0$ $I_0 \to 1$, and we have $\delta(\Gamma-\Gamma_0)$. However the expression (129) is not suitable to work with. It is better to introduce the new integration over parameter μ, since

$$\int\frac{d\mu}{\mu}\,e^{\mu(f'-f)} = \theta(f'-f)$$

and introduce new variables $f_+ = f' - f - 1$, and $f_- = f' - f$. After that, the result is

$$G_y\left(y-y_0,\,\Gamma-\Gamma_0\right) = \sqrt{\frac{q_0^2}{q^2}}\int\int\int df_+\,df_-\,\frac{\Gamma_0}{\mu}\,e^{-\left(\frac{\Gamma+\Gamma_0}{2}-\mu\right)f_-}\,.$$

$$.\,e^{\left(\frac{\Gamma-\Gamma_0}{2}\right)f_+}\,I_0\left(2\sqrt{\left(y-y_0\right)\frac{4N}{b}\int_{\frac{f_+-f_-}{2}}^{\frac{f_++f_-}{2}}\chi(f'')\,df''}\right) \tag{130}$$

All contours here are located to the right of all singularities.

For $y - y_0 \gg 1$ we can find in eq. (130) the diffusion solution. Indeed, let us suppose that $f_- \ll f_+ \ll 1$. In this case we can use the expansion (113) for the kernel, and asymptotics for I_0 in eq. (130). Finally,

$$G_y\left(y-y_0, \Gamma-\Gamma_0\right) = \int\int\int df_+\, df_-\, d\mu\, \frac{1}{\mu} \cdot$$

$$e^{-\left(\frac{\Gamma+\Gamma_0}{2} - \mu\right) f_- + \left(\frac{\Gamma-\Gamma_0}{2}\right) f_+ - \frac{1}{2}\left(\Gamma-\Gamma_0\right)}$$

$$e^{2\sqrt{\left(y - y_0\right)\omega_0\,\Gamma_0}\left(1 + \frac{\Delta f_+^2}{8}\right)\sqrt{f_-}} \quad . \qquad (131a)$$

The saddle point can be found from the following equations :

$$\frac{\Gamma - \Gamma_0}{2} - \frac{\Delta}{4} 2\sqrt{\left(y - y_0\right)\omega_0\,\Gamma_0}\sqrt{f_-^0}\, f_+^0 = 0 \qquad (132a)$$

$$-\left(\frac{\Gamma+\Gamma_0}{2} - \mu\right) + \frac{1}{2}\frac{1}{\sqrt{f_-^0}} 2\sqrt{\left(y-y_0\right)\omega_0\,\Gamma_0}\left(1 + \frac{1 + \Delta f_+^{0\,2}}{8}\right) = 0 \; .$$

From eq. (132) we can find f_-^0 and f_+^0, namely

$$f_-^0 = \left[\frac{\sqrt{\left(y - y_0\right)\omega_0\,\Gamma_0}}{\left(\frac{\Gamma + \Gamma_0}{2} - \mu\right)}\right]^2$$

$$f_+^0 = -\left(\frac{\frac{\Gamma - \Gamma_0}{2}}{\frac{\Delta}{2}\sqrt{\left(y - y_0\right)\omega_0\,\Gamma_0}\sqrt{f_-^0}}\right) \; . \qquad (133a)$$

Taking the integral (131) over f_+ and f_- by steepest descent method, we get the diffusion answer, namely

$$\frac{1}{\sqrt{q^2}}\int\frac{d\mu}{\mu}\, e^{\frac{\left(y-y_0\right)\omega_0\Gamma_0}{\left(\frac{\Gamma+\Gamma_0}{2} - \mu\right)} - \frac{\left(\Gamma-\Gamma_0\right)^2\left(\frac{\Gamma+\Gamma_0}{2} - \mu\right)}{4\Delta\omega_0\left(y-y_0\right)_0^{\Gamma}}} \qquad (131)$$

Since our function falls down at $\mu \to \infty$, we can take the pole (μ = 0) contribution and finally

$$G_\Gamma\left(y-y_0, \Gamma-\Gamma_0\right) = \frac{1}{\sqrt{q^2}} \cdot \frac{1}{\sqrt{\pi\Delta\omega_0\left(y - y_0\right)}}\, e^{\frac{\omega_0\Gamma_0}{\frac{\Gamma+\Gamma_0}{2}}\left(y-y_0\right)}$$

$$\cdot\, e^{-\frac{\left(\Gamma-\Gamma_0\right)^2\left(\frac{\Gamma+\Gamma_0}{2}\right)}{4\Delta\omega_0\Gamma_0\left(y-y_0\right)}} \quad . \qquad (132)$$

So eq. (132) gives just the diffusion answer in which $\alpha_S(\Gamma_0)$ changes and α_S depends on $\frac{\Gamma + \Gamma_0}{2}$: ($\alpha_S(\Gamma_0) \to \alpha_S(\frac{\Gamma_0 + \Gamma}{2})$). Now let us discuss when eq. (132) would be valid. The condition for that is $f_-^0 << f_+^0 << 1$, or

$$\frac{2}{\Delta}\left(\frac{\Gamma - \Gamma_0}{2}\right) << \frac{\Gamma + \Gamma_0}{2} \qquad (133)$$

Since eq. (133) should be valid for all $(\Gamma - \Gamma_0)$ of the order of

$$\left(\frac{4\Delta\,\omega_0\,\Gamma_0(y-y_0)}{\frac{\Gamma+\Gamma_0}{2}}\right)^{1/2}$$ it induces the restriction for $y - y_0$, namely

$$\left(\frac{4\Delta\,\omega_0\,\Gamma_0\left(y-y_0\right)}{\frac{\Gamma+\Gamma_0}{2}}\right)^{1/2}\frac{2}{\Delta} \ll \frac{\Gamma+\Gamma_0}{2}$$

or

$$\frac{16\,\omega_0\,\Gamma_0\left(y-y_0\right)}{\Delta} \ll \left(\frac{\Gamma+\Gamma_0}{2}\right)^3$$

or

$$\frac{\omega_0\,\Gamma_0\left(y-y_0\right)}{\frac{\Gamma+\Gamma_0}{2}} \ll \frac{\Delta}{16}\left(\frac{\Gamma+\Gamma_0}{2}\right)^2 . \qquad (134)$$

So, you see, that once more we got some restriction for the kinematical region where we can prove the diffusion formula, but now constraint (134) depends on running virtuality, but not only on initial one. However, eq. (134) gives the condition when we can use the steepest descent method for integral (131). We made some assumption to receive eq. (131) from eq. (130), namely, we assumed that f_- and f_+ are small enough to expand $\chi(f'')$ in seria. It should be stressed, that we used such an expansion for function in exponent. So the condition when we can use such an expansion is

$$\frac{5}{8}\Delta\,2\left(\omega_0\,\Gamma_0\left(y-y_0\right)\right)^{1/2}\sqrt{f_-^0}\,f_-^{0\,2} \ll 1$$

$$2\left(\omega_0\,\Gamma_0\left(y-y_0\right)\right)^{1/2}\sqrt{f_-^0}\,f_-^{0\,3} \ll 1 . \qquad (135)$$

The first from eqs. (135) gives

$$\frac{5}{8}\cdot 2\Delta\left(\omega_0\,\Gamma_0\left(y-y_0\right)\right)^{1/2}\left(\frac{\sqrt{\omega_0\,\Gamma_0\left(y-y_0\right)}}{\frac{\Gamma+\Gamma_0}{2}}\right)^5 \ll 1$$

or

$$\Delta\left(\omega_0\,\Gamma_0\left(y-y_0\right)\right)^3 \ll \left(\frac{\Gamma+\Gamma_0}{2}\right)^5$$

or

$$\omega_0\,\Gamma_0\left(y-y_0\right) \ll \frac{1}{\Delta^{1/3}}\left(\frac{\Gamma+\Gamma_0}{2}\right)^{5/3} . \qquad (136)$$

Eq. (136) is stronger than eq. (134).

The second of eqs. (135) leads only to trivial restriction, namely,

$$\frac{\omega_0\,\Gamma_0\left(y-y_0\right)}{\frac{\Gamma_0+\Gamma}{2}} \gg 1 . \qquad (137)$$

Let us estimate the condition (136) for standard case $q_0^2 = 5$ GeV^2 and $\Lambda = 100$ MeV, for $\Gamma \to \Gamma_0$ we have

$$y - y_0 \leqslant 3 \qquad (138)$$

but for $q^2 = 10^3$ eq. (136) gives us

$$y - y_0 \leq 16 \qquad (139)$$

while eq. (137) leads to

$$y - y_0 \geqslant 2 \quad . \qquad (140)$$

Thus, in G_y we have sufficiently large kinematical region for diffusion in $\ell n\, q_+$. Of course solution (130) contains much more information about Green function that we have discussed. However, analysis of this solution looks to be complicated enough, so I prefer to stop this discussion namely at this point.

Really these two Green function contain the answers on all questions, but analysis of so cumbersome expression cannot be transparent from physical point of view. To this reason, I would like to consider quite different method of solution, which has restricted accuracy, but looks very simple and can be applied to search of the solution for non linear equation. The last point is especially important for us, because we should consider the shadowing corrections that lead to non linear equation.

7. The trajectory method

In this section I would like to discuss the trajectory method of solution, which is valid only for semiclassical approach. Let us try to find solution in semi classical form, namely

$$\varphi = C\, e^{\omega(\Delta\Gamma)y - K(\Delta\Gamma)\Gamma} = e^{\Psi} \quad . \qquad (141)$$

Eq. (141) has a good chance to describe the solution of our LL(x)A equation only if $\frac{\Delta K}{K} << 1$ and $\frac{\Delta\omega}{\omega} << 1$.

Using eq. (141) we can introduce two sets of remarkable lines.

The first is so-called phase trajectory, or the set of lines on which the phase ψ of solution (141) are constant. It means that the points (y_1, Γ_1) and (y_2, Γ_2) are on the same phase trajectory if

$$\omega(\Delta r)\, y_1 - K(\Delta r)\, r_1 = \psi_1$$
$$\omega(\Delta\Gamma)\, y_2 - K(\Delta\Gamma)\, \Gamma_2 = \psi_2 \quad \text{and } \psi_1 = \psi_2 \quad .$$

So

$$U_{ph} = \frac{\Gamma_1 - r_2}{y_1 - y_2} = \frac{\omega(\Delta\Gamma)}{K(\Delta\Gamma)} \quad . \qquad (142)$$

Of course, we assume that Γ_1, y, and Γ_2, y_2 are close to each other.

Another set of characteristic lines is the group trajectories. The maximum of the packet propagates along these trajectories, so $\frac{d\psi}{d\Delta r} = 0$ for them, or

$$\frac{d\omega}{d\Delta r} y_1 - \frac{dK}{d\Delta\Gamma}\Gamma_1 = 0$$
$$\frac{d\omega}{d\Delta\Gamma} y_2 - \frac{dK}{d\Delta\Gamma}\Gamma_2 = 0$$

for different "times" y_1 and y_2.

Directly from above equation we can calculate the group velocity, which is

$$U_{g\Gamma} = \frac{r_1 - \Gamma_2}{y_1 - y_2} = \frac{\frac{d\omega}{dr}}{\frac{dK}{d\Gamma}} = \frac{d\omega}{dK} \quad . \qquad (143)$$

Now let us find, what means our equation (104) for the semiclassical solution (141). Since

$$\int K(q', q)\, e^{(K-1)\Gamma'}\, d^2q' = \chi(1 - K)\, e^{(K-1)r} \qquad (144)$$

for function K which is almost constant for $\Gamma' - \Gamma \sim 1$ inside the integral (144), we have

$$\omega = \frac{N_c\, \alpha_S\left(q^2\right)}{\pi}\, \chi(1 - K) \qquad (145)$$

directly from eq. (104).

The second equation for K we can easily get on the group trajectory, namely

$$\left.\frac{dK}{dy}\right|_{g\Gamma} = \frac{\partial K}{\partial y} + U_{g\Gamma}\frac{\partial K}{\partial \Gamma} = -\frac{\partial}{\partial y}\left(\frac{1}{\varphi}\frac{\partial \varphi}{\partial r}\right) + \frac{\partial \omega}{\partial K}\frac{\partial K}{\partial \Gamma} =$$

$$= +\frac{1}{\varphi^2}\frac{\partial \varphi}{\partial y}\frac{\partial \varphi}{\partial \Gamma} - \frac{1}{\varphi}\frac{\partial}{\partial \Gamma}(\omega\varphi) + \frac{\partial \omega}{\partial K}\cdot\frac{\partial K}{\partial \Gamma} = +K\omega - \frac{\partial \omega}{\partial \Gamma} - \omega K + \frac{\partial \omega}{\partial K}\frac{\partial K}{\partial r} =$$

$$= -\left.\frac{\partial \omega}{\partial r}\right|_{K=\mathrm{const}} = \frac{N_c}{\pi}\frac{4\pi}{b\Gamma^2}\chi(1 - K) =$$

$$= \frac{N_c\, \alpha_S}{\pi\Gamma}\chi(1 - K)^2\, \frac{K}{\Gamma}\, U_{ph} \quad . \qquad (146)$$

Thus for semiclassical solution (141) we can write the system of equations :

$$\left.\frac{d\psi}{dy}\right|_{g\Gamma} = K\left(U_{ph} - U_{g\Gamma}\right) \qquad (147)$$

$$\left.\frac{dK}{dy}\right|_{gr} = \frac{1}{\Gamma}K\, U_{ph} \qquad (148)$$

$$U_{ph} = \frac{\alpha_S\, N_c}{\pi}\, \frac{\chi(1 - K)}{K} \qquad (149)$$

$$U_{g\Gamma} = -\frac{\alpha_S\, N_c}{\pi}\chi'(1 - K) \quad . \qquad (150)$$

The above system of equations gives us the possibility to calculate the value of φ in any points of the group trajectory if we know φ at initial r_0 and y_0.

To solve eqs. (147-150) we need to know $\psi(y_0, \Gamma_0)$ and $\psi'_r(y_0, \Gamma_0)$.

The main properties of solution are defined by the typical behaviour of the kernel $\chi(1 - K)$. At $K \to 1$ $\chi \to 1/1\text{-}K$, at $K \to 0$ $\chi \to 1/K$ and for $K \to 1/2$ $\chi(K) = \omega_0(1 + \Delta(K\text{-}1/2)^2)$. The full function $\chi(K)$ is shown in fig. 10. Directly from this figure we see that the difference between correct kernel and kernel of LL(q)A equation (1/K) is small, and would be important only for $|K - 1/2| \le 1/4$. Eq. (148) shows you that K increases along the trajectory. Let us estimate this increase numerically. Assume the worst case, that we started with $K = K_0 = 1/2$ at $q_0^2 = 5$ GeV ($\Lambda = 100$ MeV) or $\Gamma = \Gamma_0 = 6$. From eq. (148) we can calculate

$$\frac{dK}{dy} = 0.1 \quad .$$

So, two units in rapidity becomes enough to reach value $K = 0.75$ $(K_0 + \frac{dK}{dy}\Delta y)$ where the difference between LL(x)A kernel and LL(q^2)A one is negligible. The typical value of rapidity for one cell of LLA ladder is $\omega_0\Delta y \sim 1$ (or $\Delta y \sim 1/\omega_0$). For our example $\Delta y \sim 1.5$. It means that in real situation the main difference between LL(x)A and LL(q)A solution is concentrated in the first one or two ladder cells.

8. Comparison the solutions of LL(x)A and LL(q^2)A equations

The above discussion has explained yet why the difference between LL(x)A and LL(q^2)A is not very big. Let me summarize here the main arguments :

1) only in the several first cells of our LLA ladder we have typical f close to 1/2 ($\nu << 1$) where the correct kernel $\chi(f)$ differs from LL(q^2)A one (1/f).2) namely in the several first steps of our evolution the cut-off on transverse momentum is very important and decreases the value of kernel in comparison with $\chi(f)$ makes it closer to LL(q^2)A one. For example if cut-off Q_g is equal to q_0, the value of the kernel in the first cell is two times smaller that $\chi(1/2)$. It means that such cut-off can even reproduce the solution of LL(x)A which gives smaller value of the structure function than in LL(q^2)A equation.

The detail analysis of the trajectories and influence of the value cut-off Q_g on the solution one can find in ref. [11]. Much work is needed to understand the specific properties of LL(x)A equation, and I would like to draw your attention, that trajectory method allows us to understand the general properties of hadron production in deep inelastic processes. Indeed, trajectories really give us the kinematical parameter of the particles that are produced in the typical inelastic event for deep inelastic scattering. So trajectories give the structure the typical inelastic event in deep inelastic processes. I have no time to discuss this subject, and refer the reader to ref. [11] in which much more information could be found concerning dominant particle production in deep inelastic processes.

9. The conservation of energy

Here, I would like to mention the problem which is very important, in the case when we try to apply the LL(x)A equation to real structure function. This problem is the energy conservation. The point is that in LL(x)A we neglected the energy conservation

because the loss of energy is important only in the next to leading order. But practically, such conservation is very important. Indeed, roughly speaking the deep inelastic structure function grows as $\left(\frac{1}{x}\right)^{\omega_0}$. It means that the momentum of gluons (or their energy) is equal to

$$\int_b^1 x^{-\omega_0}\, dx = \frac{1}{1 - \omega_0} > 1$$

and because $\omega_0 \simeq 0.65$ for our so-called typical case $q_0^2 = 5$ GeV and $\Lambda = 100$ MeV, we see tremendous violation of the momentum conservation. Strictly speaking $\omega_0 \sim \alpha_S$ and this violation is of the order of α_S, but practically we face with the momentum violation in 2-3 times. Our hope is only one, that all this non conservation real concentrated in the first (or may be two first) cells of our ladder. So we can take this $O(\alpha_S)$ correction only renormalize in $(1/1-\omega_0^{-1})$ times our result. However, from point of view of the theory we should get the new equation which takes into account the energy conservation and may be other $O(\alpha_S)$ correction. It is very interesting, that the only way how we can do this job now, is only Monte Carlo simulation in which the energy conservation was taken into account (see refs. [10, 11]). The numerical solution shows that the idea about renormalization factor works, (see also ref. [12], where this problem was investigated in details).

Lecture 8 : Evolution equation at $x \to 0$

1. Equation

LL(x)A equation with running α_S describes all qualitative features the correct evolution equation in the region of low x. All insertions inside this LL(x)A ladder lead to loss at least one ℓn 1/x. For example, the quark square in fig. 11a has no log contribution over energy S_0. Indeed, each cell gives the contribution which is proportional to $S_i^{\sigma_i+\sigma_2-1}$ where σ_i is the spin of exchanging particles. So the diagram of fig. 11a is proportional to $A \sim S_1^1\, S_2^1 \ldots S_n^1 . S_0^0$, or for the cross section $\sigma \sim S_0^{-1}$ since S_1 $S_2 \ldots S_0 \equiv S$. Of course this property is the direct consequence of the value of spin. Thus, all contributions of $(\alpha_S\, \ell n\, q^2\, \ell n\, 1/x)^1$ and $(\alpha_S\, \ell n\, 1/x)^n$ type come from pure gluon diagrams, which are described by LL(x)A equation with running α_S. However, we should take into account also the contribution of $(\alpha_S\, \ell n\, q^2)^n$-type, because in the region where $\ell n\, 1/x \approx \ell n\, q^2$, such diagrams are essential and provide the correct matching procedure between LL(x)A and LL(q^2)A equations. Such job was done in ref. [1] and really that we needed for it, is to make some insertions of quark diagrams inside LL(x)A gluon ladder. Why ? The main property, which we used, is so-called factorization in Feynman diagrams. It means, that in diagrams of non ladder type, for example in diagrams of fig. 11b, the new integrations over the momentum K are not logarithmic and that the momentum K, which appears in the propagators of the K ladder rungs crossed by this gluon, kills all the logarithmic terms which could a priori appear in them through integration. So, the bloc outlined in fig. 11b can be considered as a pointlike (without any logs) correction α_s^n to the kernel of LL(x)A

equation. Thus, we should only improve our ladder to receive the correct evolution equation which takes into account both logs α_S $\ell n\, q^2$ and $\alpha_S\, \ell n\, 1/x$.

The resulting system of equation is shown in fig. 11c and can be written in the following form for

$$\varphi(\omega, q^2) = \int_0^1 \varphi(\ell n\, 1/x, q^2)\, x^\omega \frac{dx}{dx} \tag{151}$$

$$\varphi_G(\omega, q) = \int \left[\frac{4N\, K(q, q')}{\omega} \varphi_G(\omega, q') + \frac{4C_2}{q^2\omega} \varphi_F(\omega, q')\right] \frac{\alpha_S(q')}{4\pi} \frac{d^2q}{\pi}$$

$$+ \int_{q_0^2}^{q^2} \left[\Phi_G^G(\omega)\, \varphi_G(\omega, q') + \Phi_F^G(\omega)\, \varphi_F(\omega, q')\right] \frac{\alpha_S(q')}{4\pi} \frac{dq'^2}{q'^2}$$

$$\varphi_F(\omega, q) = \int_{q_0^2}^{q^2} \left\{\Phi_F^F(\omega)\, \varphi_F(\omega, q') + 2\, n_f\, \Phi_G^F(\omega)\, \varphi_G(\omega, q'^2)\right\} .$$

$$\frac{\alpha_S\left(q'^2\right)}{4\pi} \frac{dq'^2}{q'^2} \tag{152}$$

where $C_2 = \frac{N^2-1}{2N}$ and K_f is the number of quark flavours. K(q q') is the same, as for LL(x)A equation (see eq. (74)) we emphasize that from the point of view of the integration with respect to the transverse momentum q', the kernel K has been written down exactly.

The remaining kernels Φ_G^G, Φ_F^G, etc describe cells in which a logarithm of the transverse momentum arises but no ℓn 1/x term is present. These kernels are identical to the kernels of GLAP

equation if we subtract from that kernels the singularity $1/\omega$, which is already included in the kernel K. We have

$$\Phi^G_G(\omega) = \int_0^1 dZ \left[4N\left(Z - Z^2 - 2 + \frac{1}{1-Z}\right) Z^\omega - \frac{4n}{1-Z}\right] -$$

$$- \frac{2n_f}{3} + \frac{11N}{3} \to \frac{11N}{3} - \frac{2n_f}{3} \text{ at } \omega \to 0$$

$$\Phi^F_F(\omega) = C_2 \int_0^1 \left[\frac{2\left(1+Z^2\right)}{1-Z} Z^\omega - \frac{4}{1-Z}\right] dZ + 3\,C_2 \to 0 \text{ at } \omega \to 0$$

$$\Phi^G_F(\omega) = C_2 \int_0^1 dZ\, Z^\omega (2Z - 4) = -\,3\,C_2 \text{ at } \omega \to 0$$

$$\Phi^F_G(\omega) = \int_0^1 dZ\, Z^\omega \left(Z^2 + (1-Z)^2\right) \to 2/3 \text{ at } \omega \to 0 \quad . \qquad (153)$$

2. Solution of evolution equation

To solve eqs. (152) we still use the double Mellin transform (82) for both function φ_G and φ_F. It is easy to check that this solution has the form (see ref. [1] for details).

$$\varphi_{G,F} = \int \int \frac{df\, d\omega}{(2\pi i)^2} \bar{\varphi}^{(\omega)}_{G,F}\, r\, f^\gamma \ .$$

$$. \exp\left(\omega y + (f-1)\Gamma + \frac{4N}{b\omega} \int_f^{1/2} \chi(f')\, dt'\right) \qquad (154) \quad ,$$

and γ is given by equation :

$$\gamma^2 - \frac{\gamma}{b}\left[\frac{4N}{\omega} - \Phi^G_G - \Phi^F_F\right] = \frac{2n_f}{b^2}\Phi^F_G\left[\Phi^G_F + \frac{4\,C_2}{\omega}\right] + \frac{\Phi^G_G}{b^2}\left[\frac{4N}{\omega} - \Phi^F_F\right] \ . \qquad (155)$$

For $\omega \to 0$ we have the solution of eq. (155) in the simple form

$$\gamma \to -\frac{1}{b}\left(\Phi^G_G + \frac{2n_f\, C_2}{N}\Phi^F_G\right) \qquad (156)$$

$\bar{\varphi}_F(\omega)$ and $\bar{\varphi}_G(\omega)$ connected by equation

$$\bar{\varphi}_F(\omega) = \bar{\varphi}_G(\omega) \frac{2n_f\, \Phi^F_G}{\frac{4N}{\omega} - \gamma b - \Phi^F_F} \ . \qquad (157)$$

The solution (154) together with eqs. (155-157) looks rather complicated but really, all improvements in comparison with LL(x)A lead to factor f^γ in eq. (154). So the main qualitative, even quantitative properties of solution of LL(x)A equation with running α_S, that have been discussed in the previous lecture remain to be the same for correct equation. I do not want to repeat them once more.

3. Accuracy of the equation

Let us discuss, in what kinematical region we can use the system (152) and what the accuracy of the solution (154). Of course, it means that we should discuss the influence on the equation and its solution the higher order corrections. Factorization property of Feynman diagrams says us that α^n_S corrections are local and can be interpreted as the corrections to

the kernel of our equation. This correction gives new part of our kernel $\bar{K}(q, q')$, so the resulting kernel can be written as

$$K(q, q') = K_{LLA}(q, q') + \alpha_S \bar{K}(q, q') \quad . \tag{158}$$

It should be stressed that $\bar{K}$ is of course quite different function in comparison with $K_{LLA}(q, q')$ (see eq. (74)), but it is still homogeneous function of the following type

$$\bar{K}(q, q') = \frac{1}{q'^2} \mathcal{H}\left(\frac{q'}{q}\right) \quad .$$

It means that the kernel $\chi(f)$ in our solution can be also replaced by expression $\chi(f) + \alpha_S \bar{\chi}(f)$. As has been discussed at fixed virtuality our solution behaves as $(\frac{1}{x})^{\alpha_S \chi(1/2) + \alpha_S^2 \bar{\chi}(1/2)}$. We can express this result as

$$\frac{\Delta\varphi}{\varphi} = e^{\alpha_S^2 \, y \, \bar{\chi}(1/2)} \quad . \tag{159}$$

The formula (159) shows that higher order correction to our solution is small only when

$$\alpha_S^2 y << 1$$

or

$$y << \ell n^2 q^2 \quad . \tag{160}$$

So in the whole region to the right of the curve $\varphi \sim \ell n^2 q^2$ we can guarantee the solution but within accuracy

$$\varphi = \left(1 + O\left(\alpha_S^2 \, \ell n \, 1/x\right)\right) \varphi_{LLA} \tag{161}$$

where φ_{LLA} is the solution of eq. (154).

I would like to draw your attention to the fact that eq. (161) looks at least strange from old "additive" point of view. Indeed, we can write φ as a series in $\alpha_S \, \ell n \, q^2$, $\ell n \, 1/x$:

$$\varphi = \sum_n \left(\alpha_S^n \sum_{K,m=0}^{n} \ell n^K \, 1/x \, \ell n^m \, q^2\right) \tag{162}$$

and corrections to this seria at first sight looks quite the same to lose both logs in one cell, to lose only $\ell n \, q^2$ but in two cells. For example $\alpha_S^3 \, \ell n^2 \, 1/x \, \ell n^2 \, q^2$ can come as α_S contribution in one cell, and $\alpha_S \, \ell n \, 1/x \, \ell n \, q^2$ in two others, and also $\alpha_S \, \ell n \, 1/x \, \ell n \, q^2$ contribution in one cell, $\alpha_S \, \ell n \, 1/x$ in another and $\alpha_S \, \ell n \, q^2$ in the third cell. We claim that the most important contributions namely the last two, but the first we consider as corrections of the order of α_S to the last two contributions. Strange ! Is not it ?

The answer to this apparent paradox is that we do not use an "additive", but a "multiplicative" approach to the corrections as follows from eq. (161). This approach is possible due to the factorization of the corrections, as we have discussed above, any correction (except multiladder ones discussed below) can be written as next order corrections to the kernel of our ladder and its contribution reads $\Delta\varphi$ = (something) φ. If this "something" is small (as it happens for $\ell n \, 1/x << \ell n^2 \, q^2$) the contribution of such a correction is small as compared to the large value of φ, though it can be quite large from point of view of "additive" expression (162). Thus, the most important idea in our approach is the new understanding the problem of the accuracy of our approach. Namely this new idea (see ref. [1] for details) allows us to formulate the linear evolution equation which is correct to the right of the curve

$\ell n\ 1/x \sim \ell n\ q^2$ (see fig. 11d). This approach we called LL(x)A + LL(q)A.

Lecture 9 :
Shadowing corrections in Deep Inelastic Scattering (violation of S-channel unitarity and qualitative picture of screening in DIS)

In previous lectures I covered the situation with so-called evolution equation in deep inelastic processes. Here I would like to discuss the shadowing corrections in the same process. The first problem which we face in LLA looks very unpleasant indeed the solution of LLA equation violates the S-channel unitarity, since in perturbative QCD the interaction amplitude grows very rapidly at high energy. Indeed, at low x, our φ is proportional

$$\varphi \sim \frac{1}{q} \frac{1}{\sqrt{\pi \Delta \omega_0 y}} e^{\omega_0 y - \frac{\Gamma^2}{4\Delta\omega_0 y}} \quad \text{for LL(x)A equation or}$$

$$\varphi \sim \frac{1}{q^2} e^{\sqrt{\frac{6N}{b} \ell n\, \Gamma y}} \quad \text{for LL(x) A equation} \quad .$$

It is the common property for the both above solution ; that φ increases very rapidly at $x \to 0$.

The total cross section of virtual γ-quantum absorption (in electron deep inelastic scattering, for example) is proportional to

$$\sigma_{\gamma^*} = \frac{\alpha_{em}}{q^2} F\left(x, q^2\right) = \frac{\alpha_{em}}{q^2} \int_{q_0^2}^{q^2} \varphi\left(x, q'^2\right) dq'^2 = \alpha_{em}\, \varphi\left(x, q^2\right) \quad .$$

Thus, we see that at small x

$$\sigma_{\gamma^*} = \alpha_{em}\, \varphi\left(x, q^2\right) \geq \sigma_n = \pi R_h^2 \qquad (163)$$

where R_h is the radius of a proton.

Equation (163) is even stronger, since really instead of α_{em} α_S stands here, see ref. [1] for detail discussion. However for qualitative discussion such subtle question does not matter.

Value of $x_{c\Gamma}$ is different for different LLA equations, namely, $x_{c\Gamma} \sim \ln q^2 \ln q_0^2$ for LL(x)A equation and $x_{c\Gamma} \sim \ln^2 q^2/\ln \ln q^2$ for LL(q^2)A one. However both of them tell us that inequality (163) occurs at sufficiently large virtualities. Virtualities are large but smaller than $e^{\sqrt{ay}}$ or $\Gamma^2 \leqslant ay$, so we can apply for them the LLA equations.

Thus we face the inequality (163) at so large virtualities, where we are sure, that the unknown confinement forces cannot change the behaviour of the amplitude. Therefore, we must find some correction to the LLA within perturbative QCD (α_S is still smaller than unity ($\alpha_S << 1$) for virtualities, when the constraint (163) works) that will save unitarity.

To understand what phenomena we missed in LLA, let us consider the picture of the parton cascade for a fast hadron (see fig.12a). Even the first glance on picture in fig. 12a shows us the number of partons becomes extremely large since each parton can decay in many daughters partons. To clarify the situation with LLA, let us consider the parton distribution in the transverse plane. At $x \sim 1$ we see only several partons that are distributed in the hadron disc. So the distance between partons is larger than the proper size of them. It means, that we can neglect the interaction between quarks and gluons. Thus the only emission of gluons are essential and, namely, this property of parton cascade was basical for LLA evolution equation. However for smaller x the number of partons increases and at some value of $x = x_{c\Gamma}$ partons become to populate densely in the whole disc of hadron. For $x < x_{c\Gamma}$ quarks and gluons must overlap spatially and begin to interact in a whole disc that they occupy. For such small x the processes of the annihilation and recombination of partons should be essential as well as emissions of gluons. Thus the structure of the parton cascade at small x

should be result of competition of two main processes : the emission of gluon that is proportional to the parton density (φ) and the annihilation of parton which depends only on φ^2. In the last processes the number of partons is decreased and this property allows us to restore unitarity. It occurs at the value of φ when the annihilation becomes comparable with the emission. In other words, when $\varphi = v\,\varphi^2$ where v is the typical interaction volume, which is the new phenomenological parameter for the parton cascade. Of course the resulting parton density φ should be of the order of 1/v (see fig. 12b).

Naturally, this is only qualitative picture of the parton cascade, but even it gives us the understanding what was missed in LLA. Indeed, in LLA we usually omitted the interaction of partons. So our conclusion from this primitive parton picture is that for small x we have to take into account new phenomena, namely the recombination of partons, which could save and really save the unitarity (see ref. [1]). Even more, this qualitative picture allows us to estimate the value of $x_{c\Gamma}$. Indeed, let us introduce the new parameter

$$W = \frac{\alpha_S}{q^2}\,\frac{x\,G\left(x, q^2\right)}{\pi R_h^2} = \frac{\alpha_S\,\varphi}{\pi R_h^2}\,. \qquad (164)$$

In eq. (164) $x\,G\left(x, q^2\right)$ is the number of partons and the ratio $\frac{x\,G(x\,q^2)}{\pi R_h^2}$ is the density of partons in the transverse plane. The first factor in eq. (164) is nothing more than the cross section of quark interaction (recombination) inside of the parton cascade. Thus the parameter W has a very transparent. physical meaning, namely, it is the probability of interaction (recombination) of two quark inside the parton cascade. The unitarity constraint

$$W \leqslant 1 \quad \text{or} \quad \frac{\alpha_S \, x \, G\left(x \, q^2\right)}{q^2} < \sigma_n \tag{165}$$

means that the probability of the interaction of two partons should be smaller than unity. Let us estimate at what value of $x = x_{c\Gamma}$ W becomes of the order of unity. Indeed

$$W = \frac{\alpha_S \, x \, G\left(x \, q^2\right)}{q^2 \, \pi \, R_h^2} \approx \frac{\alpha_S \left(x \, G\left(x, q^2\right)\right)_{LLA}}{\pi \, R_h^2} \approx 1 \quad . \tag{166}$$

If we put the solution of LL(x)A in eq. (166), we see

$$\frac{\alpha_S \, x^{\omega_0(q^2)}}{q^2 \, \pi \, R_h^2} \approx 1 \, , \quad \text{or} \; \alpha_S\left(q^2\right) \ell n \, 1/x \approx \ell n \, q^2 \tag{167}$$

since $\omega_0(q^2) \sim \alpha_S(q^2)$. Eq. (167) means that

$$\ell n \, 1/x_{c\Gamma} \sim \ell n^2 \, q \quad . \tag{168}$$

It is worthwhile mentioning, that $x \, G(x, q^2) \sim x^{\omega_0}$ looks very natural in such parton picture (see fig. 12c). Indeed, the multiplicity of the "wee" partons that interact with the target (N) is proportional

$$N \sim e^n \tag{169}$$

where n is the number of steps in our diffusion (number of the cells in LLA ladder), which is the order of $n = \omega_0 y = \omega_0 \, \ell n \, 1/x$. So we can read eq. (169) as

$$N \sim e^{\omega_0 y} \sim e^{\omega_0 \ell n 1/x} = \left(\frac{1}{x}\right)^{\omega_0} \quad . \tag{170}$$

So from the parton point of view the increase of the total cross section is closely related to increase of the multiplicity of "wee" partons. The same increase reveals itself in the parton recombination which becomes essential at $x \leqslant x_{c\Gamma}$.

Thus, I hope, that I have convinced you that is the region of small $x \leq x_{c\Gamma}$ we faced new problem, namely, large screening corrections due to parton recombination inside parton cascade. However, the above qualitative discussion can be only the basis of our intuition rather than the way of correct calculation. Perhaps, it is even some problem for us that we could not transform such transparent picture directly in the equations. Of course, if it will happen, it will lead us to deeper understanding of the problem. We went the other way, and developed new reggeon like technique in QCD to penetrate in the region where the parton interaction becomes essential. The short presentation of the main ideas of this approach will be the subject of the next lecture.

Lecture 10 : Reggeon-like diagram technique in QCD

The main idea of our approach to the problem of shadowing (screening) corrections in deep inelastic scattering processes is to use two small parameters, namely

$$\alpha_S\left(q^2\right) < 1$$

$$W = \frac{\alpha_S}{q^2} \cdot \frac{x\, G\left(x\, q^2\right)}{\pi\, R_h^2} < 1 \qquad (171)$$

(or $\alpha_S\, \varphi/\pi\, R_h^2 < 1$)

as we have discussed, for $y << \Gamma^2$ the main contributions give so-called ladder diagrams or, better to say, diagrams which correspond the linear evolution equation. I tried to convince you that all other contributions are small of the order of

$$\frac{\Delta\varphi}{\varphi_{LLA}} \sim \alpha_S^2\, y \ . \qquad (172)$$

However, when y tends to Γ^2 we can study these corrections and extract among them such contributions which are the most important. We claim that the most important contributions lead to corrections

$$\frac{\Delta\varphi}{\varphi_{LLA}} \sim \alpha_S \frac{\varphi_{LLA}}{\pi\, R_h^2} \approx W \qquad (173)$$

and we developed the technique to calculate these contributions. Corrections (173) are large due to the large value of φ_{LLA} at small x, namely the idea to use this large value of the solution of LLA

equation was the most important and absolutely new idea which led to new, modified evolution equation.

Technically, we developed the reggeon-like technique to calculate the corrections of the order of W^n. It means the corrections of the eq. (173) type we can calculate using the following prerscription. We can consider the LLA("ladder") diagrams and their interaction only introducing new vertices for "ladder" interactions which we are able to calculate in framework of perturbative QCD. The above long sentence really contains the main ideas of our reggeon-like diagram technique. However I would like to draw your attention to the fact that this sentence contains at least two non trivial statements. First one, we proclaim that we can introduce vertices which are local in rapidity and transverse momemtum. This is not trivial, and the hot discussion in our institute especially with L.N. Lipatov showed that even such local vertices do not apparently exist in the region $y >> a\Gamma^2$. The second statement is that our integration over transverse momentum is concentrated in the region of sufficiently large transverse momenta where we are able to use perturbative QCD to calculate these vertices. Of course, even in these lectures I have no time to discuss the prove of the diagram technique in very details. However, I shall try to show you the main way of thinking that leads to this technique and reopen the hidden assumption that we usually made to prove this way of calculation.

1. The simplest diagram

Let us consider the simplest diagram of fig. 13a to illustrate the reggeon-like technique in QCD and to show the difference from usual reggeon technique (or Reggeon Calculus).

The full expression for these diagrams looks as follows using the notation shown in fig. 13a.

$$\varphi^1 = \int dK^2\, dK'^2\, \frac{d\ell^2}{\ell^2}\, \frac{dm^2}{m^2}\, \frac{d\ell'^2}{\ell'^2}\, \frac{dm'^2}{m'^2}\,.$$

$$\int d^2Q_t\, \alpha_S\left(K^2\right)\, \alpha_S\left(K'^2\right)\, \int dy'\, dy''$$

$$\varphi\left(y-y',\, q'^2,\, K^2\right)\, \varphi\left(y'-y'',\, m^2,\, m'^2,\, Q_t^2\right)$$

$$\varphi\left(y'-y'',\, \ell^2,\, \ell'^2,\, Q_t^2\right) \cdot \varphi\left(y'',\, K'^2,\, q_0^2\right)$$

$$\gamma\left(\frac{K^2}{\ell^2},\, \frac{K^2}{m^2},\, \frac{Q_t^2}{K^2}\right) \gamma\left(\frac{K'^2}{\ell'^2};\, \frac{K'^2}{m'^2};\, \frac{Q^2}{K'^2}\right)\,. \qquad (174)$$

Here we introduced the local vertex γ for triple "ladder" interaction, the fact that γ depends on ratio of virtualities is evident directly from dimensionless character of QCD. Of course, I am going to discuss the explicit expression for γ a little bit below. $\varphi(y, m^2, m'^2, Q_t^2)$ and $\varphi(y, \ell^2, \ell'^2, Q_t^2)$ are also new elements we have not discussed them yet. These φ's are related to deep inelastic scattering amplitude but not at the angle (transferred momentum) equal to zero. Roughly speaking the main properties of $\varphi(y-y', m^2, m'^2, Q_t^2)$ are

1. the exponential increase in y, namely,

$$\varphi \sim e^{\Delta(y-y')}\, \tilde{\varphi}(m, m') \quad \text{for } Q_t^2 \le m'^2 \qquad (175)$$

where $\Delta \equiv \omega_0 \sim \alpha_S\left(m'^2\right)$.

2. φ does not depend on Q_t^2 (as seen from eq. (175)) if $Q_t^2 \leqslant m'^2$. Indeed, in our "ladder" all vertical lines carry momenta m_{it} + Q_t. So if Q_t is much smaller than each m_{it} our "ladder" cannot feel its value.

3. Rapid decrease of φ for $Q_t^2 >> m'^2$. Indeed, if $Q_t > m_{it}$ namely Q_{it} plays the role of the minimal virtualities and it is enough, if $Q_t > m'_t$, (m'^2_t is the minimal virtualities in the "ladder") but smaller than all other virtualities to provide the rapid decrease of φ, since $\varphi \sim \frac{1}{m'^2} \approx \frac{1}{Q_t^2}$. More detail analysis of Q_t dependence you can find in ref. [1].

In eq. (179) the dependence of the vertices on the virtualities ℓ^2, m^2, ℓ'^2, m'^2 is also new in comparison with the usual reggeon calculus.

Using eq. (175) we can calculate the integral over y' and y" and it is easy to see that the dominant contribution comes from the region $y-y' \sim 1$ and $y''-y_0 \sim 1$ at least at first sight. It means that the diagram of fig.13a is reduced to unenhanced diagram of fig. 13b which is of the order of

$$\varphi^{(1)}(\text{fig. 13b}) = q_0^2\, \varphi^2\left(q^2,\, y-y_0\right) = \frac{q_0^2}{q^2}\, x\, G\left(x,\, q^2\right) \varphi \qquad (176)$$

so

$$\frac{\Delta\varphi}{\varphi_{LLA}} = \frac{\varphi^{(1)}(\text{fig. 13b})}{\varphi_{LLA}} = \frac{q_0^2}{q^2}\, x\, G\left(x\, q^2\right) \qquad (177)$$

and thus this contribution is still small for all $y = \ell n 1/x < \ell n \frac{2q^2}{q_0^2}$.

However eq. (176) shows us that we can get even larger contribution from the diagram of fig. 13c type. Indeed, we lose

some contribution in rapidity region from y' to y, since $\varphi^2(y - y') >> \varphi(y - y)$ but for $y' << y$ we have the typical virtuality (χ^2) which is smaller, so our φ is larger since $\varphi \sim 1/K^2$. The contribution of the diagram of fig. 13c can be estimated as

$$\varphi^{(1)}(\text{fig. 13c}) = \int \varphi\left(y-y', q^2, K^2\right) \varphi\left(y', K^2, q_0^2\right) \cdot$$

$$\cdot\, \alpha_S \frac{q_0^2}{K^2} x' G\left(x', K^2, q_0^2\right) dy'\, dK^2 \quad . \qquad (178)$$

The factor q_0^2 in the nominator comes from integration in respect to Q_t in our basical diagram of fig. 13a. Integration in respect to K^2 we can estimate as

$$\varphi^{(1)} = \varphi\left(y, q^2, q_0^2\right) \cdot \int \alpha_S \frac{q_0^2}{K'(x)^2} x' G\left(x', K^2(K')\right) dy' \quad (179)$$

where we used that

$$\int \varphi\left(y-y', q^2, K^2\right) \varphi\left(y', K^2, q_0^2\right) dK^2 = \varphi\left(y, q^2, q_0^2\right)$$

and $K^2(x')$ is the typical transverse momentum in our LLA "ladder" for rapidity $y' = \ell n\, 1/x'$. So once more, we got that $\frac{\varphi^{(1)}}{\varphi} \sim W$, where

$W = \frac{\alpha_S\, x\, G\left(x, K^2\right)}{K^2 R^2}$ and $R^2 = 1/q_0^2$. Parameter W turns to be larger for "fan" diagram of fig. 13c, than for unenhanced diagram of fig. 13b. I would like to note also, that considering the

semienhanced ("fan") diagrams we also include in calculation of the region $y' \approx y$ in which such sort of diagrams transforms into unenhanced ones.

It should be stressed that in this diagram the new dimension phenomenological parameter $R^2 \sim 1/q_0^2$. As we discussed, this parameter defines the characteristic interaction volume or the correlation radius inside of our parton cascade.

2. The simplest "fan" diagram in DLA

To demonstrate the main ideas of the new reggeon-like diagram techniques, let us consider the simplest "fan" diagram of fig. 13c in DLA. The explicit form of DLA solution for $\varphi(y, q^2)$ looks simpler in the variable $\xi = \ell n \frac{\Gamma}{\Gamma_0}$ instead of $\Gamma = \ell n\, q^2/\Lambda^2$. Indeed, in ξ and y

$$\varphi(y, \xi) = \frac{1}{q^2} e^{\sqrt{\frac{16N}{b} y\xi}} \quad .$$

Putting the above expression inside the diagram we can reduce it to the form

$$\varphi_f(y, \xi) = \int dy_1\, \varphi\left(y-y_1, \xi-\xi_1\right) \cdot \gamma\, \varphi^2\left(y_1, \xi_1\right) \alpha_S^2\left(\xi_1\right) d\Gamma_1\, d^2Q_t$$

or

$$\varphi_f(y,\xi) \sim \frac{1}{q^2} Q_0^2 \int dy_1\, d\xi_1\, e^{\sqrt{\frac{16N}{b}\left(y-y_1\right)\left(\xi-\xi_1\right)}} \cdot e^{2\sqrt{\frac{16N}{b} y_1 \xi_1}} \cdot e^{-e^{\xi_1} - \xi_1} .$$

The integration over dy_1 and $d\xi_1$ can be performed by the steepest descent method. You can easily see, that we have the saddle point with

$$\xi_1^0 = \frac{1}{2} \ln y/\xi << \xi$$

and

$$y_1^0 = 4 \cdot \frac{16N}{b} \frac{y}{\xi} \ln \frac{y}{\xi} < y .$$

In the kinematical region where $y >> \xi$ we can find the contribution of this diagram, which is equal to

$$\varphi_f \sim \frac{1}{q^2} Q_0^2/\Lambda^2\, e^{\sqrt{\frac{16N}{b} y\xi}} \cdot e^{\left(\frac{3}{4}\sqrt{\frac{16N}{b} y/\xi}\right)\ln(y/\xi)} .$$

So from the above expression we see that :

1) this answer is large as compared to $\varphi(y, \xi)$ for $y >> \xi$.

2) the value of typical virtuality (q_1^2) in the vertex is large enough, so we can apply perturbative QCD here.

Of course, this calculation is of little practical use, because we can be very careful to use here DLA. However, even such simple example, shows us, the main qualitative features of our approach.

Of course, we should sum all the "fan" diagram in order to obtain the true answer. This will be done in the following sections.

3. Triple ladder vertex

Now let us consider the perturbative calculation of triple "ladder" vertex γ that appeared in our expression for reggeon-like diagrams.

This vertex was considered in ref. [1, 2], but only in ref. [12] all hidden assumptions were extracted, and final result was received in different kinematical regions.

I would like to draw your attention to the fact, that the value of γ is not well defined since we have the factor q_0^2 due to d^2Q_t integration which is pure phenomenological one. However, such a calculation should clear up how we can get γ which is local in rapidity.

Let us consider the Born diagram for process of diffraction dissociation in Deep Inelastic Scattering (see fig. 14a) in three jets (quark, antiquark and gluon). This diagram is the simplest one for triple "ladder" (Pomeron) interaction. As usually, let us use Sudakov variables, but instead of vector Q we introduce vector Q' for which $Q'^2 = 0$. So

$$q = \alpha Q' + \beta p + q_G, \quad S = 2(pQ')\, p^2 = Q'^2 = 0$$
$$Q' = Q + \beta_a p, \quad \beta_a = x_B = \frac{|Q^2|}{S} . \qquad (180)$$

For simplicity we use also specific axial gauge, namely $A_\mu p_\mu = 0$. So the gluon propagator looks as follow

$$\frac{d_{\mu\nu}(K)}{K^2} = \left[g_{\mu\nu} - \frac{K_\mu p_\nu + p_\mu K_\nu}{(pK)}\right]\frac{1}{K^2} \qquad (181)$$

$d_{\mu\nu}$ obeys the following properties :

$$p_\mu d_{\mu\nu} = 0 \quad . \quad Q'_\mu d_{\mu\nu} = -\frac{K_{t\nu}}{\alpha_K} - \frac{2\beta_K p_\nu}{\alpha_k} \approx K_{t\nu}/\alpha_K \qquad (182)$$

and also for $K^2 = 0$. $K_\mu d_{\mu\nu}(K) = 0$, $d_{\mu\nu} = 2$, $d_{\mu\nu}(K)\, d_{\nu\rho}(K) = d_{\mu\rho}$ we would like to calculate triple reggeon vertex (see fig. 14a) only in the kinematical region when

$$|Q^2| >> q_t^2 >> K_t^2,\ m_t^2,\ \ell_t^2 >> \mu^2$$

$$\alpha_1 \sim 1 >> \alpha_2 >> \alpha_K >> \alpha_1, \alpha_m$$

$$\beta_\ell, \beta_\mu >> \beta_Q \sim \beta_2 >> \beta_1 \quad . \qquad (183)$$

Here μ is some characteristic mass of our amplitude. As we discussed above, only longitudinal polarizations of gluons in t channel (vertical ones in fig. (14a)) give the contribution at x = 0. So, we can rewrite $d_{\mu\nu}(K)$ as

$$d_{\mu\nu} = \frac{p_\mu Q'_\nu + Q'_\mu p_\nu}{(pQ')} + g^\perp_{\mu 0} - \frac{K_\mu p_\nu + p_\mu K_\nu}{(pK)} =$$

$$\approx \frac{p_\mu Q'_\nu}{(pQ')} - \frac{p_\mu K_\nu}{(pK)} = -\frac{p_\mu K_{\nu t}}{(pK)} = -\frac{p_\mu K_{\nu t}}{\alpha_K\ S/2} \quad . \qquad (184)$$

Deriving eq. (184) we used that $Q'_\mu M_\mu(\ ) = 0$, where M_μ is the top part of our diagram. It is very easy to see that directly from Feynman rules for QCD, the vertices are equal

$$= \frac{-K_{t\mu}}{\alpha_K\ S/2} p_\nu F_{\mu\nu\rho} = -2 K_{t\rho} \qquad (185)$$

for emission of S-channel gluon from t-channel one and

$$p_\delta \Gamma_{\rho\delta\sigma}/(pQ') = 2\ \alpha_K\ g_{\rho\delta}$$

for interaction with the S-channel gluon.

We cannot restrict ourselves by consideration the only diagram of fig. 14a, and should take into account the two groups of analogous diagrams (see figs. 14b and 14c) in which the t-channel gluon ℓ or ℓ' touch each quark line. Let us consider once more the first one (fig. 14a). It is easy to see that this diagram depends on K_t in the following way.

$$M^a_{\mu\sigma} = \frac{K_{\mu t} K_{\sigma t}}{K^2} M_\mu(q, Q) \quad . \qquad (186)$$

Here μ is the polarization of gluon K emitted from quark-antiquark pair.

We can return to trick which was discussed in fourth lecture to understand why this amplitude gives such polarization. There I showed that we can use polarization $K_{t\mu}$ instead of p_μ if we act on $M_\mu(q, Q)$. M_μ is the amplitude that describes the emission of gluon K by quark-antiquark pair. It should be stressed also that in eq. (185) we used the kinematical restriction of eq. (183) since $q_t >> K_t$ we neglect the dependence on the K_t in $M_\mu(q, Q)$ in eq. (186)*) . Of course, we can express the amplitude for diagrams of figs. 14b and c in the same way, namely :

$$M^b_{\mu\sigma} = \frac{(K + \ell')_{t\mu} (K + \ell')_{t\sigma}}{(K + \ell')^2} M_\mu(q, Q)$$

$$M^c_{\mu\sigma} = \frac{(K - \ell')_{t\mu} (K - \ell')_{t\sigma}}{(K - \ell)^2} M_\mu(q, Q) \quad . \qquad (187)$$

---

*) Of course factor $K_{t\mu}$ describes the dipole emission of gluon in our kinematical region, where $K_t << q, Q$.

The square of the whole amplitude is equal to

$$|M\Sigma|^2 = |M^a + M^b + M^c + M^d| \quad . \qquad (188)$$

where $\mu^d = \mu^a$.

After integration over azimuthal angles we can easily calculate that the dependence on K, ℓ, and m can be factorized in the following form

$$(\Sigma M)^2 = R(K, \ell)\, R(K, m) \,.\, M_\mu(q, Q)\, M_\mu(q, Q)$$

where

$$R(K, \ell) = \theta\left(\ell^2 - K^2\right) + \frac{\ell^2}{K^2}\theta\left(K^2 - \ell^2\right) \quad . \qquad (189)$$

Finally, the photon dissociation cross section can be written in the form,

$$\frac{d\sigma^D}{dt}(\gamma^* \to q\bar{q}\, g) = 2\,\Sigma\, e_t^2 \frac{4\pi\,\alpha_{em}}{|Q^2|}\left(\frac{\alpha_S}{\pi}\right)^2\left(\frac{\alpha_S}{\pi}\right)$$

$$\times \frac{2\left(Z^2 + (1 - Z)^2\right)}{e^2\, m^2\, q_t^2}\varphi(\ell)\,\varphi(m) \,.$$

$$.\, d\ell_t^2\, dm_t^2\, d^2K_t\, dZ\, R\left(K_t, \ell_t\right) R\left(K_t, m_t\right) \frac{d\,\beta_K}{\beta_K} \quad . \qquad (190)$$

Comparing eq. (190) with eq. (179) we see that our triple "ladder" vertex is equal to

$$\gamma = R(K, \ell)\, R(K, m) \qquad (191)$$

all other factors in eq. (190) really in eq. (190) were included in functions φ's. Integration over $d\beta_K$ is the same as integration over dy'.

Of course eq. (190) corresponds the "fan" diagram of fig. 13c rather that eq. (174) but all deviations is clear. The problem here, is only one, we really calculated only process of diffraction dissociation, so we need to prove so-called AGK cutting rules to reconstruct the reggeon-like diagram from one process.

4. AGK-cutting rules

AGK-cutting rules[13] establishes the well known connection between different processes which can be described by the same ladder (reggeon) diagrams. For example the simplest two ladder diagrams (see fig. 15a) is responsible for quasielastic scattering (fig. 15b), multiparticle production of all particles in one ladder (fig. 15c) and also multiparticle production of particles in two ladder (with multiplicity in two times large than for diagram of fig. 15c) (see fig. 15d). The ratio between these different processes was proved in ref. [13] for Reggeon Calculus and equal

$$\text{Fig. 15b} : \text{Fig. 15c} : \text{Fig. 15b} = 1 : (-4) : (2) \quad . \qquad (192)$$

Formally speaking, AGK proved these cutting rules using assumption that all amplitudes fall down as function of virtualities at fixed energy (or x in the case of deep inelastic processes). For our ladder amplitude we have such decrease, but the problem is to prove that such decrease can provide us the convergency of all integrations. In ref. [1] we considered more direct way to prove AGK and saw that AGK cutting rules are correct at least in LLA. I do not want to reproduce here this sufficiently long calculation. However for us it is very important that the resulting contribution of our basical diagram of fig. 13 has sign minus. Namely, this sign provides the screening of the cross section in deep inelastic process.

Concluding this lecture I would like to make some resumé. Thus, we developed the diagram technique, in which

1. the main object is LLA ladder which plays the role of pomeron in usual Reggeon Calculus.

2. The interaction "pomeron" with "pomerons" and hadrons can be described by vertices which are local in rapidity.

3. The vertices can be calculated in perturbative QCD.

4. All rules for signs here are the same as in Reggeon Calculus, namely the exchange of two ladder gives you sign minus. Hence ladders lead to positive contribution and so on.

5. Each additional ladder exchange gives the smallness of the order of W.

It means that exchange of two "ladders" is of the order of W in respect to one "ladder" exchange, three ladders give W^2 contribution and so on.

The only difference is the fact that we cannot formulate the reggeon field theory, since all our amplitudes depend on virtualities (transverse momenta) and such integrations as well as the "ladder" propagator look very complicated.

Thus the answer on the question what diagrams are the most important in the kinematical region where the structure function becomes large is the following one. We should sum all "ladder" diagrams and interaction between ladders.

Lecture 11
Modified Evolution Equation

Thus, we faced very unpleasant problem. LLA violates unitarity and we should sum all interactions of our "ladders" (pomerons), using in some sense usual reggeon approach. Our experience shows us that such problem seems to be very complicated and could not be solved in microscopic way. At first sight, we can suggest now only phenomenological approach and our theory has a great chance to be degenerated in a lot of phenomenological models which are quite far from theoretical understanding of the problem. Frankly speaking, many of our colleagues were disappointed of such situation in old reggeon theory and left this field of high energy physics. So now, we reduce the pure theoretical problem of evolution equation in deep inelastic processes once more to sum of reggeon-like diagrams and once more we should sum all of them. The only thing encouraged us was the fact that we faced with this typical for "soft" processes problem at large transverse momentum where we could apply perturbative QCD. So we can make an attempt to solve this typical reggeon problem at large virtualities and have some answer which can tell us what could be natural in the region of small virtualities.

1. Equation

The main step to derive the new modified evolution equation has been made. Indeed, in the previous lecture I proved that the main contribution in deep inelastic processes gives so-called "fan" diagram of fig. 13c. Thus we should sum all LLA diagrams ("ladder") and all "fan" diagrams of fig. 15 type.

The equation that sums these diagrams has the form (see [1])

$$\frac{\partial\varphi}{\partial y} = \int \frac{N_c\,\alpha_S\left(q'^2\right)}{4\pi}\,\frac{d^2q'_t}{\pi}\,K(q,q')\,\cdot$$

$$\left\{1 - \alpha_S\left(q'^2\right)\,\frac{\varphi\left(q'^2\right)}{\varphi_0}\right\}\varphi\left(q'^2\right)\,. \qquad (193)$$

Fig. 16 shows how this equation generates the ladder and "fan" diagrams, in several orders of α_S. φ_0 can be expressed through the triple "ladder" vertex and value of q_0 or $R^2 = \int dQ_t^2$. Value φ_0 is really our new phenomenological parameter : so for us it is not very important to calculate φ_0 through R^2. However, since R^2 has some transparent physical meaning we can write this relation, namely

$$\varphi_0 = 16\pi\left(4\pi R^2\right)\frac{\sqrt{N_c^2 - 1}}{N_c}\,(1 - f)^2 \qquad (194)$$

where $\quad 1 - f = -\dfrac{\partial\,\ell n\,\varphi}{\partial\,\ell n\,q^2}\quad$ and $\quad 1/R^2 = \int dQ_t^2\,.$

I would like to draw your attention to the sign minus in front of the second term in eq. (193). This sign is the result of AGK cutting rules and leads to shadowing that stops the increase of φ in the region when φ becomes large. However this sign means that equation (194) has no probabilistic interpretation, at least we have not known such interpretation. It is very important to understand this point. Indeed, I discussed sufficiently simple and transparent physical picture of parton cascade in lecture 9. But up to now we have failed to write the equation directly from this picture. We had to classify diagram, extract some specific set of such diagrams and only after this job we were able to write equation in which we

introduce new phenomenological parameter that describes the interaction between partons inside the parton cascade. I think, that this is not the most compact and simplest way of discussing such physical phenomenon as parton-parton interaction, but only such derivation of the master equation (193) we have had.

Thus we cannot use the simplest probabilistic interpretation of function φ or structure function. We face also very practical difficulties. We cannot solve eq. (193) using Monte Carlo simulation due to above property. However namely this sign minus provides the Unitarity constraints, since the factor in the bracket becomes smaller when φ increase. This is the way how the equation restores unitarity.

2. High twist correction and screening

If you will look at the master equation more carefully, you shall see that this equation contradicts all ideas of theoretical description of deep inelastic processes. Indeed, our starting point for theoretical discussion of the behaviour of the deep inelastic structure function was the fact that DIS occurs at small distances where we can apply the methods of perturbative QCD since $\alpha_S << 1$ and so-called Wilson operator expansion for deep inelastic structure function. Wilson operator expansion means that we can write for deep inelastic structure function the following seria

$$F_2\left(x, q^2\right) = F_2^0\left(x, q^2\right)^{LLA+HO} + \frac{1}{q^2}F_2^1\left(x, q^2\right) + \frac{1}{q^4}F_2^2\left(x, q^2\right) + \ldots\,. \qquad (195)$$

Our main theoretical idea was that for large transferred momentum q^2 only the first term in the above seria survives and, namely, for this term we developed evolution equation in LLA and even can calculate the higher order corrections (see ref. [14] for example).

However, the nonlinear term in our equation means without any doubts that we take into account the high twist correction in evolution equation. Indeed, $\varphi = \frac{x\,G(x\,q)}{q^2}$, and it is clear that non linear term is suppressed as power $1/q^2$ in comparison with the first one. Thus we have direct contradiction with the traditional approach.

Of course, the solution of this puzzle is very simple. Indeed, let us rewrite the seria (195) in more traditional form, for moments of $F_2(F_2(\omega) = \int_0^1 x^\omega F_2(x, q^2)\frac{dx}{x})$

$$F_2\left(\omega, q^2\right) = F_2^0\left(\omega, \ell n\, q^2\right) + F_2^1\left(\omega, \ell n\, q^2\right)\ 1/q^2 + $$
$$+ F_2^2\left(\omega, \ell n\, q^2\right)\ 1/q^4 + \ldots \quad . \qquad (196)$$

As we discussed, for moment the solution of our evolution equation we can write in the form

$$F_2^2\left(\omega, q^2\right) = F^i\left(\omega, q_0^2\right) . e^{\gamma_i(\omega)\ell n \ell n q^2} \qquad (197)$$

where $\gamma(\omega)$ is so-called anomalous dimension. Really in old our approach was hidden assumption that $\gamma_i(\omega)$ could not be so large to compensate the power-like decrease in the seria (196). Now let us return to GLAP equation (or even to DLA equation). We saw that in DLA

$$\gamma_0(\omega) = \frac{4N}{b\omega} \qquad (198)$$

$\gamma_0(\omega)$ becomes very large at $\omega \to 0$. If $\gamma_1(\omega)$-$\gamma_0(\omega)$ remains to be large, this difference can compensate the smallness due to extra power of $1/q^2$. So the second twist can be important if

$$\frac{e^{\left(\gamma_1(\omega)-\gamma_0(\omega)\right)\ell n \ell n q^2}}{q^2} \to 1 \quad . \qquad (199)$$

Really in our equation we sum the diagram for which $\gamma_1 = 2\gamma_0(\omega)$. So in our case eq. (199) means $\frac{e^{\gamma_0(\omega)\ell n \ell n q^2}}{q^2} \sim 1$ or

$$\frac{4N}{b\omega_{c\Gamma}} = q^2/\ell n\, \ell n\, q^2 \quad . \qquad (200)$$

So at very small ω, our next twist contribution should be important. In $y = \ell n\ 1/x$ variables the condition (200) means that

$$F^0 = \int e^{\omega y + \gamma_0 \ell n \ell n q^2} d\omega$$

$$F^1 = \int e^{\omega y + \gamma_1(\omega) \ell n \ell n q^2} d\omega$$

and

$$F^{(0)} \sim e^{\sqrt{\frac{16N}{b} y \ell n \ell n q^2}}$$

and

$$F^{(1)} \sim e^{2\sqrt{\frac{16N}{b} y \ell n \ell n q^2}} \quad .$$

Finally

$$\frac{F^{(1)}}{q^2 F^{(0)}} \to 1 \quad . \tag{201}$$

means that

$$e^{\sqrt{\frac{16N}{b} y \ell n \ell n q^2}} \sim q^2 \tag{202}$$

or $\quad \ell n\, 1/x_{c\Gamma} \sim \frac{b}{16N} \ell n^2 q / \ell n\, \ell n\, q^2$.

So we see that high twist corrections could be important and even large namely in the same kinematical region as our reggeon-like diagrams. Really, reggeon-like diagrams allowed us to sum all high twist contribution in the region where they become essential. Of course we used for estimate (201) our assumption that $\gamma_1 = 2\gamma_0$. However, really I am sure that this is not even assumption, and now some prove of this statement is in progress. I would like also to mention here that all previous discussion arose as a result of hot discussions in DESY during low x workshop (May 1990). This presentation is a short résumé of the paper of J. Bartels, M. Ryskin, A. Shuvaev and me which is in progress.

3. Hidden assumption

Let us discuss the assumptions that have been made to get the master equation (193). Really, there are two main hypothesis.

1. The first one is the assumption that exchange of two and more ladders lead to larger contribution at low x than exchange of some more complicated diagram (see for example the diagrams in fig. 17). This assumption is equivalent to our hypothesis that $\gamma_1 = 2\gamma_0$ in previous section. Now we have had one support of this more less ad hoc hypothesis, namely L.N. Lipatov[15] proved that at least in six gluon channel the exchange of three ladders gives larger contribution at $x \to 0$ than exchange of two odderons, which are the

new set of diagrams in three gluon channel. It turns out that $3\Delta_P > 2\Delta_{odd}$.

The second assumption was the eikonal approximation for emission of ladder by hadron (see fig. 18a) which means that the amplitude of n-"ladder" emission is equal to g^n/n !. The physical interpretation of this assumption is very simple. We neglect the correlation for "ladder" emission on the first step of our understanding. In any case we need some hypothesis about the hadron structure, since we cannot control it in perturbative QCD. We hope that our hypothesis is the simplest and clearest from physical point of view and can be improved very easily.

4. Solution

Thus we should solve the master equation, and in some sense we have to looking for the explicit solution since the numerical methods as Monte Carlo cannot help us. Fortunately, we were able to do this, at least in semiclassical approach[1] (see eq. (141) and all discussion around this equation) using the trajectory method that has been described in lecture 7.

The first important observation that the equation (193) can be rewritten as a system of two ordinary differential equations along the group trajectory.

Indeed

$$\left.\frac{d\varphi}{dy}\right|_{gr.tr} = K\left(U_{ph} - U_{gr}\right)\varphi + O(\alpha_S)$$
$$\left.\frac{dK}{dy}\right|_{gr.tr} = \frac{4N_c}{b\Gamma^2}\chi(1-K)\cdot\left[1 - \frac{K\varphi}{K_0\,\varphi_0}\right] \tag{203}$$

and $\frac{d\Gamma}{dy} = U_{gr}$ is the equation for group trajectory. (For details I refer you to lecture 9). In the first equation we missed the nonlinear correction because they are small. The only thing that this nonlinear term makes it diminishes the slope K when $\varphi \to \varphi_0$, as seen from eq. (203). To study the property of the nonlinear

equation let us start from the initial condition which is typical for Green function, of linear equation, namely at $y = y_0$ $\varphi = \delta(\Gamma - \Gamma_0)$. So we have a bunch of group trajectories that start from the point (y_0, Γ_0) in our (y, Γ) plane and they have all different K's at equal rate. Of course such trajectories cannot cross each other, since the system (203) has the unique solution.

It should be stressed that among all group trajectories of nonlinear equation (193) there is one, which coincides with the phase trajectory. For this unique trajectory we have

$$U_{ph} = U_{g\Gamma} \quad ; \quad \text{or} \quad \frac{\chi(1 - K_0)}{K_0} = -\chi'(1 - K_0) \quad . \tag{204}$$

Eq. (204) defines the value of K_0 and numerically $K_0 = 0.63$ for $N_c = 3$ (see ref. [1] for details). Directly from the second equation in system (203) follows that if $K\varphi = K_0\varphi_0$ K is constant, so it means that $\varphi = \varphi_0$. For critical line $U_{ph} = U_{g\Gamma}$. So $\frac{d\varphi}{dy} = 0$ from the first equation in system (203). I would like to draw your attention to the fact that nonlinear term in our equation provides the constant value of φ along this critical line. The equation for critical line looks as

$$y = \frac{0.21}{8N_c}\Gamma^2 + C\,\Gamma + y_0 \quad . \tag{205}$$

The last two constants C and y_0 cannot be defined directly from the equation. They should be found from matching procedure.

Now we can divide the whole kinematical plane in three parts, if we draw the critical line, and the trajectory of linear equation that touches this critical line (see regions A, B and C in fig. 18b), for region A, all trajectories of linear equation even do not touch the critical line and for all this region we can use LLA equation that was discussed in lecture 8. Of course the answer depends crucially on the initial condition for φ on the vertical line (for

fixed $\Gamma = \Gamma_0$ or $q^0 = Q_0^2$). In region B, the group trajectories of the linear equation cross the critical line. It means that the trajectory of nonlinear equation looks as shown in fig. 18b (see curve 1 there). The trajectory goes as for linear equation and the point when it could cross the critical line, the trajectory envelops it. So the resulting trajectory goes in the vicinity of the critical line till the second cross of the critical line by the trajectory of the linear equation (see dash line 1 in fig. 18b), for large $\Gamma = \ell n\, q^2$ our trajectory of nonlinear equation coincides once more with the trajectory of the linear LLA equation. Now it is easy to understand that we can solve our nonlinear equation to the right of the critical line, using the solution of linear equation with the initial condition on the critical line $\varphi = \varphi_0$. Especially if you note, that all trajectories that start from the point (y_0, Γ_0) with $K > K_0$ accumulate to the critical line.

Such a solution was found in ref. [1] and roughly speaking, we can parametrize this solution in sufficiently primitive way, namely

$$\varphi = \varphi_0\left(\alpha_S\left(q^2\right)\right)^{1/6} H(\kappa)\, q^{2(f(\kappa)-1)} \tag{206}$$

for function $H(\kappa)$ and $f(\kappa)$ you can find the expression in ref. [1], but $f(\kappa)$ can be also parametrized in the simple way within 5 % accuracy :

$$f(\kappa) = \sqrt{\kappa(1-0.21\,\ell n\,\kappa)} \quad . \tag{207}$$

In eqs. (206) and (207)

$$\kappa = \frac{8N_c\,\ell n\,1/x}{0.21\,b\,\ell n^2\left(q^2/\Lambda^2\right)} = \frac{8N_c\,y}{0.21\,b\,\Gamma^2} \quad . \tag{208}$$

In region C we have not found the solution of our nonlinear equation, all our trajectories with $K < K_0$ go in some sense along of the y axis and penetrate just through the corner where the critical line crosses the vertical line $\Gamma = \Gamma_0$. More that we have no equation in the region C, since new parameter W here is not small and we cannot use this parameter to select some set of Feynman diagrams.

I am going to discuss this particular region in the next lecture.

I hope that you understood all problems that we faced trying to prove and solve the new nonlinear evolution equation.

Much work is needed to clarify a lot of problem here, but the main step was made. Namely we demonstrated[2] that we can touch this problem and even solve it, in spite of the number of additional hypothesis that have been assumed.

Lecture 12 : Saturation of the parton density at low x

As I have discussed in the previous lecture, inside of the region C in fig. 18b we have no theoretical approach. So we can use practically any assumption. However I would like to draw your attention to the fact that we face the very unusual situation here, namely small coupling constant α_S and large parton density. So here, at the moment we have only phenomenological assumption.

1. Parton density saturation hypothesis. Our phenomenological assumption is, so-called, parton density saturation hypothesis. Let us describe this hypothesis which looks oversimplified and even primitive. So for $q_t > q_0(x)$ we have solution (206) in which $\varphi \to \varphi_0$ at $q_t = q_0(x)$. As I discussed in lecture 10 the picture for distribution of partons in the transverse plane is very simple for $q_t = q_0(x)$ (or $x = x_{c\Gamma}$) namely partons populate densely in the whole hadronic disc that they occupy. The idea of parton density saturation is to assume that this picture preserves even for $q_t < q_0(x)$ or inside of the region C in fig. 18b. It means that $\varphi(q_t^2)$ behaves as shown in fig. 19a. Of course inside the region C in fig. 18b a lot of diagrams becomes important, not only "fan" ones which describe the interaction between partons. Such an interaction becomes even more important inside this region. So physical motivation of the parton density saturation looks transparent. Indeed, each parton with $q_t < q_0(x)$ lives in enviromnent of other partons so it has to interact with them. As result of this interaction the transverse momentum of this parton increases and becomes equal to the mean momentum of our parton medium. The mean momentum is the largest one for which interaction inside this parton cascade is still essential. So this is just our $q_0(y)$, since for $q_t > q_0(y)$ we can consider the parton-parton interaction only as a perturbation effect in comparison with parton emission as has been discussed in previous lectures.

So our hypothesis that for $q_t < q_0(x)$ the fast hadron is a collection of partons with proper size $1/q_0(y)$ where y is the

rapidity of a parton. This distribution of partons of course is the result of the strong parton-parton interaction inside the parton cascade, so if we want to have some theoretical arguments supporting such a picture, we should take some system with large number of parton but to which we can apply some theoretical technique to prove something.

2. The parton cascade for nucleus. Such a system is heavy nucleus (A is the atomic number ; and A >> 1). Indeed, in lab. frame the proper life-time of the gluon (parton) inside the parton cascade is equal to

$$\tau = \frac{q_{oi}}{q_{ti}^2} = -\frac{2mq_{oi}}{2m\, q_{ti}^2} = \frac{1}{2mx_i} \qquad (209)$$

where q_{oi} is the energy of i-th parton and $q_{ti}^2 = -q_i^2$ is the virtuality of this parton, m is the nucleon mass.

We can also introduce the mean free path for such a parton, which is equal to

$$\ell_i = \left(\sigma_i \rho\right)^{-1} \qquad (210)$$

where σ_i is the cross section for i-th parton-nucleon interaction. It is obvious that $\sigma_i \sim \frac{1}{q_{it}^2}$, and ρ is the density of nucleons in the nucleus. So when

$$\tau_i \gg \ell_i \qquad (211)$$

our parton takes part in τ_i/ℓ_i interactions. Of course this is correct only for $\tau_i \ll 2\, R_A$, since the parton "i" cannot interact with more that $\rho\, 2R_A = A^{1/3}$ nucleons. Thus

$$1 \ll \tau_i/\ell_i \ll A^{1/3} \qquad (212)$$

and this parameter can be large for large nucleus and for sufficiently small transverse momentum. Indeed eq. (212) could be rewritten in the form

$$1 \ll \frac{1\, \rho\, \sigma}{2mx_2} \sim \frac{\rho\, 1/q_{ti}^2}{2mx_i} \ll A^{1/3}$$

so for $q_{ti}^2 \le \frac{2mx_i}{\rho} = \bar{q}$, our parton interacts essentially with the nucleons of the nucleus.

This interaction changes crucially the condition for emission of gluons in our parton cascade, and inside of the nucleus we can develop new approach for parton cascade which is quite different from usual LLA. Namely we would like to use the following parameters to describe the evolution of the parton cascade inside the nucleus.

$$\left.\begin{array}{l} \alpha_S\, \ell n\, 1/x \sim 1 \\ \alpha_S\, A^{1/3} \sim 1 \\ \alpha_S \ll 1 \end{array}\right\} . \qquad (213)$$

Indeed, as we discussed in all previous lectures, our cross section (deep inelastic structure function) in LL(x)A can be represented as a sum of the following type

$$\Sigma \frac{1}{n\,!} \prod_i \left(\int \alpha_S\, K\left(q_{it}\right)\right)\left(\frac{dE_i}{E_i}\, d^2\, q_{it}\right) \sim \Sigma \frac{1}{n!} \alpha_S \left(\ell n\, s/q_t^2\right)^n \qquad (214)$$

Summation in eq. (214) leads to the cross section $\sigma(s)$ which is proportional to

$$\sigma(S) \sim \alpha_S^2 r_B^2 \left(S\, r_B^2\right)^{\omega_0} \tag{215}$$

where r_B is the nucleon size and $\omega_0 = C\,\alpha_S$ ($C = 2.65$ for $N_c = 3$). However, in order to obtain the log each intermediate gluon q_i must be emitted coherently by its parent q_{i-1} during a time τ_i (see eq. (209)). From the spacetime point of view the logarithm of the energy $\frac{dE_i}{E_i} = \frac{dx_i}{x_i}$ corresponds to log integration over proper time of a parton (τ_i)

$$\int \frac{dq_{oi}}{i\, q_{o\,i}} = \int dq_{oi} \int e^{iq_0 x}\, dt = \int \frac{d\,t}{i\,t} \; .$$

If during the time τ_i there are several collisions between the parton parent q_{i-1} and other nucleons of the nucleus (figs. 19b, c) in which its colour charge is changed, then the coherent emission amplitude decreases as ℓ_i/τ_i and conditions for log integration over dx_i are violated.

The last statement we can, illustrate by introducing an effective absorption potential $v_i = \frac{i\sigma\rho}{2}$ or $1/2\ell_i$. This causes the energy denominators $1/\Delta E = (-\,q^2/2E)^{-1}$ to be replaced by $1/\Delta E + v$, that is the propagator $1/q^2$ are replaced by $1/q^2 + 2E_i\, v_i$

$$= \frac{1}{q_i^2\left(1 + \frac{i\sigma\rho}{2mx}\right)} = \frac{1}{q_i^2\left(1 + i\,\frac{\tau_i}{\ell^i}\right)} \; .$$

The probability for the emission of a new gluon with $\tau_0 > \ell$ now no longer contains the log

integration $\frac{d\tau_i}{\tau_i}$ which could compensate for the small factor α_S and it remains parametrically small in the coupling α_S.

As a result, a log ladder of fast gluons is not formed inside the nucleus. Intermediate gluons (fig. 19a) are emitted only near the nuclear fragmentation region where their formation time τ_i does not exceed ℓ.

So we have discussed the qualitative picture for the parton cascade inside the nucleus, now we would like to write the evolution equation inside the nucleus, using the above qualitative arguments. Introducing $\varphi(q, x)$ for gluon with virtuality q^2, we can write the linear equation

$$\varphi\left(x,\, q^2\right) = \int_x^1 \frac{dx'}{x'}\, K(q, q')\, \frac{\alpha_S\left(q'^2\right) N}{\pi}\, \frac{d^2 q'_t}{\pi} \tag{216}$$

as the first step let us include one-gluon rescatterings with large momentum transfer $q_i > q_m > \bar{q}$. In this case graphs like that in fig. 20a actually are dominant. The more complicated interference diagrams (fig. 20c) contain an extra propagator $1/q_t^2$ and are suppressed like the parameter $\bar{q}/q_m$. Summation of the diagrams of fig. 20a leads to multiplication of the propagator of gluon i (that is the kernel K) by the factor $\exp\left(-\,\sigma_\mu\, \rho\, \ell_i/2\right)$ corresponding to the amplitude for the absorption of the gluon i on a segment ℓ_i of its trajectory with cross section $\sigma_m = 6\pi\, \alpha_S^2/q_m^2$. If the lifetime $\tau_i = 1/2m\; x_i$ is larger than the nucleus size then $\ell_i = 2R(b)$ and for small times $\tau_i << R_A$, that is, $x > x_A = 1/2\, R_A$ the gluon is absorbed throughout the entire path $\ell = \tau_i$ and the new kernel is

$$K = K \exp\left[- \sigma_m \rho / 4mx_i\right) \quad . \qquad (217)$$

The resulting equation is

$$\frac{d\varphi(y, q^2)}{dy} = \int K(q, q') \frac{\alpha_S N}{\pi} e^{-\sigma\rho/4mx} \frac{d^2q'}{\pi} \varphi\left(y, q'^2\right) \qquad (218)$$

where $\sigma = 6\pi\, \alpha_S^2/q'^2$.

Eq. (218) does not even need to be resolved. It is sufficient to study it carefully. The argument of the exponential ($\sigma\rho/4mx$) grows with decreasing x as a result of the increase of the proper life time of a parton. So at $x \to 0$, rescatterings exp ($-\sigma\rho/4mx$) begin to suppress the probability for new gluons to be emitted. When the argument $\frac{\sigma\rho}{4mx}$ becomes of the order of unity the effective kernel K decreases sharply and further growth of the cross section (the function φ) practically ceases. Starting at this instant $x = x_0$ ($\rho\sigma/4mx_0 = 1$) there is no more formation of new, faster partons in the LLA of QCD, and the cross section $\sigma(x < x_0, q^2) = \sigma(x_0, q^2)$ remains constant in the range $x_A < x < x_0$.

For the actual calculation of the value x_0 it is necessary to know the value of the cross section $\sigma \sim \alpha_S^2/q^2$. Of course, we have no physical reason for choosing $q_n \geq \bar{q}$. This inequality just simplifies the selection of the graphs. It is most natural to take the cross section σ to be total interaction cross section

$$\sigma\left(x, q^2\right) = \int_{q^2} \varphi\left(x, q'^2\right) \alpha_S \, dq'^2/q'^2 \quad . \qquad (219)$$

So we can suggest nonlinear equation which looks as eq. (218) but σ is replaced by $\sigma(x, b)$ from eq. (2.19). This equation possesses the same features as eq. (218).

So, we can summarize the above dicussion as the following statement. Due to interaction inside the nucleus, there is no partons with $q_t \leqslant \bar{q}$ in the parton cascade of a fast nucleus and the $\varphi(x\ q^2)$ firstly grows until the parameter $\sigma\rho/4mx_0$ reaches unity, after that $(x < x_0)$ φ remains constant. More detail information about structure of the parton cascade for nucleus you can find in ref. [16].

3. Semiquantitative description of parton distribution in the saturation region. The above examples gives us some intuition to understand what could be in the region C in fig. 18b where we assumed the hypothesis of the parton density saturation. Really only this example gives us some theoretical basis for discussion, but nevertheless I think even more I am sure that only physical assumptions which take into account the main property of the parton cascade in the region C in fig. 18b, namely, the large parton density, could help us to understand the situation here. I do not believe that here we can sum all dominant diagrams and something like this.

So in this section I would like to present our current understanding of the problem and our today intuition, based mainly on the above theoretical consideration for nucleus case.

The main lesson from the above example, that in LLA it is natural to expect that the picture of the interaction is considerably simplified to the left of the boundary. The point is that the emission of new "ladder" gluons with sufficiently small momenta are $q_t << q_0(y)$ tends to be strongly suppressed. Therefore the value of φ should be reduced with respect to one gluon exchange result (up to the α_S correction) or the simplest diagram of Born approximation. The main reason is the same as was in nucleus case.

Indeed, directly from uncertainty principle the emission time of a gluon with momentum q_i in the rest frame of the target is

$$\tau_t \approx 1/\Delta E = \frac{2E_i}{q_{t\,i}^2} \approx \frac{1}{2mx_i}$$

on the other hand, the total probability for the rescatterings shown in figs. 20b and c during the entire lifetime of the gluon q is determined by $\varphi(x, q_t)$. I would like to recall that parameter W, which shows us how rescatterings are important is proportional to φ so $W \approx \varphi/\varphi_0$. It means that the rescattering should be taken into account, if $\varphi \approx \varphi_0$. If we look on the expression for parameter W, we see that we can express W through the mean free path, namely

$$W = \frac{\alpha_S}{q^2} \frac{x\,G(x\,q^2)}{\pi R^2} = \sigma.N \qquad (220)$$

where $\sigma_0 = \frac{\alpha_S}{q^2}$ is the cross section for parton-parton interaction and N is the density of parton in the transverse plane. If we use the analogy with the nucleus case $N = \int \rho\, dZ$ is the optical width of the nucleus. So to extract from eq. (220) the expression for the mean free path of our parton, we should rewrite W as follows.

$$W_i = \sigma_0\, \rho\, \tau_i = \sigma_0\, \rho\, 1/2m\, x_i \qquad (221)$$

where τ_i is the proper time of the parton "i". So

$$\ell_i = \left(\frac{W_i}{\tau_i}\right)^{-1} = \frac{2mx_i}{W_i} \quad . \qquad (222)$$

So in our saturation hypothesis $\ell_i = \frac{1}{2mx_{c\Gamma}(q_t)}$. Indeed if we fix the size of the parton or in other word consider the parton with definite q_t, we see that at $x > x_{c\Gamma}(q_t)$ $W_i << 1$ and ℓ is large, so we can neglect the interaction between partons. On the boundary $W \rightarrow$

1 and ℓ_i is equal to $1/2m\, x_{c\Gamma}(q_t)$. So in the vicinity of the boundary $\tau_i/\ell_i = 1$ and our parton at least once interacts with another parton. For smaller $x << x_{c\Gamma}$ τ_i/ℓ_i increases and in this situation we lose the log integration over dx_i/x_i as was shown in the previous section.

The physical reason for this effect is very simple, and really it is the manifestation of the Landau-Pomeranchuk effect[18]. Indeed, during each collision (interaction) the parton changes its colour charge. It means, the emission of the new (secondary) gluon by this particular parton can be considered as independent emission in $n = \tau_i/\ell_i$ intervals between which there is no coherence. In LLA the emission was proportional to n^2 ($M^2 \sim n^2$) since it was very coherent process for all time of formation of our new gluon. In the case of small ℓ_i our $M^2 \sim n$ and our log integral can be transformated in

$$\int \frac{d\tau_i}{\tau_i} \frac{1}{\left(1 + \frac{\tau_i}{\ell_i}\right)} \quad . \qquad (223)$$

So all our integration inside the region C in fig. 18b have no large log 1/x contribution and so our amplitude of gluon emission turns to be very small since it is proportional to $(\alpha_S)^n$.

So, for all $q_{it} < q_0(y_i)$ we have no emission of new gluons and it means that instead full ladder-like diagram of fig. 21a we have the exchange of only one gluon from point (y_i, q_{τ_i}) to $(y_{c\Gamma}(q_{t_i}), q_{t_i})$.

The correct expression for $\varphi(x, q)$ in the region C, using the above picture, was done in ref. [17] where the formulas, that typical for nucleus case[16] were rewritten for the case of the partons, that populate densely in the hadron disc.

Thus, concluding this lecture, I would like to stress, that even inside of the region C in fig. 18b, where strictly speaking we have

no theoretically grounded prove, we can suggest the picture of the parton distribution and interaction which looks at least self-consistent and natural. Of course this detail picture reveals itself in some experimental observed properties. I have no time to discuss these predictions here, and can only recommend you the paper[17] were these predictions were partially discussed. Unfortunately, the most predictions and consequences of this approach have not been discussed. Much work is needed to estimate and list all new phenomena that could be measured using this new detailed picture for the structure of parton cascade for past hadron inside of the saturation region.

Partially, the prediction coming from the interaction of partons with $q_t < q_0(y)$ for heavy quark production was discussed in ref. [19].

Lecture 13 : Deep Inelastic scattering with nucleus

In previous lecture I have touched the problem of the deep inelastic processes on nuclei. Here I would like to discuss the old problem of so-called screening correction in deep inelastic scattering with nucleus to demonstrate how works the developed approach and how helps us to solve this problem.

It is well known that a nucleus is a target with sufficiently large size ($R_A >> 1/\mu$ where μ is the typical hadron scale). Due to this fact such a target can be used as a good probe of space-time picture of the high energy interaction. This problem has been discussed in details[20] during the last two decades.

The question arises, can our microscopic theory - QCD - add something important to the understanding of deep inelastic scattering with nucleus that has been reached in the old parton time. To answer on this question we would like to draw your attention to the fact that for γ^*A (and even for hA) interaction the typical transverse momentum is large enough, namely, $<K_t^2> \sim A^{1/3}$, since incoming virtual photon/or hadron) interacts with a sufficiently large number of nucleons, which is proportional to the optical density of a nucleus $T(b_t) \sim A^{1/3}$. Indeed, the main factor that determines the penetration of a parton into the nucleus is $\sigma T(b_t)$, and $\sigma \sim \alpha_S^2 r_t^2$ where r_t is the typical transverse size of a parton. If $\sigma T(b_t)$ is of the order of one, the interaction with the nucleus becomes essential. Thus $\sigma T \sim 1$ and $r_t^2 \sim A^{-1/3}$. Small r_t allow us to use perturbative QCD with a guaranteed accuracy, that is controlled by the smallness of the QCD coupling constant, namely, $\alpha_S(r_t^2 \sim A^{-1/3}) << 1$. It is very important property, which gives us the possibility to have a better theoretical understanding of γ^*A (or hA) interactions than $\gamma^*h(hh)$ collisions.

1. Space-time picture of interaction with nucleus

The first question that I would like to answer, is what the difference are between nucleus and hadron parton cascade. I think, there are two main differences : 1) the coherent interaction between partons from different nucleons. 2) The saturation of the parton density for a parton cascade from a nucleus is reached at smaller value of the parton density (per nucleon) than in a nucleon. The last point can be clarified direclty from unitarity constraint. Indeed, the unitarity for a nucleus says :

$$\sigma_A < R_A^2 \tag{224}$$

where σ_A is the total cross section for the interaction of a nucleus with the target (as in the hadronic case we consider here a gluon with virtuality q^2 as a target). Of course near the saturation region

$$\sigma_A = A\sigma_N = A\frac{\alpha_S}{q^2} x\, G(x, q^2) \leqslant \sigma_A = \pi R_A^2 \quad . \tag{225}$$

Thus,

$$\frac{\alpha_S \times G_N(x\, q^2)}{\pi q^2 R_A^2} = W_N \leq A^{-1/3} \quad . \tag{226}$$

So the unitarity is saturated at smaller W_N than in a nucleon case. It means that the main contribution in parton-parton recombination (that as we have discussed, is the main origin of the screening corrections) comes from the interaction between partons from different nucleons in a nucleus.

Let us estimate how many nucleons can interact with a virtual photon. The easiest way is to discuss this problem in lab. frame where the nucleus is in the rest. As we have discussed in the

previous lecture, the proper life time of the virtual photon in this frame is equal to

$$\tau^*_{\gamma a} = \frac{q_0}{|q^2|} = \frac{1}{2mx} \tag{227}$$

where q is the momentum of the virtual photon. Now we can divide the whole interval of x from 0 to 1 in three regions.

1. $\tau^*_\gamma < R_{NN}$ or $x > 1/2m\, R_{NN}$ where R_{NN} is the average distance between two nucleons in a nucleus. In this kinematical region virtual photon lives so small time that it can only interact with one nucleon. So the picture of interaction looks as shown in fig. 22a, and

$$\sigma_{\gamma A} = A\sigma_{\gamma^* N} \tag{228}$$

2. $R_A > \tau_{\gamma^*} > R_{NN}$ or $(2mR_A)^{-1} \equiv x_A < x < (2mR_{NN})^{-1}$.

In this kinematical region the virtual photon exists as a system of partons sufficiently long time. During τ_{γ^*} the partons from γ can interact with several nucleons. For fixed b_t, the number of interacting nucleons changes from 1 to $2R_A(b_t)\rho$ where ρ is the nucleon density in the nucleus (see fig. 22b). Here I do not wait the relation (228) but the average number of collisions in this kinematical region does not depend on the atomic number A.

3. $\tau_\gamma > R_A$ or $x < x_A$.

In this kinematical region virtual photon decays into parton before the nucleus. So here the interaction looks similar to hadron-nucleus scattering. Due to this reason we expect

$$\sigma_{\gamma^* A} \sim A^{2/3} \tag{229}$$

for such small x.

Thus, even from oversimplified space-time picture we expect in the region of small x ($x < x_A$) large screening corrections that lead to eq. (229) even for large value of q^2.

Therefore we face the pure theoretical problem to calculate large absorption correction for large virtuality of photon, where we can apply perturbative QCD.

2. Equation

From the previous qualitative discussion it is clear that the modified evolution equation in a nucleus should take into account the screening corrections due to the diagrams of fig. 23b which describe the rescattering off nucleons that are located at distances $\Delta Z \leqslant \tau_\gamma = 1/2mx$ from each other, as well as diagrams of the type of fig. 23a which have been included in our master equation (193) for the parton cascade in one nucleon. In the diagrams of the type of fig. 23b the typical transverse momenta Q_t transferred along the separate ladders (reggeons) φ are strongly related to the size of the nucleus or more exactly to the wave function of the nucleons in the nucleus. The role of the dimensional parameter $Q_0^2/4\pi$ is here played by the quantity $T(b_t) = \int \rho(b_t, Z)\, dZ$ where ρ is the nucleon density in the nucleus. The integration region over Z here is $\Delta Z = 1/2mx$. As a result, the rescattering probability (or parameter W) increases by factor $K = 1 + 4\pi\, T(b, \Delta Z)/Q_0^2$, while the maximal parton density $\varphi_m = \varphi_0/\alpha_S$ per nucleon in the nucleus decreases by the factor K. Thus

$$\varphi_{0A} = \varphi_0 \Big/ \left(1 + 4\pi\, T(b, \Delta Z)/Q_0^2\right) . \qquad (230)$$

The modified evolution equation looks very similar to nucleon one, namely

$$\frac{\partial \varphi_A(y, q^2)}{\partial y} = \int K(q, q') \frac{N\alpha_S(q'^2)}{\pi} \frac{d^2q'}{\pi} \cdot$$
$$\cdot \left(1 - \alpha_S(q'^2) \frac{\varphi\left(q'^2, y\right)}{\varphi_{0A}}\right) \varphi\left(q'^2, y\right) \qquad (231)$$

where

$$T(b, \Delta Z) = \begin{cases} \rho \dfrac{1}{2mx} & \text{at} \quad x > x_A(b_t) \\ 2\rho\, R_A(b_t) & \text{at} \quad x < x_A(b_t) \end{cases} \qquad (232)$$

where $x_A(b_t) = (2m\, R_A(b_t)^{-1}$ and

$$R_A(b_t^2) = \sqrt{R_A^2 - b_t^2} .$$

Just from eq. (2.32) we see two important regions in the solution : (1) $x < x_A$ where factor K is independent of x. Here the equation (2.31) looks as for nucleon. There is only one difference, namely, the boundary line $q_t = q_{tA}(x)$ shifts in the nuclear case, since the parton density on this line decreases in the nucleus being equal to $\varphi_{0A} = \varphi_0/K$. It means that such a value ($\varphi = \varphi_{0A}$) is reached at a smaller value of $y = \ell n\, 1/x$ than for nucleon. In other words, for the same value $y = \ell n\, 1/x$, for nucleus the typical momentum q_{tA} increases (see figs. 24a and b) we can describe the value of q_{0A} introducing the shift $\Delta(b_t)$[2] :

$$\ell n^2\, q_{0A} = \frac{1}{12.7} \ell n\, 1/x + \Delta(b) \qquad (233)$$

and $$\Delta\left(b_t\right) = \frac{1}{12.7} \ell n^2\, x_A\left(b_t\right) + \ell n\, x\left(b_t\right) \qquad (234)$$

more realistic estimate for real nucleus is

$$\Delta = 0.55 + 0.22\, \ell n\, A^{1/3} \quad . \tag{235}$$

Of course we averaged the value of $\Delta(b_t)$ over b_t in the nucleus, but nevertheless eq. (235) gives us the correct scale for evaluation of the nuclear effects in deep inelastic scattering.

$$(2)1 >> x > x_A \quad .$$

Here the situation is more complicated. Indeed for $x > x_A$ the parton has time to be formed inside the nucleus during time $\tau = 1/2mx \leq 2R_A(b_t)$. For this reason we need to calculate the incoherent rescattering of a parton inside a nucleus up to the development of the cascade inside the nucleus on distances $\Delta Z > 1/2mx$, besides the coherent effects related to the screening on distances $\Delta Z < 1/mx$. Fortunately, no new problems of principle arise in doing so except cumbersome calculation. Due to this fact we will restrict ourselves only to the region $x < x_A$, where all new secondary particles are formed (created) outside the nucleus. Partially $x > x_A$ has been considered in the previous lecture.

3. Solution

I have mentioned the main problem which I would like to attack. Namely, I want to understand how at large q^2 the cross section of virtual photon absorption changes the dependence on A from $\sigma_{\gamma A} \sim A$ which is standard (natural) for deep inelastic scattering to $\sigma_{\gamma^* A} \sim A^{2/3}$ which is typical for hA interaction.

At first sight these two regimes contradict each other. Is that so ? This question was first discussed by Gribov and later was called the Bjorken paradox[20]. Let us study how the A dependence of the cross section $\sigma(\gamma^* A)$ changes with increasing q^2 and $y = \ell n$

$1/x$ considering very heavy, theoretical nuclei with $A = \infty$. The ratio of the cross sections

$$\frac{\sigma(\gamma^* A)}{\sigma(\gamma^* N)} = \frac{\varphi^A\left(x, q^2\right)}{\varphi^N\left(x, q^2\right)} \sim A^{\alpha} \tag{236}$$

for fixed x and q^2 depends on two factors. The first one is $A^{2/3}$ which arises as a result of the integration over the impact parameter b_t of the nucleus

$$\varphi^A\left(x, q^2\right) = \int T(b_t)\, \varphi_{b_t}\left(x, q^2\right) d^2 b_t \sim A^{2/3} \quad .$$

The second factor is closely related to the shift of the critical line of the master equation (193) inside the nucleus by the amount $\Delta\, \ell n\, 1/x^2 = \Delta(b_t)$ (see eqs. (234) (235) and fig. 24a). Using the answer for φ_N in the form

$$\varphi_N\left(x, q^2\right) = \varphi_0 \left(\frac{q^2}{\Lambda^2}\right)^{f(\kappa)-1} \tag{237}$$

(see eqs. (206), (207) and (208) to specify all notations in eq. (237)) we can find $\varphi_{b_t}(x, q^2)$ in the form[16]

$$\varphi_{b_t}\left(x, q^2\right) = \frac{\varphi_0}{1 + 4\pi\, T\left(b_t\right)/Q_0^2} \left(\frac{q^2}{\Lambda^2}\right)^{f\left(\kappa(b_t)\right)-1} \tag{238}$$

where $\kappa(b_t) = 12.7\, [\ell n\, 1/x + \Delta(b_t)]/\ell n^2 \dfrac{q^2}{\Lambda^2}$. (239)

It turns out that the value of the effective factor α in eq. (236) is

$$\alpha = 2/3 + \frac{2}{3}\sqrt{\kappa}\,\frac{d\,f(\kappa)}{d\kappa}\sqrt{\frac{\ell n^2 A}{9{:}12.7\,\ell n\,1/x}}\ . \qquad (240)$$

For $x \to 1$, we can neglect the term $0.21\,\ell n\,1/x$ in $f(x)$, and for α we get the answer

$$\alpha = 2/3 + \frac{1}{3}\ell n\left(A^{1/3}\right)\sqrt{1/12.7\,\ell n\,1/x}$$

as is seen, for such values of x the factor α does not depend on the value of q^2 and feels only the value of x or the lifetime of the parton $\tau = 1/2\ mx$.

Only for very small x, when

$$\ell n\,1/x \gg \ell n^2 A \qquad \alpha \to 2/3\ .$$

Due to the intense absorption of slow intermediate partons on the nuclear surface the relation $\sigma(\gamma^* A) \sim \pi R_A^2 \sim A^{2/3}$ should be satisfied even for such q^2 where the cross section of the first quark-antiquark pair with a separate nucleon is small, namely, $\varphi^N(x, q^2) \ll 1/T(b_t)$. The relation $\sigma_{\gamma^* A} \sim A$ is reached either for sufficient large x $[\ell n\,1/x^2 \sim \Delta(b_t)\,\ell n^2\,A^{1/3}/12.7]$ or for very large q^2, to the right of curve (3) in fig. 24a. When the group trajectory corresponding to the point (x, q^2) $(x \ll 1)$ starts in the region $x_0 > x_A$ where $\varphi_A = A\varphi_N$.

For real nuclei $(A < 240)$ the screening correction appears not to be very large. Indeed, coherent rescattering off the neighbouring nucleons in the nucleus decreases the equilibrium saturated density φ_0 approximately by a factor K, when $K = 1 + 0.09\,A^{1/3}$, i.e. $K = 1.55$ for p_b. For such nuclei it is more convenient to use A_{eff}, which is defined as $A_{eff} = \sigma(\gamma^* A)/\sigma(\gamma^* N)$ instead of the factor α. In

the framework of the parametrization (see eqs. (238) and (239)) we get[16]

$$\frac{A_{eff}}{A} = 1 - \frac{3\pi}{Q_0^2}\rho\,2R_A\left(1 - \sqrt{\frac{\ell n\,1/x_A}{\ell n\,1/x}}\,\frac{\sqrt{\kappa}\,f'(\kappa)}{f'(1)}\right)\ . \qquad (241)$$

We would like to draw your attention to the fact that eq. (241) is almost independent of q^2 (for $x \sim 1$) as it is in the case of theoretical nuclei. The influence of the screening corrections becomes larger for small x when $\ell n\,1/x \gg \ell n\,1/x_A$, when the second term in parentheses in eq. (241) is negligibly small.

In refs. [16, 2] you can find the application of the developed technique to several other problems in $\gamma^* A$ or hA interaction such as multiparticle production or processes of diffraction dissociation.

Here I discussed this particular example only to illustrate how this new approach can help us to solve old problem.

Lecture 14 :
Basical phenomenology
New physics at HERA

In this lecture I would like to discuss the only phenomenology that we need for deep inelastic processes. Of course, the developed approach can allow us to build new phenomenology for hadron-hadron collisions as well as for hadron nucleus interactions. To some extent this problem was outlined in our review[2]. Here, I would like to consider only selected topics of this phenomenological approach. The goal of the phenomenological description for us is to extract from experimental data the necessary parameter of our approach, namely, the value of Q_0^2. Let me remind you that in our approach the value of Q_0^2 defines the

1. scale of shadowing (screening) corrections, which are proportional to the value of Q_0^2

2. the saturation value or better to say the value of φ on the boundary line $\varphi = \varphi_0 \sim \frac{1}{Q_0^2}$

3. the typical transferred momentum along the ladder which is of the order of the minimum (intristic) momentum of partons in the parton cascade

4. the typical interaction volume for the recombination of partons inside the parton cascade.

1. Phenomenology

So, we developed some phenomenology to extract from experimental data the main numerical parameter of our theoretical approach, Q_0^2. Let us outline briefly the main input of this phenomenology.

1. We simplified the general equation for critical line and reduced it to the form

$$q_0^2(x) = Q_0^2 + \Lambda^2 e^{3.56\sqrt{\ell n\, x_0/x}} \quad . \qquad (242)$$

In eq. (242) we have three pure phenomenological parameters Q_0, which we have discussed below and which we introduced in eq. (242) as an instrict momentum of partons, Λ, which is the position of infrared pole in α_S ($\alpha_S = 4\pi/b\, \ell n\, q^2/\Lambda^2$), and x_0, which tell us, what value of x is small enough.

2. For $q_t^2 > q_0^2(x)$ we use the solution of modified evolution equation in the form of eq. (206) (see also eqs. (207) and (208)).

3. For $q_t^2 \le q_0^2(x)$ we assume the hypothesis of the parton density saturation, which leads to

$$\frac{d\, x\, G\left(x, q^2\right)}{dq^2} = \frac{276\ b}{4\sqrt{2}\,\pi\ 3N_c}\ \frac{1}{Q_0^2} \quad . \qquad (243)$$

The calculation of numerical factor in eq. (243) can be found in refs. [1, 2].

Using the above input we described the experimental data for hadron production at sufficiently large transverse momenta in wide range of energy ($\sqrt{S}$ = 63-1800 GeV). I would like to mention here, that we choose namely hadron production only by the reason, that the smallest x has been reached till now only in hadron-hadron collision.

For hadron production we used standard formula (see fig. 24c), namely

$$\frac{d\sigma}{d\eta\, dq_t^2} = \int dZ\, q_t^{j\,2}\, \delta\left(q_t^2 - Z^2\, q_t^{j\,2}\right) \bar{D}^{ch}(Z)$$

$$\frac{4N_c\, \alpha_S}{(4\pi)^4\, q_t^{j\,2}} \int^{q_t^{j\,2}} \varphi\left(x_1, K_t\right) \varphi\left(x_2, K_t - q_t^j\right) d^2K_t \qquad (244)$$

where

$$x_{1,2} = 2\, q_t^j \exp\,(\pm\, \eta)/\sqrt{s}$$

$$\eta = \ell n\, \mathrm{tg}\, \theta/2 = \frac{1}{2}\, \ell n \frac{E - q_L}{E + q_L} \qquad (245)$$

$\bar{D}^{ch}$ is the fragmentation function for jet decay into hadron. Really we used oversimplified version for it, namely, $\bar{D}^{ch}(Z) = 2\,\frac{(1 - Z)^2}{Z}$. As you see from eq. (244) we follow our basic idea for multiparticle production, namely, all secondary hadrons are produced only as a result of minijet fragmentation (see ref. [2] for detail), in our attempts to describe the secondary hadron production in the typical inelastic event. However, I would like to note, that we need only estimates of our phenomenological parameters (Λ, Q_0, x_0) and we can restrict ourselves only inclusive cross section for which we have good theoretical ground to use formula (244).

Fig. 25 illustrates the quality of our description.

Now let us discuss the value of phenomenological parameters that we extracted, namely

$$\Lambda = 52\ \mathrm{MeV},\ Q_0^2 = 2\ \mathrm{GeV}^2,\ x_0 = 1/3 \quad .$$

<u>Λ = 52 MeV</u> : for such a value of Λ, the running QCD coupling constant $\alpha_S = 0.16$ for $q^2 = 20\ \mathrm{GeV}^2$ in good agreement with the EMC data ($\alpha_S = 0.16 \mathrm{l}\ 0.01$) at $q^2 = 22\text{-}5\ \mathrm{GeV}^2$) which has been found from a fit to the nucleon structure function for $x > 0.3$.

<u>$x_0 = 1/3$</u>. Really our procedure turns to be insensitive to the value of x_0. So, we used $x_0 = 1/3$ rather from additive quark model argument than from experimental data.

<u>Q_0 = 1.4 GeV</u>. The large value of Q_0 seems unnatural for many of my colleagues. Indeed, at first sight such a value should be of the order of the inverse hadron size, or $Q_0^2 \sim 1/(R_N^2)^{1/2} \sim 400$ MeV. But such argument is correct only if you have in mind the picture of the uniform distribution of produced gluons (parton) in the hadron.

The definition of Q_0 as the typical momentum in integration over momentum transferred along the one ladder in "fan" diagrams means that Q_0 characterizes rather the correlation radius between two gluons inside a hadron. So, large value of Q_0 or small correlation radius $R_G = 1/Q_0$ leads us to the picture for hadron, which is shown in fig. 25b. Here, the gluons are concentrated in several "hot" or "black" spots inside the hadron each of which has the size $R_G \sim 1/Q_0$ which is small enough. $R_Q \sim 0.1$ fm.

Under our estimates one might use the three spots corresponding to the three valence quarks, if one wanted. So now, our saturation works for each spot and comparatively early (at $x = 0{,}02$ for $Q_0^2 = 2\ \mathrm{GeV}^2$). For larger energy, (smaller x) the spots become black. This is absolutely new approach to high energy collision and as a first step this approach should be tested in deep inelastic processes at low x region. However I would like to mention here, that this new picture for the hadron structure should manifest itself in typical inelastic event for hadron-hadron

collisions and main consequences of this approach were considered in ref. [2].

2. HERA physics

HERA gives us the possibility to look inside the saturation region or at least to study the vicinity of the boundary line (see eq. (242)). In fig. 26a you can see the boundary line of eq. (242) on the HERA map. To the right of this line, the only emission of partons defines the structure of our parton cascade. So here there is no interaction between partons and in some sense our parton cascade looks as the perfect gas. Inside the saturation limit we face the strong interaction between partons, but due to the fact that α_S is still small in this region the correlation between parton looks also small enough, and we have strong interaction here mainly due to the large density of parton. The system which has analogous property is the liquid, so inside the saturation region to the left of our boundary curve we have so-called quark liquid.

So new physics at HERA is the study of this quark liquid. However more modest goal is to discover the deviation of the experimental data from the predictions of the standard approach. First of all we should define what is the standard approach to the problem. For me the standard appraoch is the solution of correct linear equation that has been discussed in lecture 8. Namely deviation from this linear equation solution will give us information about the value of shadowing correction. Such attack of the problem looks theoretically self-consistent, but nevertheless most people would like to use the solution of GLAP equation as standard one, only because they are more familiar with this equation.

I would like once more to draw your attention to the great difference between correct LLA equation at low x and GLAP equation. The point is that we need the boundary condition for GLAP solution, namely, the value of structure function at sufficiently small value of $q^2 = q_0^2$ at any x. At $q = q_0$ $x\,G(x, q^2) = F(x)$ for any

value of x. The correct LLA equation can be read as evolution equation in $y = \ln 1/x$, and for solution of this equation we need only initial condition, namely at $x = x_0$ we should know $x_0\,G(x_0, q^2) = \bar{F}(q^2)$ the structure function at any value of q^2. Unfortunately a lot of shadowing correction could be hidden in phenomenological function F(x). Even this remark shows you that we should attack the shadowing correction trying to collect all possible information, not only observing for example $F_2(x, q^2)$ behaviour at low x.

The right strategy and the full investigation how we can measure the shadowing correction in HERA kinematical region have not been done. Much work is needed to formulate the above problems in particular in the working groups at DESY. So I am going to discuss only the ideas how we can start this attack.

We would like to see in HERA experiment two important aspects of our approach :

1. large screening (shadowing) correction to GLAP equation
2. the structure of hadron, that is shown in fig. 28b.

Let us try to understand how these two phenomena can reveal themselves in HERA measurements.

1) $F_2(x, q^2)$, $F_L(x, q^2)$

The first problem which we face is how saturation behaviour of the gluon structure function (see eq. (243)) reveals itself in the behaviour of the deep inelastic structure function.

To clarify this question we calculated[21] the set of diagrams of fig. 26b, using the saturation hypothesis of eq. (243). It should be noted that the second diagram gives a very considerable contribution in the region close to saturation and has not been taken in usual evolution equation.

It is clear from figs. 26c and 26d that saturation looks quite different in gluon structure function $x\,G(x\,q^2)$ and $F_2(x, q^2)$. Even

for $q^2 < q_0^2(x)$ $F_2(x, q^2)$ grows logarithmically, namely, $F_2(x, q^2) \sim q^2R^2 \ln q_0^2(x)/q^2$. This log contribution comes from the integration over transverse momentum of quarks that belongs to the self energy of the heavy photon. The typical value of such contribution is of the order of $\alpha_{em} \ln q_0^2(x)/q^2$ and absorption can stop this increase only at reasonable large value of q^2 when $\alpha_{em} \ln q_0^2(x)/q^2$ tends to unity.

We would like to note that the estimates based on our phenomenology are in not bad agreement with current experimental data. In particular $F_2^{sea} = 0.32$ at $x = 0{,}028$ and $q^2 = 4$ GeV^2. The value of gluon structure function in saturation region also is not in contradiction with the experimental data. Indeed, if we extrapolate the conventional value of $x\,G(x = 0.15, q^2 = 5\ \mathrm{GeV}^2) = 1.2$ in the region of small x using expression $x\,G(x, q^2 = q_0^2) = \frac{(1-x)^3}{\sqrt{x}}$ the value of the saturation $x\,G(x) = dq^2 = 8$ reaches at $x = x_0 = 0{,}085$ in agreement with eq. (243) for critical line in our phenomenology.

I would like to mention that we predict $\sigma_L/\sigma_t \approx 0.3$ which is also important information about screening. Strictly speaking in LLA $\sigma_L/\sigma_t = 0$; so this value can give us more sensitive tool to see screening.

Even the slight glance on fig. 26d shows us that the differences between different approaches looks more significant rather in the slope of $F_2(x, q^2)\left(\frac{d\,F_2(x, q^2)}{d \ln q^2} \text{ or } \frac{d\,F_2(x, q^2)}{d \ln 1/x}\right)$ than in its value.

So our recommendation for experimentalists is to reach so good accuracy in the measurement of $F_2(x, q)$ to extract the slopes

of $F_2(x, q)$ from experimental data to find some indication of new physics at $x \to 0$.

2) Direct measurement of $x\,G(x\,q^2)$

Of course, the shadowing corrections first of all reveals itself in $x\,G(x\,q^2)$ as we have discussed, in the region $|q^2| < q_0^2(x_B)$, $x\,G(x, q^2) = dq^2$, where $d = 2.4$ Gev^{-2} using the values of our phenomenological parameters ($\Lambda = 52$ MeV, $Q_0^2 = 2$ GeV^2, $x_0 = 1/3$). Direct way to extract $x\,G(x, q^2)$ is to measure the inclusive production of hadron jets in deep inelastic scattering. For example, we could measure $\gamma^* + p \to C\bar{C}(b\bar{b}) + X$ processes and its cross section could be rewritten directly through $x\,G(x\,q^2)$ (see fig. 27a and discussion in ref. [22]). The main problem here, that it is very difficult to invent good trigger to extract namely this process from the typical inelastic event of secondary hadrons production.

The second problem, which is our theoretical problem is the fact that until now nobody has calculated this process using the saturation hypothesis to estimate the effect of screening in observable experimental characteristic.

3) Diffraction dissociation of virtual photon

M.G. Ryskin[12] suggested to measure the processes $\gamma N \to x+N$, or $\gamma^* N \to x_{\gamma^*} x$ processes (if $\ln M^2(x\gamma) + \ln M^2(x_n) << \ln S$ where $S = (q + p_\mu)^2 = -\frac{q^2}{x_B}(1 - x_B)$). The total cross section of this process is shown in fig. 27b and could be written in the form[12].

$$M^2 \frac{d\sigma^D}{dt\,dM^2} \sim \frac{\alpha_{em}}{Q^2} \int \frac{x}{x_K} D_j\left(\frac{x}{x_K}, Q^2, K_t^2\right) \cdot \left[x_K\, G\left(x_K, K_t^2\right) \frac{\alpha_S}{K_t^2}\right]^2 \frac{dx_K}{x_K}\, d^2K_t \quad . \qquad (246)$$

This cross section has the scale $\frac{\alpha_{em}}{Q^2}$ which is the probability of virtual γ absorption by parton. D_{γ^*} describes the probability of γ^* dissociation in several quark and gluon jets, the last of them with transverse momentum K_t and the fraction of energy x_K. $[(x_K\ G(x_K, K^2)]^2$ corresponds the density of partons in the proton-target squared, since in the process of diffraction dissociation we face the annihilation of two partons with (x_K, K_t) in one (see fig. 27c). Even more, if you look on expression more carefully you could see that our cross section is proportional to $x_K\ G(x_K, K_t^2)\ \alpha_S(K_t)^2$ which is σ_t^2 where σ_t the total cross section of the interaction of gluon "K" with the nucleon.

So our cross section is really infrared unstable since $\frac{d\sigma^D}{dt\ dM^2} \sim \int \frac{d^2K_t}{K_t^2}$ and small K_t really works. So our processes can be divided in two parts. The top one ($D\gamma^*$) turns out to be in the standard deep inelastic situation, but the bottom part looks as usual "soft" process. So we expect the cross section of the order of $\sigma^D \sim 1/K^2_{min} \sim 1/\Lambda^2$, where Λ is the infrared cut off. The estimates show that in HERA region $\sigma^{D\gamma} \sim$ 2-10 nb[23] . However, the situation changes crucially if we take into account the absorption correction, since at small K_i we cannot neglect its contribution. For $K_t < q_0(x_K)$ (or in the saturation region) $G(x_K, K_t^2) = d\,K_t^2$. It means that from our point of view the role of cut off play $K_t = q_0(x_K)$ instead of Λ in naive estimates. In our phenomenology $q_0^2(x_K) > Q_0^2 = 2\ GeV^2$. Thus we expect the value of cross section in two orders smaller than in the naive estimate[23]. Ryskin's

evaluation of the value of the cross section in the kinematical region Q^2 = 30-100 GeV^2, M^2 = 300-1000 GeV^2, x_K = (0.3-1) 10^{-3} gives the value

$$\sigma^D\left(ep \to e' + x_\gamma + p\right) = 0.01\ nb\ .$$

Due to the fact, that the cross section depends on the squared value of $(x\ G(x, K^2)$ the saturation phenomena could manifest itself here stronger, than for example in $F_2(x, q^2)$ or even in $x\ G(x, q^2)$. The main prediction for these processes can be resumed as follows :

1. saturation leads to suppression of the value of the cross section more than in 100 times in comparison with standard estimate.

2. Measurement of the cross section as a function of the transverse momenta of the fastest jets in the target fragmentation (K_t in fig. 27a) should give us the information about screening since $\frac{d\sigma^D}{dK_t^2} \sim 1/K_t^4$ for $K_t >> q_0(x_K)$ and $\frac{d\sigma^D}{dK_t^2} \sim$ const at $K_t < q_0(x_K)$. So such an experiment could check our prediction for saturation boundary line (eq. (2.42)).

Ryskin also estimated that the cross section of the double diffractive process $(\gamma^* p \to x_\gamma + x_N)$ for $M(x_N) \leqslant$ 3-5 GeV in 5-10 times larger that σ^D and has the same attractive features as σ^D.

Really the whole this section is the shortest presentation of Ryskin paper[12] and his talk this December in Saclay. Much more information you could find about diffraction dissociation in deep inelastic scattering namely in these papers.

4) Mueller idea of "hot" spot search at HERA[24]

During the low x seminar at DESY (May 1991) A.H. Mueller[24] suggested the beautiful idea of the experiment in which we can measure the absorption in situation when it should be strong. These ideas looks very simple and attractive. Let us measure the

inclusive production of gluon jet with transverse momentum K_t which is very close to q and with the fraction of energy x_K as closer to one as possible to provide small value of $\frac{x_K}{x_K}$, (see fig. 27c). Indeed, this inclusive cross section is proportional to

$$x_K \frac{d\sigma^{set}}{dx_K\, dK_t^2} = \left(x_K\, G\left(x_K, K_t^2\right) . C \left(\frac{x_K}{x_B}\right)^{\omega_0(q^2)} \frac{1}{\sqrt{\ell n \frac{x_K}{x_B}}} \quad . \qquad (247)$$

The first factor is understandable directly from fig. 27c, the second one is the solution KLF equation with α_S = const = $\alpha_S(q^2)$. Indeed, the upper part of our diagram is the "ladder" in which virtualities of all particles almost equal to each other. If q^2 is small enough to be inside of saturation region we should see the large absorption correction to this formula. If q^2 is large enough we can use perturbative QCD to get the standard prediction and so we can compare the experimental result with theoretical prediction. So this Mueller's idea looks very attractive, but I see here several difficulties which we should overcome.

1. The coefficient C has not been calculated in eq. (247)
2. γ^* interacts with quark, so instead of x_B in formula (247) should be value of $x = \bar{x} = \frac{x_B}{x_q}$ where x_q is the size of quark antiquark pair in the kinematical region of KLF equation. Unfortunately, this size has not been calculated until now.
3. Even if the final virtualities are equal we should take into account the running coupling constant of QCD, and, as we discussed, the difference between solution of KLF equation and LL(x)A equation with running α_S is very significant (see lectures 6 and 7).
4. Strictly speaking, eq. (247) is not correct since we must take into account that detected gluon jet could be produced

also in jet decay (see fig. 27d). Of course for $x_K \to 1$ this process is suppressed enough, but nevertheless we need theoretical estimation of this contribution. Let me note, that such emission crucially changes the inclusive cross section for gluon jet at sufficiently small x_K[25].

Thus, we need much work to make the tool for experimental observation of large absorption correction from nice Mueller idea.

Let me also to note, that in this experiment we could observe what will happen in the event with large gluon density, and answer the question there is or not the saturation of gluon density. Of course, we can call "hot" spot the events with saturation of the parton density. However, in this experiment we cannot distinguish between two situations : "hot" spots exist as a rare fluctuation in our hadron in which gluons distribute uniformly in average or "hot" spots is the typical structure of our hadron, as we assume from our phenomenology.

5) Structure of typical inelastic event in deep inelastic scattering

The study of spectra of the secondary particle gives us possibility to clear up how evolution of the parton cascade develops and how it forms the structure function.

As we have discussed, roughly speaking, our evolution or our structure function is the sum of ladder-like diagrams (see fig. 28a). I hope that I have convinced you, that the essential values of the energy fraction for i-th parton (gluon) x_i^0 turns out to be the function of the parton transverse momentum K_{it} (see fig. 28a). This function is so-called trajectory which we have discussed in lectures 7 and 11. The word "essential $x_i = x_0$" means the saddle point value of x_i in our solution of evolution equation. The equations for trajectories were found in lecture 7 for linear equation and in lecture 11 for non-linear one. In ref. [11] the Monte Carlo calculation of the trajectories is presented. Qualitative picture for trajectories is shown in fig. 28c. We see that partons (in linear case) try to have smaller value of K_{it}, because at smaller

K_i the value of running α_S is large. However namely in this region also the absorption corrections which lead to recombination of gluons becomes large, so the resulting trajectory for nonlinear equation looks as curve (3) in fig. 28b. So studying the distribution of the secondary hadron we could measure the form of the trajectories reconstructing from experiments the average value of $\ell n\, x_i$ at fixed K_{ti} for gluon (hadron) jet.

The main experimental problem is to invent the algorithm of the jet selection. This problem is far from to be easy, but in any case here (in deep inelastic scattering) this job looks easier than in hadron-hadron interactions.

Perhaps, we can study the flow of the transverse energy E_{t-1} as a function of rapidity for the secondary hadrons in the deep inelastic scattering. In separate events in $\frac{dE_t}{dy}$ (or $\frac{dE_t}{d\eta}$ where $\eta = -\ell n\, tg\, \theta/2$) we can observe some peaks, that are related to gluon K_i in the Feynman diagrams 2 in fig. 28a. If we know the rapidity of each peak (η_i) and its transverse energy we can calculate K_i and x_i namely, $K_{ti} = E_{ti}$, $x_i = E_{proton}/E_{ti} sh\eta$. Thus, we can reconstruct our trajectory directly from experiment, and study it versus q^2 and x_B.

Unfortunately, the calculations in ref. [11] shows us that the distribution of gluons versus the transverse momentum (K_{it}) seems to be very broad, namely $\Delta\, \ell n\, K_{it}^2 \sim 2 \div 3$. It means that it is very difficult to get the form of trajectory within sufficiently good accuracy and feel the deviation of this form from linear case.

To get the final conclusion of this kind of experiments we need more work with Monte Carlo simulation of the parton (and hadron) final station in deep inelastic scattering.

6) Correlation function analysis of the final state in Deep Inelastic Scattering

I am in the firm belief that one of the best way to measure the value of absorption correction is usual correlation function analysis of the secondary hadron production. This analysis was

discussed in details for multiparticle production in hadron-hadron and hadron-nucleus collisions (see ref. [26]) in framework reggeon approach. The main idea of this analysis is the fact that pomeron is the collection of uncorrelated particles. This fact can be seen directly from Kancheli-Mueller diagrams[27] for inclusive cross section. Indeed, single inclusive cross section

$$\frac{d\sigma}{dy_1} = \int \frac{d\sigma}{dy_1 dK_t^2} dK_t^2$$

we can draw as diagrams of fig. 29a double inclusive cross section $\frac{d\sigma}{dy_1\, dy_2}$ could be described by diagram of fig. 29b. It is easy to understand that

$$\frac{d\sigma}{dy_1} = g_1\, g_2\, e^{\Delta(y-y_1)+\Delta(y_1-y_0)}\, a$$

$$\frac{d\sigma}{dy_1\, dy_2} = g_1\, g_2\, a^2\, e^{\Delta(y-y_1)+\Delta(y_1-y_2)+\Delta(y_2-y_0)} .$$

So, the correlation function

$$R\left(y, y_2\right) = \frac{\frac{1}{\sigma_{tot}} \frac{d\sigma}{dy_1\, dy_2}}{\left(\frac{1}{\sigma_t} \frac{d\sigma}{dy_1}\right)\left(\frac{1}{\sigma_t} \frac{d\sigma}{dy_2}\right)} - 1 \qquad (248)$$

is equal to zero if we take into account that $\sigma_t = g_1 g_2\, \ell^{\Delta(y-y_0)}$ (see fig. 29c).

Thus, $R(y_1\, y_2)$ differs from zero due to so-called short range (in rapidity) correlation, namely, when particles with rapidities y_1 and y_2 has so small difference $\Delta y = y_1 - y_2$ which is smaller than correlation length Δ_{SR} ($\Delta y \leqslant \Delta_{SR}$). To estimate Δ_{SR} we used to

draw the diagram of fig. 29d type, where P' is the secondary reggeon trajectory ($\alpha(0)_{P'} \sim 1/2$, so $\Delta_{SR} = 2$).

The second origin of $R(y_1\ y_2) \neq O$ is so-called long range correlation which are originated from shadowing diagrams of fig. 29e type.

So the full answer for $R(y_1\ y_2)$ we can write in the form

$$R\left(y_1\ y_2\right) = \frac{N_1^2}{g_1\ g_2} + SR(0)\ e^{-\frac{\Delta y}{\Delta_{SR}}} . \qquad (249)$$

So the first term in eq. (249) does not depend on rapidity and its value is really the value of our screening corrections.

In above discussion I would like only to recall you our standard approach to correlation analysis of the multiparticle production. This analysis allowed us to understand the general properties of the hadron inelastic event and still is the origin of the phenomenological description of hadron-hadron and hadron-nucleus collisions (see for example [28]).

What is our advantage in the case of deep inelastic scattering ? Let me suggest you some glossary, from which my hopes will be clear.

Pomeron in deep inelastic scattering is our "ladder" or solution linear equation.

Long range correlation is contribution of our shadowing (screening) diagrams.

Short range correlation is either correlation between two hadrons in the decay of one gluon jet or the correlations between two emitted gluons in our "ladder" (see diagrams in figs. 30a and 30b).

Now, I would like to answer, why I hope that this analysis will be useful in the case of deep inelastic processes. Let us consider the correlations between two gluons with rapidities y_1 and y_2 in KLF equation. So I would like to calculate the diagram of fig. 30c and compare it with diagrams in fig. 30d for inclusive cross section and if fig. 30e for total cross section. In the case when all

y_i is large ($y = \ell n\ 1/x_B >> 1\ y_1 >> 1\ y_2 >> 1$), we can use the diffusion solution (see eq. (93)).

So we can write the diagram of fig. 30c as follows.

For KLF solution we can rewrite the diagram of fig. 30a for $\frac{d\sigma}{dy_1\ dy_2}$ in the form

$$\frac{d\sigma}{dy_1\ dy_2} = \int \varphi\left(y-y_1,\ q^2,\ q_1^2\right) \frac{d}{dy_1} \varphi\left(y_1-y_2,\ q_1^2\ q_2^2\right)$$
$$\frac{d\varphi}{dy_2}\left(y_2-y_0,\ q_2^2\ q_0^2\right) \frac{dq_1^2}{q_1^2}\ \frac{dq_2^2}{q'^2_2} \qquad (250)$$

we use the KLF equation (see lecture 5) to get eq. (250). Indeed, after integration over K_{1t} and K_{2t} the emission of gluons 1 and 3 in fig. 30a gives $\frac{\alpha_S N}{\pi} K(q_1, q'_1)$ and $\frac{\alpha_S N}{\pi} K(q_2, q'_2)$ so

$$\frac{d\sigma}{dy_1 dy_2} = \int \varphi\left(y-y_1,\ q^2,\ q_1^2\right) K(q_1, q_1^1)\ \varphi\left(y_1-y_2,\ q'^2_1\ q_2^2\right)$$
$$K\left(q_2\ q'_2\right)\ \varphi\left(y_2-y_0,\ q'^2,\ q_0^2\right)\left(\frac{\alpha_S N}{\pi}\right)^2 .$$
$$\frac{dq_1^2}{q_1^2}\ \frac{dq'^2_1}{q'^2_1}\ \frac{dq_2^2}{q_2^2}\ \frac{dq'^2_2}{q'^2_2} \qquad (251)$$

using KLF equation we have

$$\frac{\alpha_S N}{\pi} \int K\left(q_1, q_1^1\right) \varphi\left(y_1 - y_2, q_1'^2, q_2^2\right)$$
$$= \frac{d}{dy_1} \varphi\left(y_1 - y_2, q_1^2, q_2^2\right) .$$

Eq. (250) we can rewrite as follows

$$\frac{d\sigma}{dy_1 dy_2} = \int d\Gamma_1\, d\Gamma_2\, e^{\frac{\alpha_S N}{\pi}\chi\left(f_1\right)\left(y - y_1\right) + \left(f_1 - 1\right)\left(\Gamma - \Gamma_1\right)} e^{\frac{\alpha_S N}{\pi}\chi\left(f_2\right)\left(y_1 - y_2\right) + \left(f_2 - 1\right)\left(\Gamma_1 - \Gamma_2\right)} \times$$
$$\times e^{\frac{\alpha_S N}{\pi}\chi\left(f_2\right) \times \frac{\alpha_S N}{\pi}\chi\left(f_3\right)\left(y_2 - y_0\right) + \left(f_3 - 1\right)\Gamma_2} \cdot \frac{df_1\, df_2\, df_3}{(2\pi i)^3} . \quad (252)$$

Here, $\Gamma_1 = \ell n \frac{q_1^2}{q_0^2}$ and $\Gamma_2 = \ell n \frac{q_2^2}{q_0^2}$. After integration over Γ_1 and Γ_2, you can easily see that eq. (252) reduces to the form

$$\frac{d\sigma}{dy_1\, dy_2} = \int e^{\left(y - y_0\right) \frac{\alpha_S N}{\pi}\chi(f) + (f-1)\Gamma} \frac{df}{(2\pi i)} \cdot \chi^2(f) \left(\frac{\alpha_S N}{\pi}\right)^2 =$$
$$= \frac{d^2}{dy^2} \sigma_{tot}\left(y - y_0, \Gamma\right) . \quad (253)$$

The same approach gives for $\frac{d\sigma}{dy_1}$ (see fig. 30d) the answer

$$\frac{d\sigma}{dy_1} = \frac{d}{dy} \sigma_{tot}\left(y - y_0, \Gamma\right) .$$

Therefore our correlation function $K(y_1, y_2)$ is equal to

$$R\left(y_1, y_2\right) = \frac{\frac{1}{\sigma_t} \frac{d\sigma}{dy_1\, dy_2}}{\frac{1}{\sigma_t} \frac{d\sigma}{dy_1} \frac{1}{\sigma_t} \frac{d\sigma}{dy_2}} - 1 =$$
$$= \frac{\frac{d^2}{dy^2} \ell n\, \sigma_t\left(y - y_0\right)}{\left(\frac{d}{dy} \ell n\, \sigma_t\left(y - y_0\right)\right)^2} \quad (254)$$

as example let us calculate $K(y_1, y_2)$ for diffusion solution, when

$$\sigma_t = \frac{N_0(r)}{\sqrt{\pi \Delta\omega_0 y}} e^{\omega_0(q_0^2)(y - y_0) \frac{\Gamma^2}{\Delta\omega_0 y}}$$

$$R\left(y_1, y_2\right) = \frac{\left(1/2 - \frac{2\Gamma^2}{\Delta\omega_0 y}\right)}{\left(\omega_0 y - \frac{1}{2} + \frac{\Gamma^2}{\Delta\omega_0 y}\right)^2} . \quad (255)$$

Strictly speaking $R(y_1\ y_2)$ turns out to be equal to zero - since in diffusion solution $\omega_0 y >> 1$; but we see also some dangerous, namely, $K(y_1\ y_2)$ falls down only logarithmically. In double log limit

$$\sigma_t = \frac{N(r)}{\sqrt[4]{\frac{\alpha_S N}{\pi}\Gamma\left(y - y_0\right)}} \cdot e^{\sqrt{\frac{2\alpha_S N}{\pi}}\Gamma(y-y_0)}$$

and $R(y_1\ y_2)$ is equal to

$$R(y_1\ y_2) = \frac{\left(1 - \sqrt{\frac{2\alpha_S N}{\pi}\left(y - y_0\right)\Gamma}\right)}{\left(\sqrt{\frac{2\alpha_S N}{\pi}\left(y - y_0\right)\Gamma} - \frac{1}{2}\right)^2} = \frac{1}{\sqrt{\frac{2\alpha_S N}{\pi}\left(y - y_0\right)\Gamma}} << 1 \ . \qquad (256)$$

So, you can see, that once more the correlation function turns out to be parametrically small. The above two examples I hope should encourage us to attack this problem seriously. It means that I am sure, that we should make some attempts to develop correlation function analysis for deep inelastic processes, using the theoretical information about structure of our "charm" (pomeron) which is the solution of LLA equation.

Of course much work we need to clarify this problem and I am happy that A. Capella, A. Krzywicki and J. Tran Thanh Van joint me to attack this problem and we have started our discussion on the subject.

7) Dissociation of the target hadron

Let me discuss once more interesting exclusive process in deep inelastic scattering, namely, reaction

$$\gamma^0 \to p \to \psi\left(\rho^0, \ldots\right) + M \ .$$

The cross section for this reaction can be written in the following form (see fig. 31a)

$$M^2 \frac{d\sigma}{dM^2 dt} = \int d^2K'\ \varphi^2\left(y-y',\ Q_t,\ K^2\right) \cdot \alpha_2^2\left(K^2\right) \cdot$$

$$G_{3p}\ \varphi\left(y',\ K^2,\ q_0^2\right)\left(t = \left(Q_t^2\right)\right) \ . \qquad (257)$$

The most interesting measurement here is the t-dependence. Indeed, $\varphi(y-y',\ Q^2,\ q^2)$ depends on $t = |Q^2|$ only if $|t| \geqslant q_0^2(x')$ $= q_0^2\left(\frac{M^2}{S}\right)$. For $|t| \leq q_0^2(x')$ our amplitude is really independent of t. Of course this is prediction only if we reach the saturation region and our phenomenology gives sufficiently good estimation for critical line.

Unfortunately, we have now no numerical estimate of the cross section in spite of the fact, that really we have all theoretical ingredients to make necessary calculation.

I would like also to draw your attention to the fact, that qualitative picture of the dissociation process is very similar to diffraction dissociation on nucleus. We know that such dissociation has very pronounced features in the case of saturation (see ref. [29]).

This process is the last one which I would like to discuss at the moment. The problem is that of course, new approach leads to many consequences but most of them even have not been estimated if in rough way.

As a whole situation with experiment at HERA could be expressed in simple words. We have a lot of idea and even theoretical understanding of the problem. Perhaps it is better to speak, we understand the theoretical problems and can specify the kinematical region where we have sufficiently good theoretical description of the problems. However, the numerical estimates are

only for several processes and even they are far from final version that can give the reliable predictions for experimental observation.

I am not sure the HERA working groups can prepare such calculation in short period of time, because the main problem is that we have only several experts in theory of deep inelastic processes at low x.

I hope that these lectures could be my small contribution in agitation and preparation of the theoreticians for professional discussion the general situation in the region of low x. I would like to mention once more that low x deep inelastic scattering is not only specific processes but physics at low x here opens new perspectives in understanding the high energy hadron (nucleus) collisions (see ref. [2]).

Lecture 15 : Problems and hopes

In this lecture, which is the last one, I am going to list the problems which we need to solve in the nearest future. My main aim in this talk is to show for all theoreticians that we have a lot of unsolved theoretical problems which are difficult enough to be attractive and most of them could be solved even now without developing new technique. However much more work, even routine one is needed to achieve some remarkable progress. Really most of these problems have been mentioned in the previous lectures, but I hope that the systematic listing of them will give the right impression on the current situation in this field of high energy physics.

1. The main theoretical problem for linear LL(x)A is to <u>find the next to leading order corrections</u>. This problem looks quite different for LL(x)A and LL(q^2)A for which next order correction has been calculated[14]. Indeed, partially such corrections that was calculated for GLAP equation have been taken into account directly in LL(x)A. Unfortunately, we have had no systematic investigation of this problem, but the solution of the above problem is extremely important. Indeed, I have mentioned that LL(x)A violates the energy conservation, so next order correction is necessary to restore such fundamental property as energy conservation.

2. <u>Numerical solution of LL(x)A equation</u> is also only in the beginning of systematic study. I would like to draw your attention to the fact, that LL(x)A could be solved both as evolution equations in $\ell n\ q^2$ and in $\ell n\ 1/x$. If the first way of solution which is close to solution of usual (GLAP) evolution equation has been treated in several papers (see the reports of Kwiecinsky, Krawczyk, Marchesini and Webber at low x seminar in DESY (May 1990)), the second one has not been touched in numerical approach. However, the little experience of solution of evolution equation in $\ell n\ 1/x$

shows that the numerical answer depends very significantly on the value of momentum cut off (Q_{OS} in ref. [11]).

3. We have found the solution of LL(x)A with the running α_S as evolution equation in $\ell n\ 1/x$, but this solution looks too formal and we do not understand the precise behaviour of our asymptotic in the region of small x.

4. In LL(x)A the inclusive cross section of gluon jet, heavy quark pair production and so on have not be studied systematically from numerical point of view. Especially interesting to calculate the value of correlation function in LL(x)A. As I discussed in previous lecture, these calculations will allow us to formulate systematic approach for the multiparticle production in deep inelastic scattering. We need also theoretical calculations of the distribution of gluons in typical LL(x)A "ladder" to understand the structure of the typical inelastic event. I would like to draw your attention that even for single inclusive production of gluon jet the correct formula was written only for large transverse momentum. On the other hand we have some experience that namely in the region of low x the inclusive spectrum changes crucially due to emission of sufficiently soft gluons[25]. Unfortunately, I do not understand for example how I can describe the result of ref. [25] using Kancheli-Mueller diagram technique[27], which was proved on sufficient general ground.

5. Next order correction for inclusive production

We know that this correction could be very important numerically, at least the experience in usual LL(q^2)A teaches us that so-called K-factor in processes of inclusive production could be of the order of 2-3.

This problem is very important from numerical point of view, because for example in our phenomenology we extract the normalization of gluon structure function directly from inclusive production and if the calculated K factor appears to be large it

means that the normalization of $F_2(x, q^2)$ should be suppressed in $1/\sqrt{K}$ times.

6. Systematical study of high twists contribution

We argued that the theorem that the operators of different twists cannot mixture is correct only when the anomalous dimension of high twists operator is smaller than one. ($\gamma_n - \gamma_0 \leqslant 1$). For small x γ_n grows very rapidly, so we should face the mixture of the operator of different twists. Namely, this situation was realized in the reggeon-like diagram technique. Thus we should study once more the problem of operator expansion of deep inelastic moments in the region small x (or $n \to 1$).

7. The right most singularities of "ladder" with 3, 4 ... gluons in t-channel induces the behaviour of the above exchanges as power $(1/x)^{\Delta_n}$. We assumed, that Δ_n for all these exchanges is smaller than Δ_0 for our LL(x)A ladder or $n\Delta_0$ for exchange of 2n gluon in t-channel. We need prove of these assumptions or some example that this assumption is incorrect.

8. We need to calculate the triple ladder diagram but in situation when the momentum, transferred along the ladders is not equal to zero. If we will know this vertex, we can write the correct LL(x)A equation with screening correction for the parton density in impact parameter plane. We discussed this problem in ref. [2] using some model simplification for this vertex. I understand that this work is very difficult but we really need it.

9. We proved the modified evolution equation using reggeon-like diagram technique, but physical meaning of obtained equation is very simple. Namely, it looks as some equilibrium in parton cascade between emission and recombination of partons. We need the ideas that allow us to prove the modified evolution equation directly from these ideas, without complicated diagram technique.

10. Inside the saturation region we have very interesting system of parton which are interacting with small coupling constant but the density of these partons are sufficiently high. We have even some detail hypothesis how interact parton in this region and why the emission of all gluons with $q_t < q_0(x)$ is suppressed. So the system of partons in the saturation region looks as collection of partons with well defined proper size which is proortional to $1/q_0(x)$. However we need some study of the problem of the inclusive production in this saturation region taking into account the rescattering gluons and so on. Some first attempts were made in ref. [30] for heavy quark production, but we should investigate this problem theoretically and the physical meaning and momentum structure of Sudakov-like form factor which appears in this case.

11. Exclusive processes in deep inelastic, especially the diffraction dissociation is still open problem

We have only one paper of Ryskin devoted this problem and, of course, this problem should be studied. For example, the case of target fragmentation was only touched in ref. [2] in spite of the fact that now we know that saturation should immediately manifest itself in this process.

12. As we discussed, that the most interesting and general feature of low x phenomena is so-called diffusion in $\ell n\, q_t$. This diffusion leads to large average $\langle \ell n^2\, q_t \rangle$ in our deep inelastic processes, namely, $\langle \ell n^2 q_t \rangle \sim \alpha_S\, \ell n\, 1/x_B$. It means that partons with low q_t also could be very essential in the whole evolution processes in our parton cascade. I think also, that this problem is very important in the σ_t problem. We would like to study this problem in more theoretical basis.

13. Deep inelastic scattering, especially at not very high virtuality of photon looks at most aspects as hadron-hadron interaction. So we should wait for increasing of proton radius versus x_B ($x_B \to 0$).

Untill now we have neglected this effect in deep inelastic processes. This phenomena could be even some origin of new phenomenology for simultaneous description of low q^2 and high q^2 deep inelastic data.

14. In saturation region I am not sure that parton language is very useful for us. So we need some picture and language to discuss all phenomena in the saturation region in the simplest way.

Frankly speaking, the situation in low x region as a whole reminds the old reggeon calculus. Once more we face the problem of taking into account a lot of diagram. Of course, only when you will recognize these facts, the first, natural wish should be run away from this field of our activities.

I hope, that I convince you, that in deep inelastic scattering we have one very important difference, namely, we can study screening corrections theoretically in the kinematical region where they are small. This study allows us to understand better what the system of partons in our parton cascade on microscopic level.

I hope, that we could attack the saturation region theoretically, even more we have microscopic hypothesis how our parton cascade inside the saturation region looks like. So, now we are seeking for appropriate technique to describe the modified equation and the parton system in the saturation region on microscopic, parton level, directly through interaction and collisions of parton inside the parton cascade, without reggeon-like technique.

I hope, that new generation of deep inelastic experiments will give us the necessary information to make the next theoretical step.

I hope, that you understand that we have the greatest advantage even at the moment. We understand the problems and can formulate the nearest aim to solve them.

The whole situation at low x, I am trying to present in fig. 32. Namely, in my opinion, the hadron looks as traditional russian toy "Matrjoshka". If we look in hadron with sufficient bad resolution, we see hadron as a whole and it looks nice. When the resolution of

our microscope becomes better we see several quarks inside the hadron, which are also nice. But microscope with even better resolution cannot open this toy once more. On some level, these quarks look rather as balloons with quark liquid. If we make small hole in this balloon, we see the jet of quark gas. And even now we know something about jet production. But if we make the hole, which size large enough and put there the tape, we can get the drop of quark liquid. The HERA I hope is this tape and our aim (I mean the aim of theoreticians) to prepare a good glass to catch this drop. Unfortunately, this glass is not prepared yet. But we are on the way, at least we have impression about general construction of this glass.

Conclusions

I must tell you that for me it was first and very interesting experience to deliver this more-less systematic course of lectures on low x deep inelastic scattering. Of course, these lectures are only introduction to the problem, even more, only theoretical introduction. I hope, that in nearest future. I'll write some lectures on the physics at low x and even more generally at large energy (LHC, SSC region).

I am very grateful to all participants of seminar at L.P.T.H.E. Orsay for encouraging discussion and permanent interest in the problem.

I would like to thank D. Schiff, who organized these lectures and stimulated them.

I am especially indebted to A. Capella and A. Krzywicki, for hot discussion of the subject and interesting questions than were very useful for me.

It is pleasure for me to thank Mlle M. Calvet for typing the manuscript. Without her assistance this paper could not appear on the whole.

References

1. L.V. Gribov, E.M. Levin and M.G. Ryskin, Phys. Rep. 100C (1983) 1.
2. E.M. Levin and M.G. Ryskin, Phys. Rep. 189C (1990) 268.
3. Yu. L. Dokshitzer, V.A. Khoze, A.H. Mueller and S.I. Troyan, Rev. Mod. Phys. 60 (1988) 373.
4. V.N. Gribov and L.N. Lipatov, Sov. J. Nucl. Phys. 15 (1972) 78, 1218.
   L.N. Lipatov, Sov. J. Nucl. Phys. 20 (1974) 181.
5. G. Altarelli and G. Parisi, Nucl. Phys. B126 (1977) 298.
6. Yu. L. Dokshitzer, D.I. Dyakonov and S.I. Troyan, Phys. Rep. 58C (1980) 270.
7. V.S. Fadin, E.A. Kuraev and L.N. Lipatov, Phys. Lett. B80 (1975) 30, JETP 71 (1976) 890, 72 (1977) 371.
8. I.I. Balitsky and L.N. Lipatov, Sov. J. Nucl. Phys. 28 (1978) 654.
9. I.S. Gradshteyn, I.M. Ryzkik, "Table of Integrals, Series and Products", Academic Press NY (1965) (formula 8.361).
10. G. Marchesini and B.R. Webber, Cavendish preprint-HEP-90/6 (1990).
11. E.M. Levin, G. Marchesini, M.G. Ryskin and B.R. Webber, Cavendish preprint-HEP-90/9, LPTHE Orsay 90/44.
12. M.G. Ryskin, DESY 90-050 and to appear in Proceedings of the Small x Workshop, DESY, May 1990 (to be published in Nucl. Phys.).
13. V.A. Abramowsky, V.N. Gribov and O.V. Kanchely, Sov. Nucl. Phys. 18 (1974) 308.
14. J. Morfin and Wu-Ki Tung preprint Fermilab-Pub. 90/74 (1990) Wu-Ki Tung Proceedings of the Small x Workshop, DESY, May 1990.
15. L.N. Lipatov, Proceedings of the Small x Workshop, DESY, May 1990.
16. E.M. Levin and M.G. Ryskin, Nucl. Phys. B304 (1988) 805, Sov. Nucl. Phys. 47 (1988) 1397.
17. M.G. Ryskin, Sov. Nucl. Phys. 51 (1990) 320.

18. L.D. Landau and I.Ya. Pomeranchuk, Dokl. Akad. Mamk 95 (1953) 535, 735 (in Russian).
A.B. Migdal, Sov. Phys. JETP 32, 527 (1957).
19. E.M. Levin et al., preprint LVPI-1664, Leningrad (1990) LPTHE Orsay 91/01, January 1991.
20. V.N. Gribov, Sov. Phys. JETP 57 (1969) 1306.
T.H. Bauer, R.D. Spitel, O.K. Yennie and P.M. Pipkin, Rev. Mod. Phys. 50 (1978) 261.
N.N. Nikolaev, Sov. Phys. UFN 134 (1981) 369.
E.M. Levin, Proceedings XXI LNPI Winter School (Leningrad, 1986) p. 31.
L.L. Frankfurt and M.I. Strikman, Phys. Rep. 160 (1988) 235.
21. E.M. Levin and M.G. Ryskin, Sov. Journal of Nucl. Phys. 41 (1985) 300.
22. S. Catani et al., Phys. Lett. B242 (1990) 97.
23. G. Ingelman and P.E. Shlein, Phys. Lett. 152B, 256 (1985).
K.H. Streng, CERN-TH-4949, January 1988, Proceedings of the HERA Workshop, Hamburg, October 12-14 (1987) p. 365.
24. A.H. Mueller, preprint CU-TP-475 and in Proceedings of the Small x Workshop, DESY, May 1990.
25. L.V. Gribov, Yu.L. Dokshitzer, V.A. Khoze and S.I. Troyan, Sov. Phys. JETP Letter 94 (1988) 12.
26. E.M. Levin and M.G. Ryskin, Sov. J. Nucl. Phys. 21 (1975) 206.
A. Capella and A. Krzywicki, Phys. Rev. D18 (1978) 4120.
27. A.H. Mueller, Phys. Rev. D2 (1970) 2963.
O.V. Kancheli, JETP Lett. 11 (1970) 267.
28. A. Capella, U. Sukhatme, C.-I. Tan and J. Tran Thanh Van, Phys. Lett. B81 (1979) 68.
A.B. Kaidalov and K.A. Ter-Martirosyan, Phys. Lett. B117 (1982) 247 ; Sov. J. Nucl. Phys. 39 (1989) 1545, 40 (1984) 211 and review : A. Capella, U. Sukhatme, C.-I. Tan and J. Tran Thanh Van, Dual Parton Model LPTHE Orsay (1987).
29. E.M. Levin and M.G. Ryskin, Sov. J. Nucl. Phys. 45 (1987) 150.

Figure Captions

Fig. 1 : Scattering of two composite particles with the different sizes R_A and R_B in Born Approximation of QED.

Fig. 2a : The simplest diagram for e^+e^- annihilation.

Fig. 2b : The emission of gluons in the quark decay.

Fig. 3 : The space-time picture for deep inelastic scattering (a) and e^+e^- annihilation (b).

Fig. 3c : Evolution equation in DLA.

Fig. 4 : The parton cascades for deep inelastic scattering (a) and e^+e^- annihilation (b).

Fig. 4c and 4d : Kinematical region for DLA for α_S = const (c) and running α_S (d).

Fig. 5a : The parton decay in LL(q^2)A (space-time picture).

Fig. 5b : The graphical form of evolution equation in LL(q^2)A (GLAP equation).

Fig. 6a : Space-time picture in LL(x)A for parton decay.

Fig. 6b : Born Approximation for quark-quark scattering amplitude in QCD.

Fig. 6c : α_S^3 corrections for quark-quark scattering amplitude in QCD (production of secondary gluon).

Fig. 6d : Definition of gauge invariant amplitudes M_μ and M_ν in α_S^2 order of perturbative QCD.

Fig. 6e : Resulting amplitude for secondary gluon production in α_S^3 order of perturbative QCD.

Fig. 6f : α_S^2 contribution to quark-quark scattering amplitude in perturbative QCD.

Fig. 6g : Graphical relations between colour factor in colour SU(3) group.

Fig. 7 : LLA "ladder" diagram with reggeized gluons and new vertices.

Fig. 8 : The structure of the parton cascade.

Fig. 9 : The gluon structure function for GLAP equation (one loop) and KLF equations (all loops) in region of small x. The picture is taken from the paper of Marchesini and Webber[10].

Fig. 10 : The kernels $\chi(\gamma)$ and $X(\gamma) = \int_\gamma^{1/2} \chi(\gamma')\, d\gamma'$. LL(x)A (all loops) and LL(q^2)A (one loop).

Fig. 11a : The diagram with one quark loop in gluon "ladder".

Fig. 11b : The factorization property of QCD diagrams.

Fig. 11c : The graphical form of LL(q^2)A + LL(x)A equation for deep inelastic structure function at $x \to 0$.

Fig. 11d : Kinematical region for LL(x)A + LL(q^2)A.

Fig. 12a : The structure of the parton cascade for a fast hadron.

Fig. 12b : Emission and annihilation processes in the parton cascade.

Fig. 12c : The difference between the number of diffusion steps and the multiplicity of "wee" partons, in LL(x)A.

Fig. 13a : Enhanced diagram for Deep Inelastic Scattering (DIS) amplitude.

Fig. 13b : Non enhanced diagram for DIS amplitude.

Fig. 13c : The simplest "fan" diagram for DIS amplitude.

Fig. 14a : The diagrams for triple ladder vertex in Born Approximation of QCD.

Fig. 14b : LL(x)A generalization for triple "ladder" vertex.

Fig. 15 : Illustration of AGK cutting rules.

Fig. 16a : "Fan" diagrams for DIS amplitude.

Fig. 16b : The equation taking into account multiladder "fan" diagrams.

Fig. 16c : Some iterations of this equation.

Fig. 17 :

Fig. 18a : Multiladder vertices.

Fig. 18b : The trajectories of linear (dashed line) and nonlinear evolution equations.

Fig. 18 c : What and where we know about DIS structure function ?

Fig. 19b : Structure of interactions with nucleus.

Fig. 20a :

Fig. 20b : The interaction of partons inside the saturation region.

Fig. 21a : The resulting structure of the parton cascade inside a nucleus.

Fig. 22 : The space-time picture for DIS with nucleus
a) for $\tau_{\gamma^*} < R_{NN}$ $(x > x_{NN})$
b) for $2\,R_A > \tau_{\gamma^*} > R_{NN}$ $(x > x > x_A)$
c) for $\tau_{\gamma^*} > 2R_A$ $(x < x_A)$.

Fig. 23 : The semi-enhanced multiladder diagram inside a nucleus.

Fig. 24a : The boundary (critical) line for the nucleon structure function in vacuum (1) and inside a nucleus (2). All cross sections are proportional to A below curve (3).

Fig. 24b : The unitarity constraint for φ_N in vacuum and in nucleus.

Fig. 24c : Process $h+h \to h(p_t)+x$.

Fig. 25a : The comparison of our phenomenological approach with the experimental data.

Fig. 25b : The structure of hadron ("hot" spots picture).

Fig. 26a : The HERA map - the kinematical regions for Quark Gas (QG) and Quark Liquid (QL).

Fig. 26b : The diagrams for F_2^{sea} near the saturation region.

Fig. 26c : The result of calculation of F_2^{sea}, using the saturation hypothesis.

Fig. 26d : The comparison of different approaches for F_2^{sea} at $Q^2 = 50\ GeV^2$.

Fig. 27a : $\gamma^*+p \to C\bar{C}\ (b\bar{b}) + x$ processes.

Fig. 27b : Diffraction dissociation of virtual photon. (1) and typical DD kinematics for HERA collider. (Pictures are taken from Ryskin's talk at Saclay (Dec. 1990)).

Fig. 28a :

Fig. 28b : Energy flow distribution for typical inelastic event in DIS.

Fig. 29 : Mueller-Kancheli diagrams for correlation function in reggeon approach.

Fig. 30 : Mueller-Kancheli diagrams for correlation function in QCD.

Fig. 31 : Diffraction dissociation of the target hadron in deep inelastic scattering.

Fig. 32 :

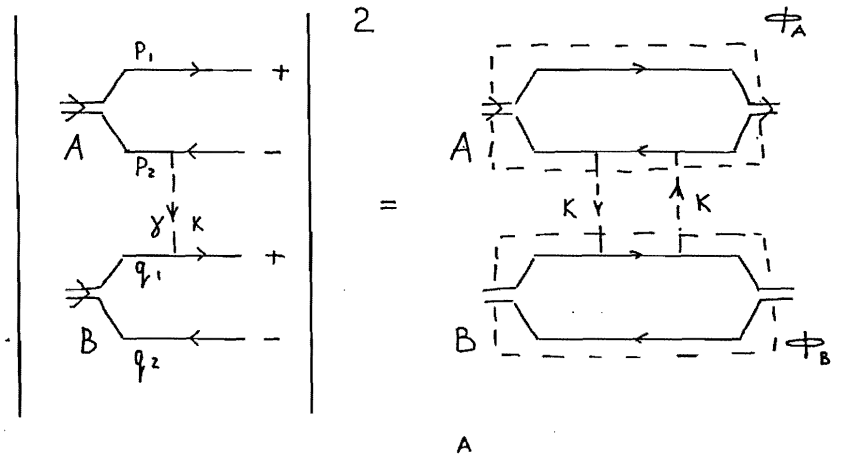

A

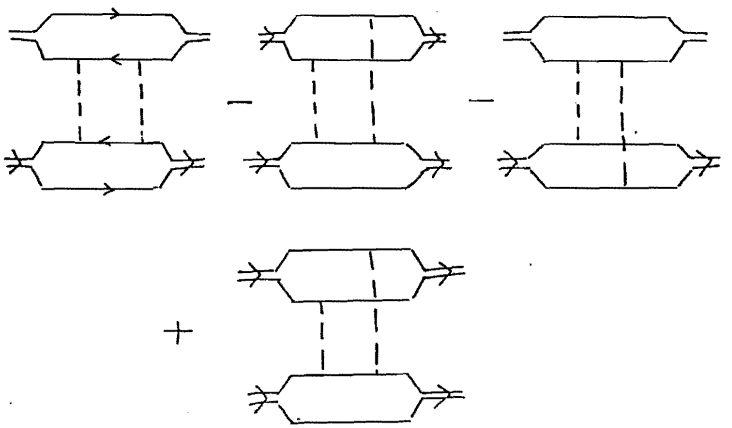

B

Figure 1

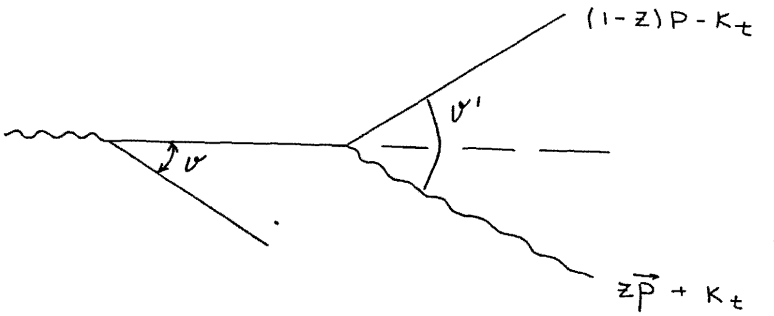

Figure 2a

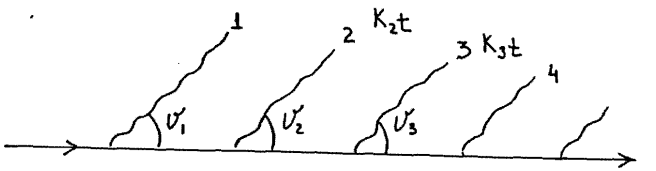

Figure 2b

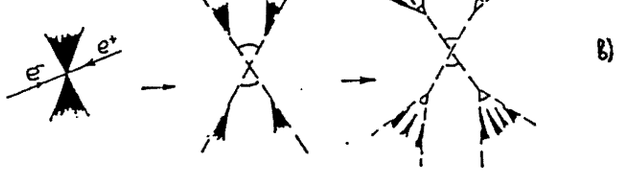

Figure 3

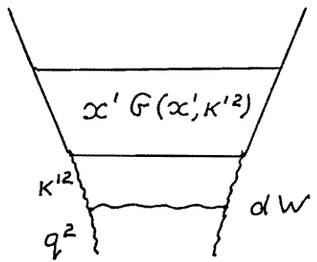

Figure 3c

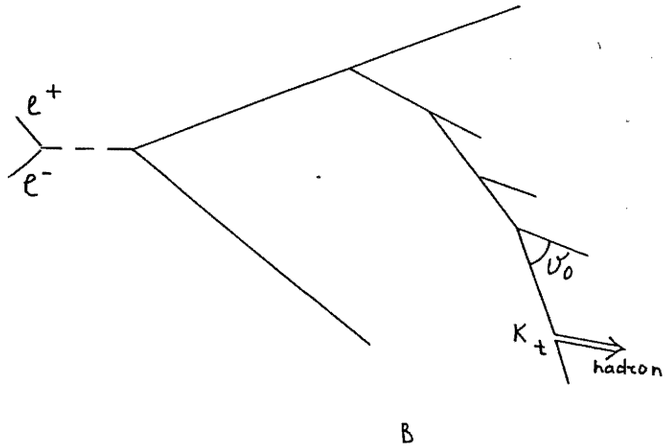

Figure 4

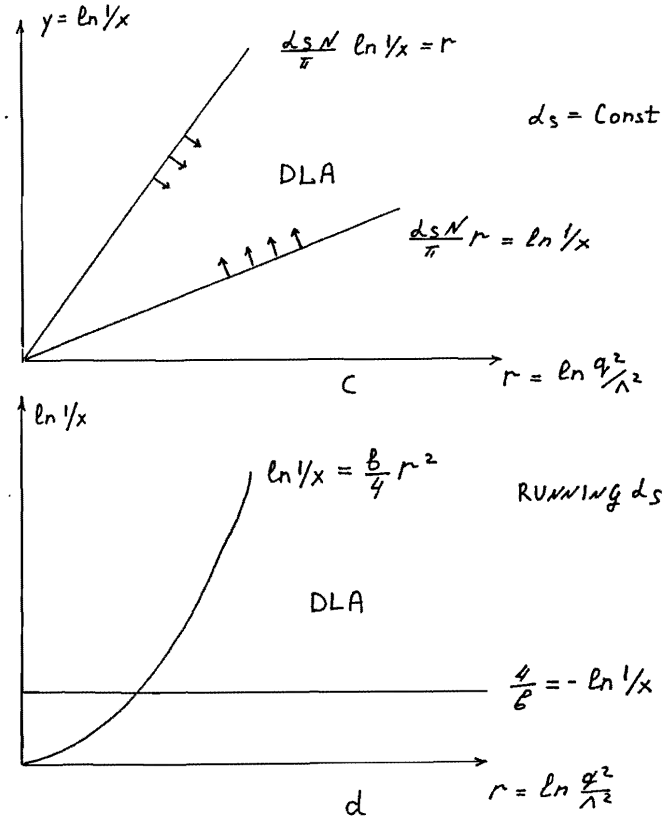

Figure 4

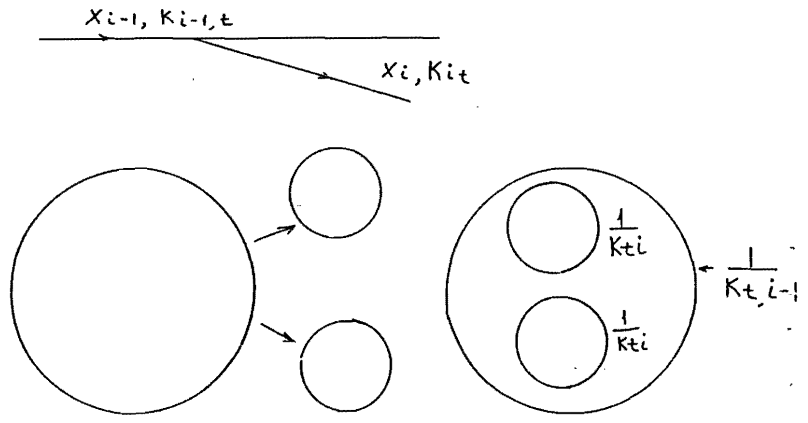

Figure 5a

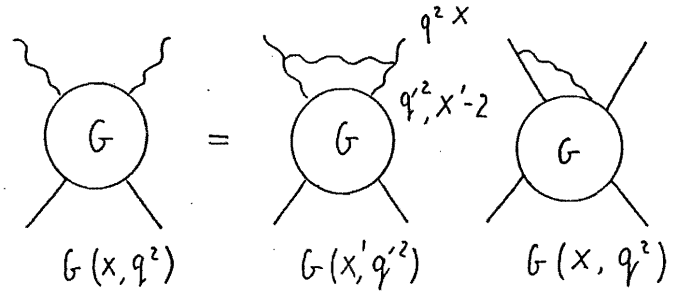

Figure 5b

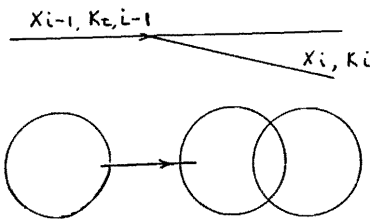

Figure 6a

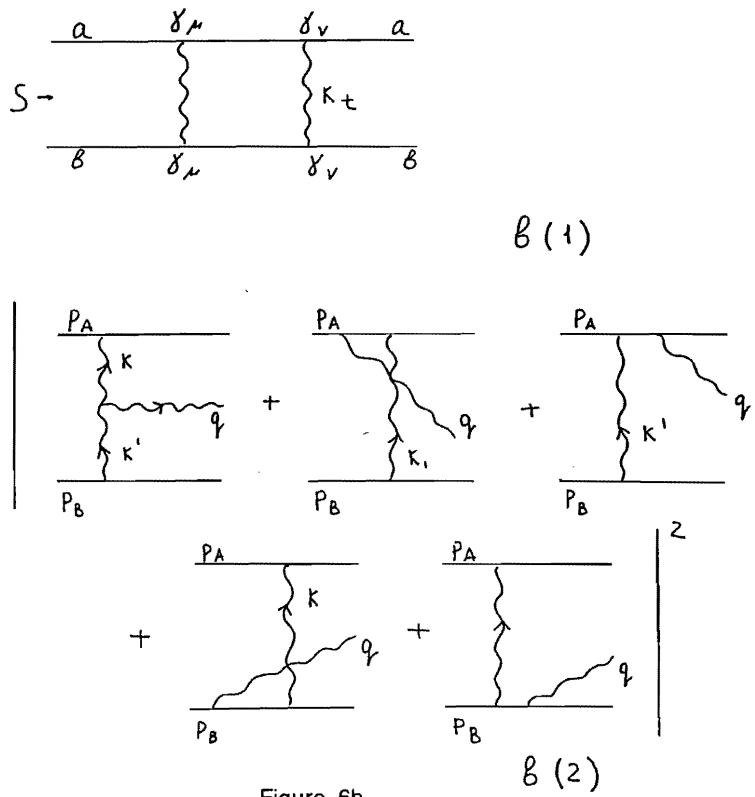

Figure 6b

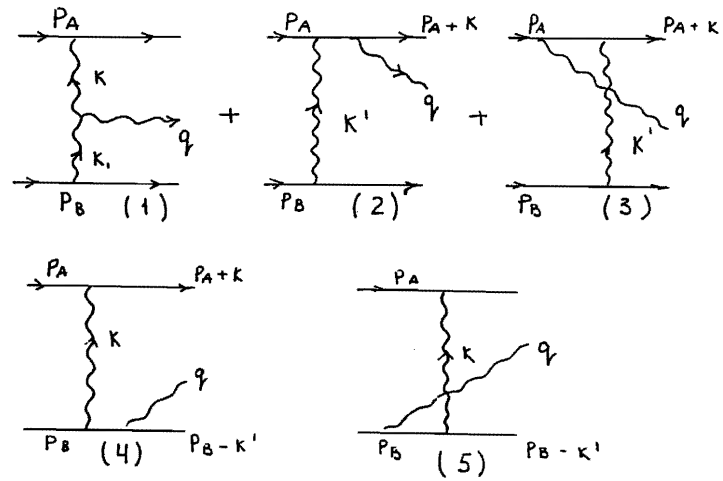

Figure 6c

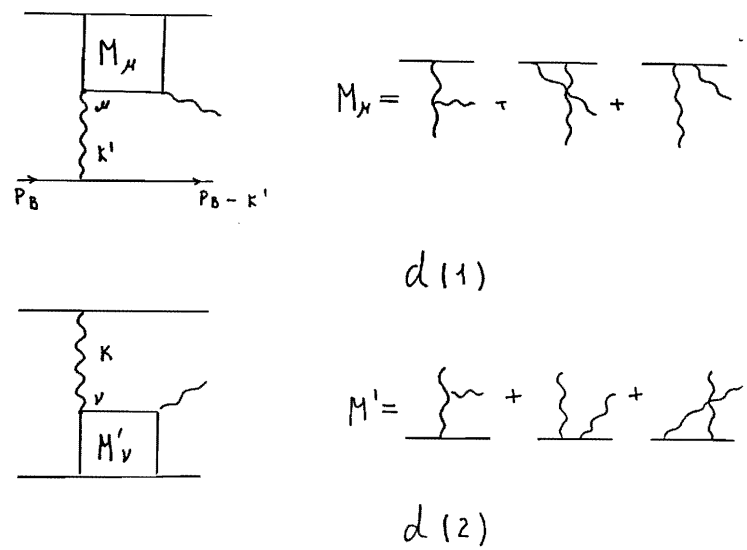

Figure 6d

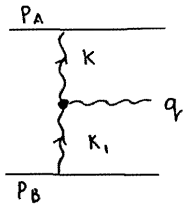

Figure 6e

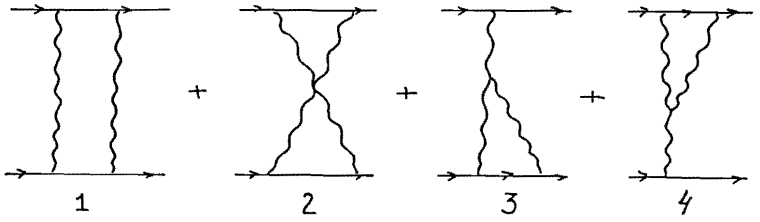

Figure 6f

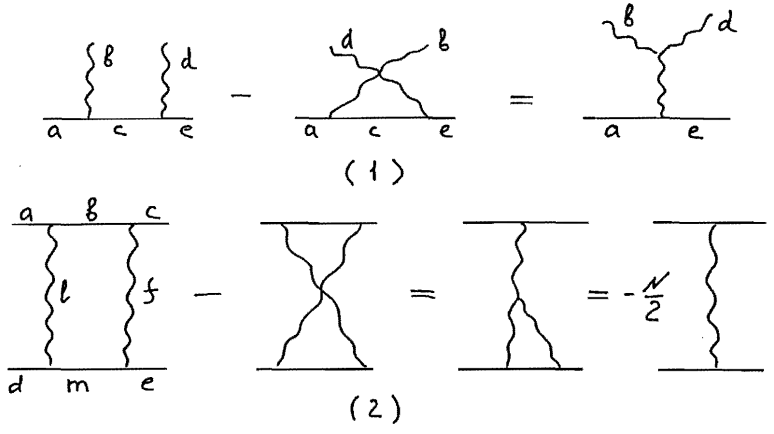

Figure 6g

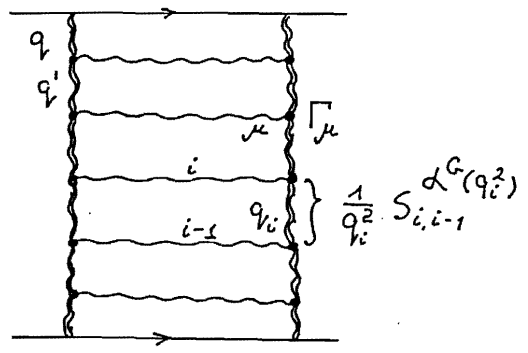

Figure 7

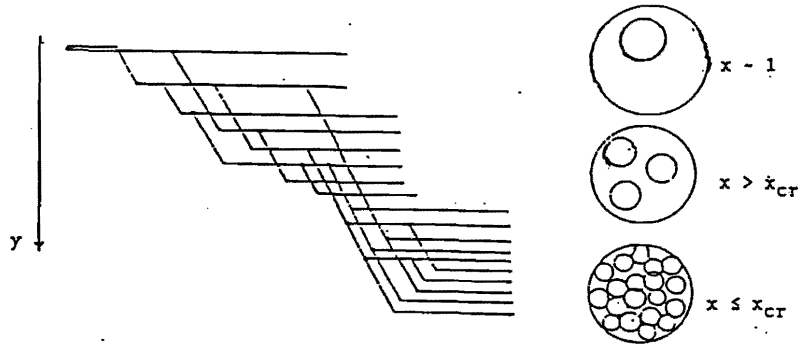

Figure 8

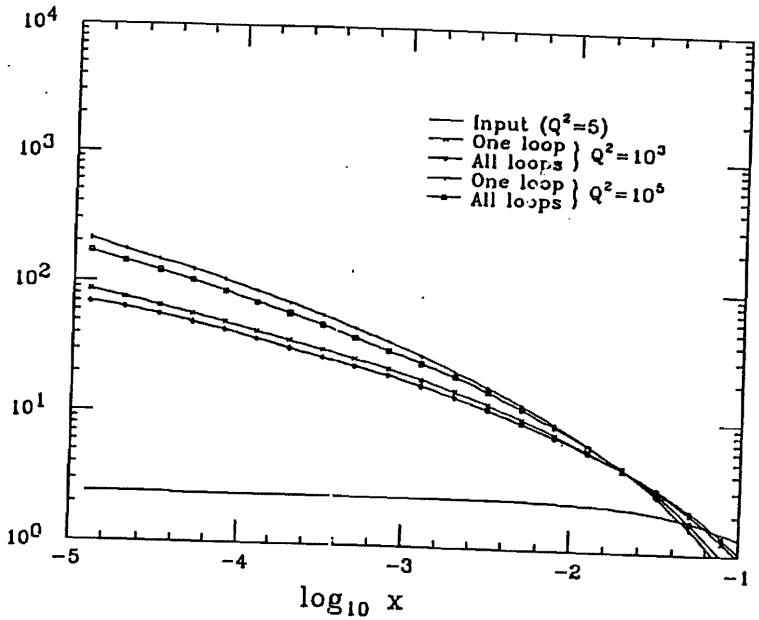

Figure 9

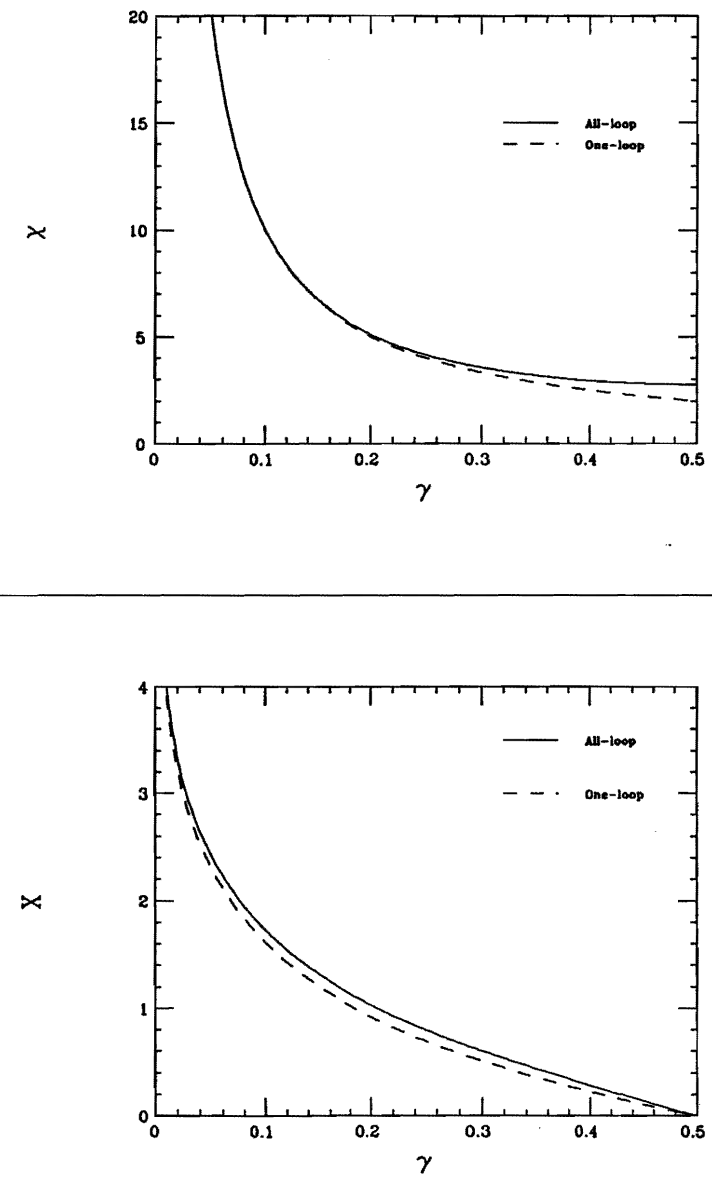

Figure 10

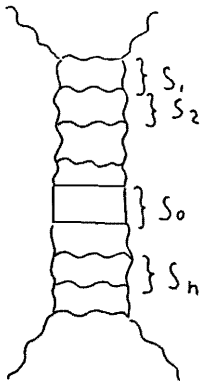

Figure 11a

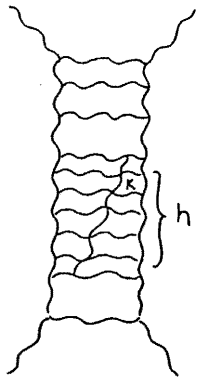

Figure 11b

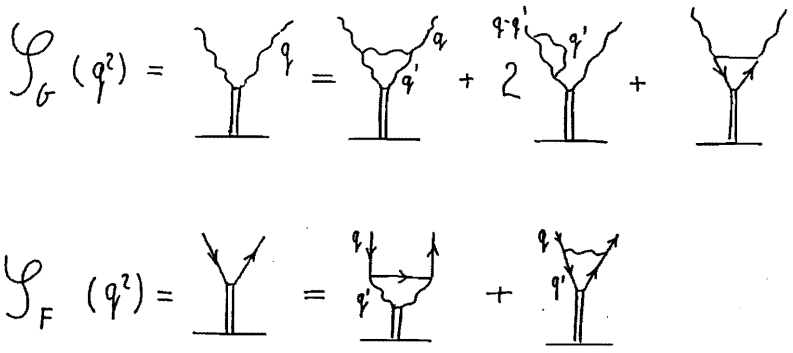

Figure 11c

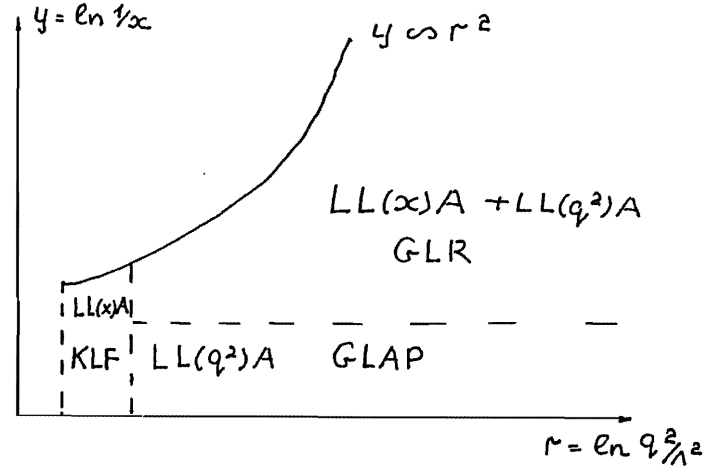

Figure 11d

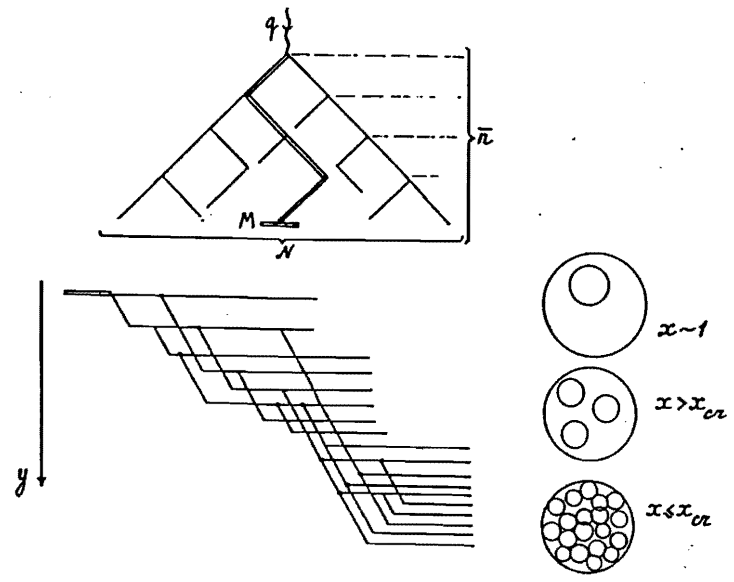

Figure 12a

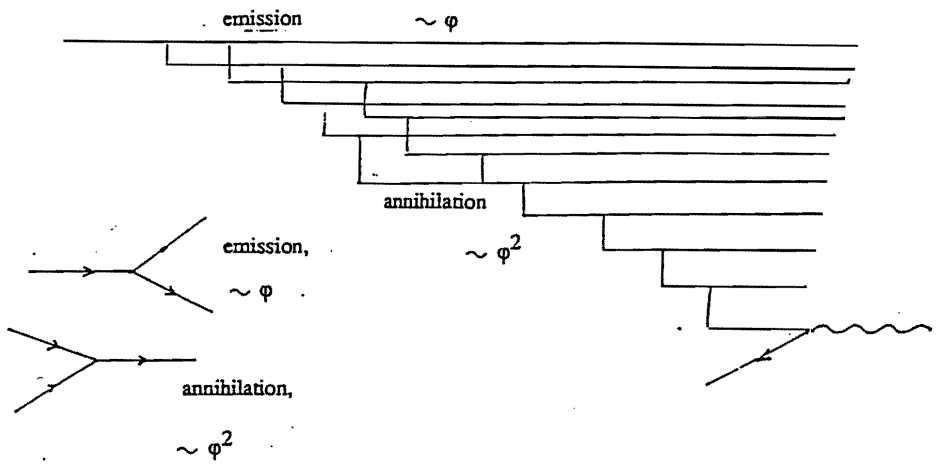

Figure 12b

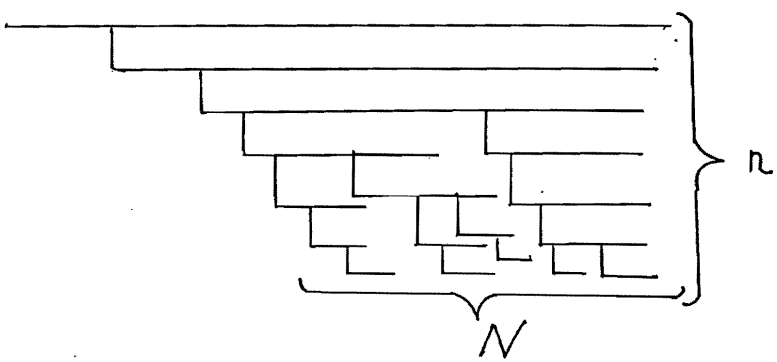

Figure 12c

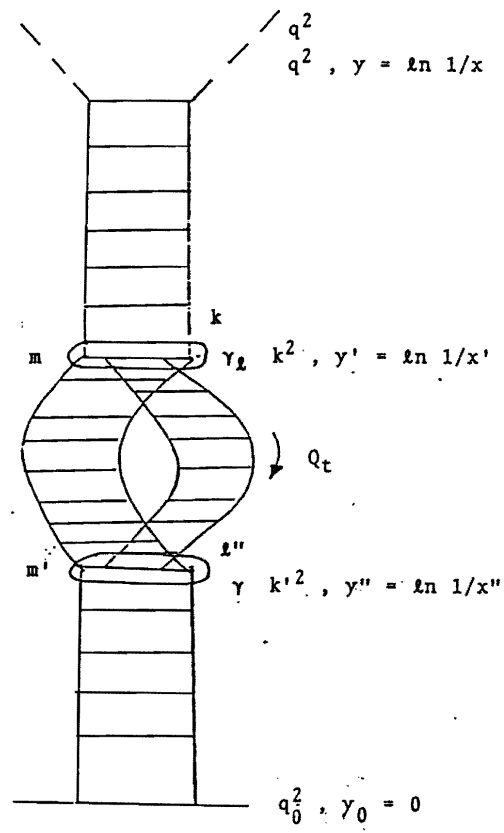

Figure 13a

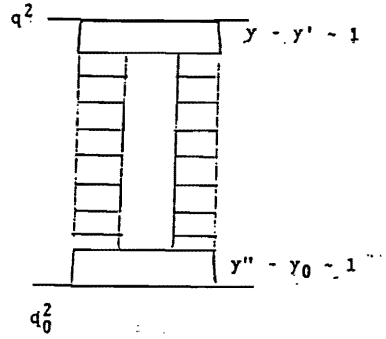

Figure 13b

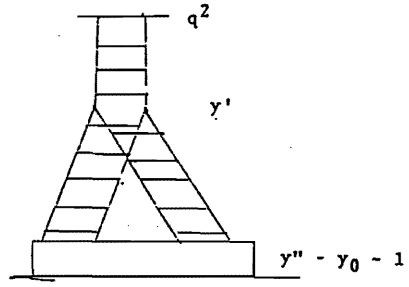

Figure 13c

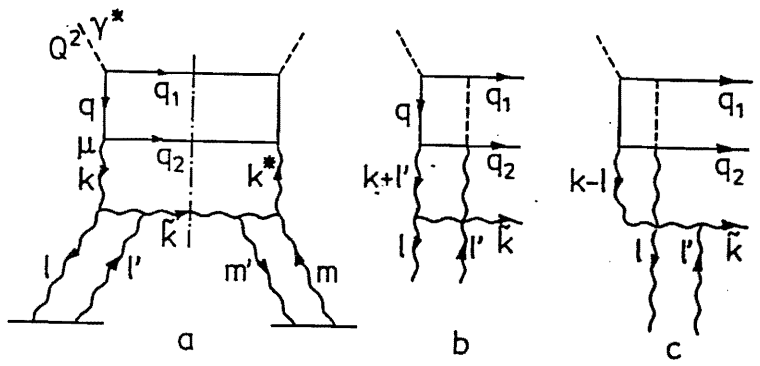

Figure 14a

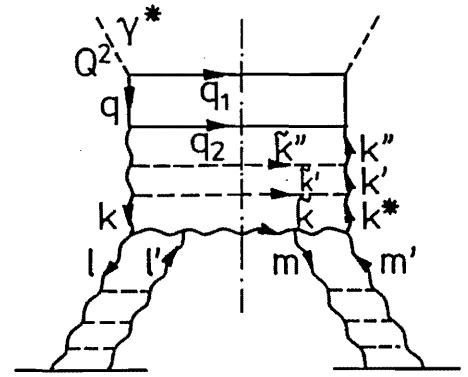

Figure 14b

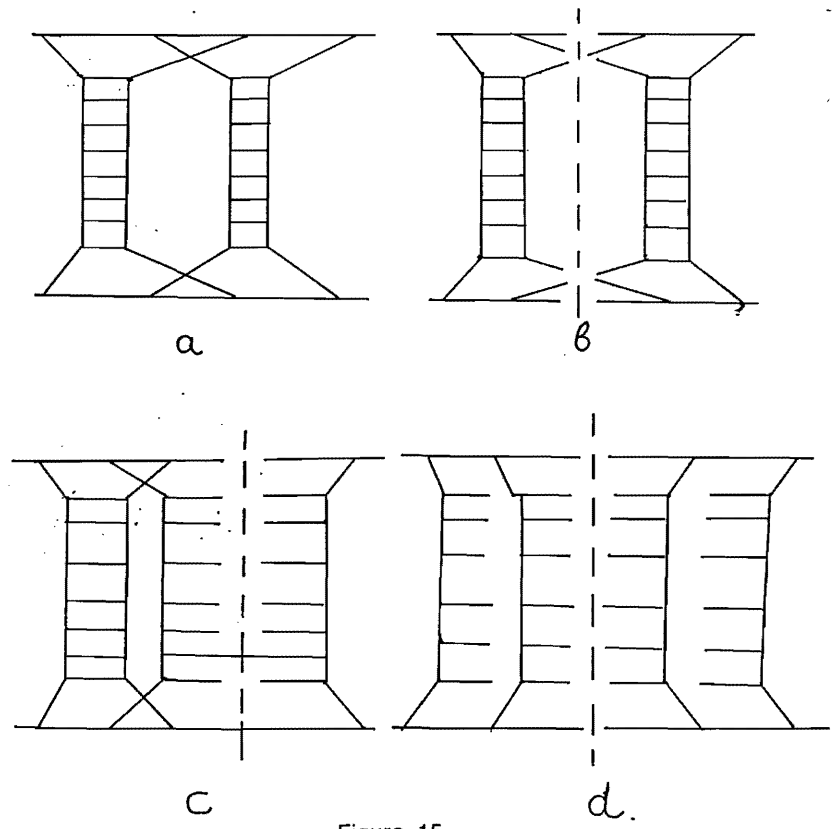

Figure 15

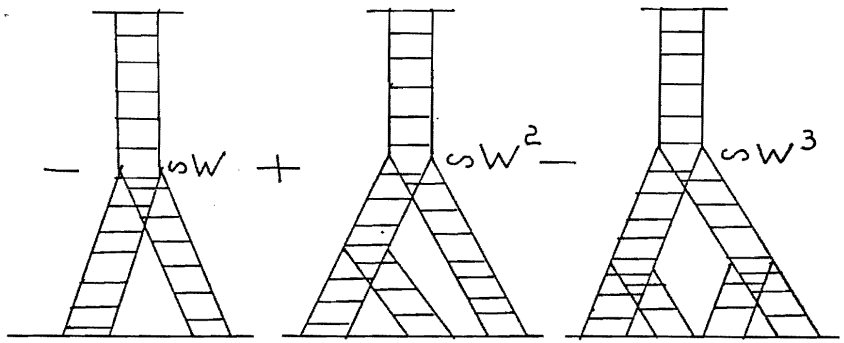

Figure 16a

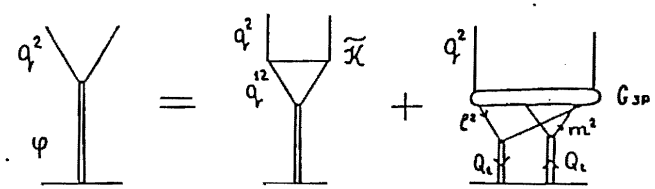

Figure 16b

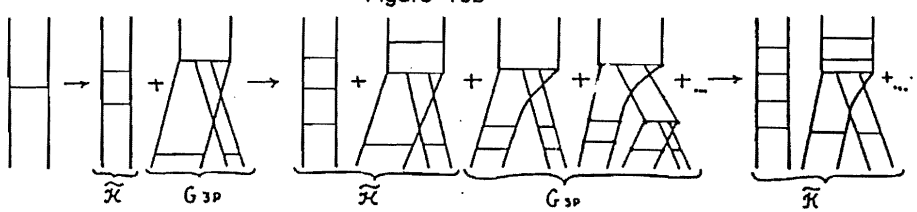

Figure 16c

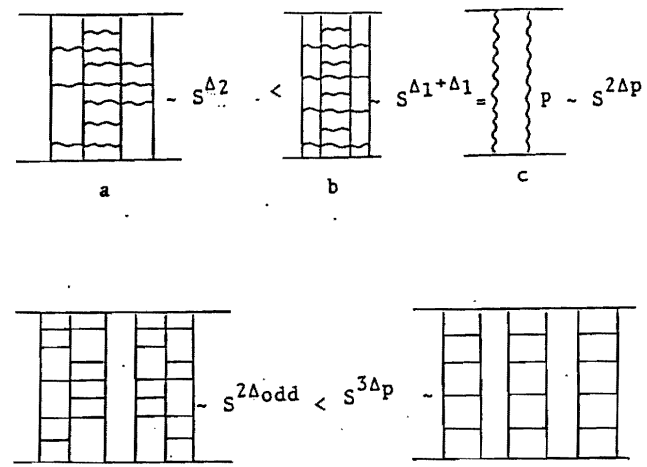

Figure 17

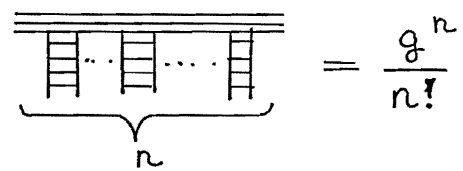

Figure 18a

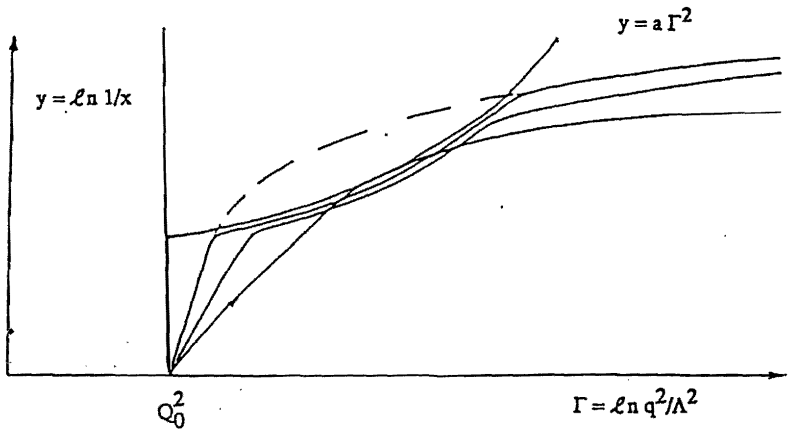

Figure 18b

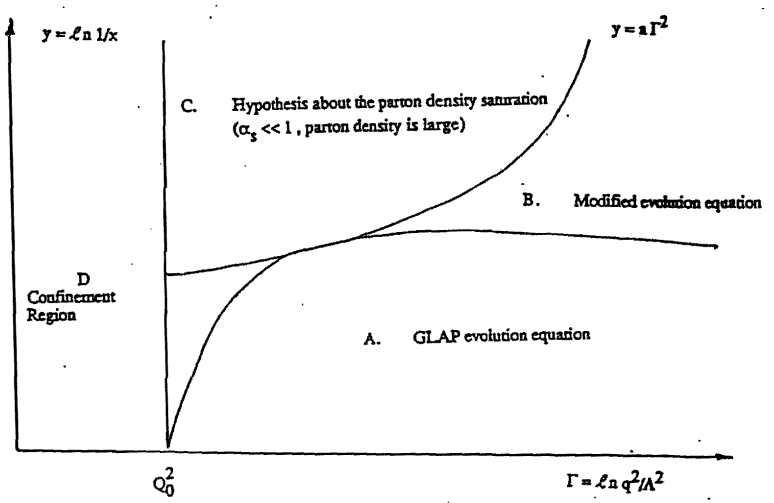

Figure 18c

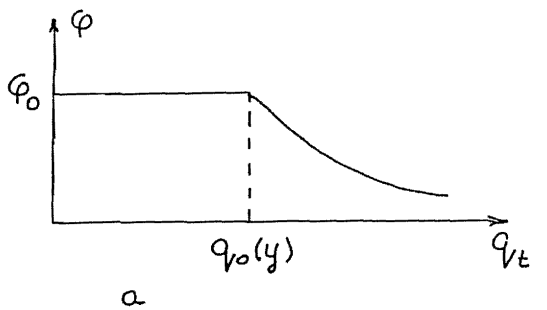

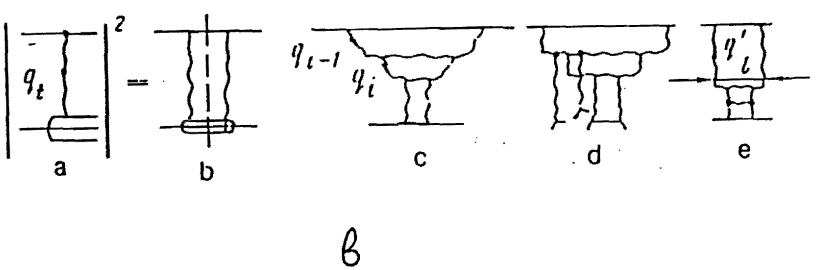

Figure 19

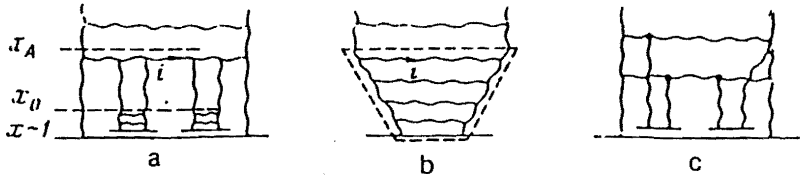

Figure 20a

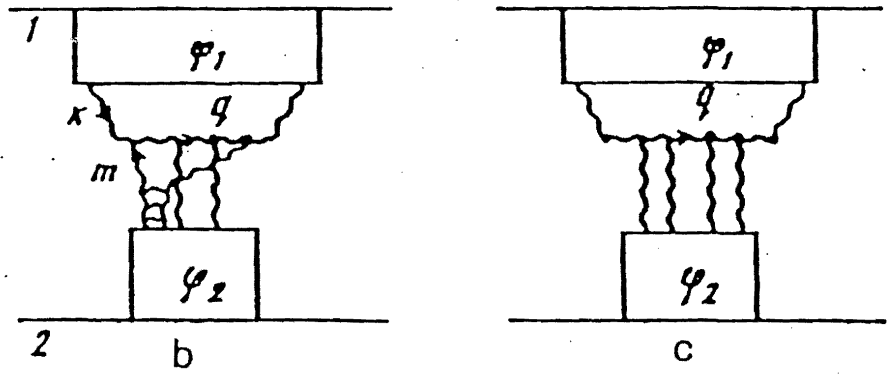

Figure 20b

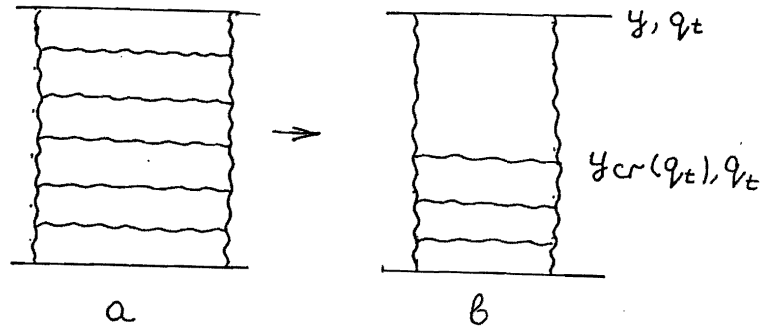

Figure 21

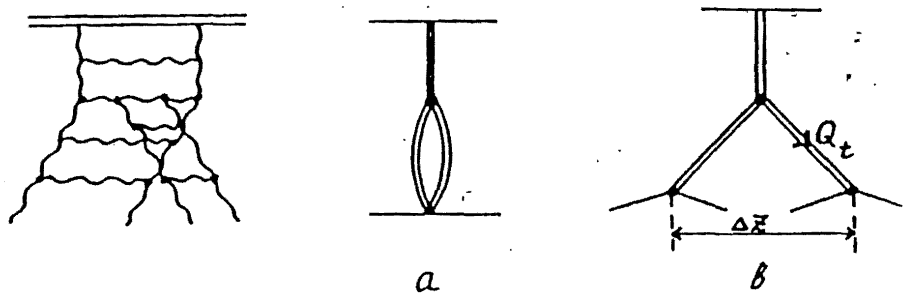

Figure 23

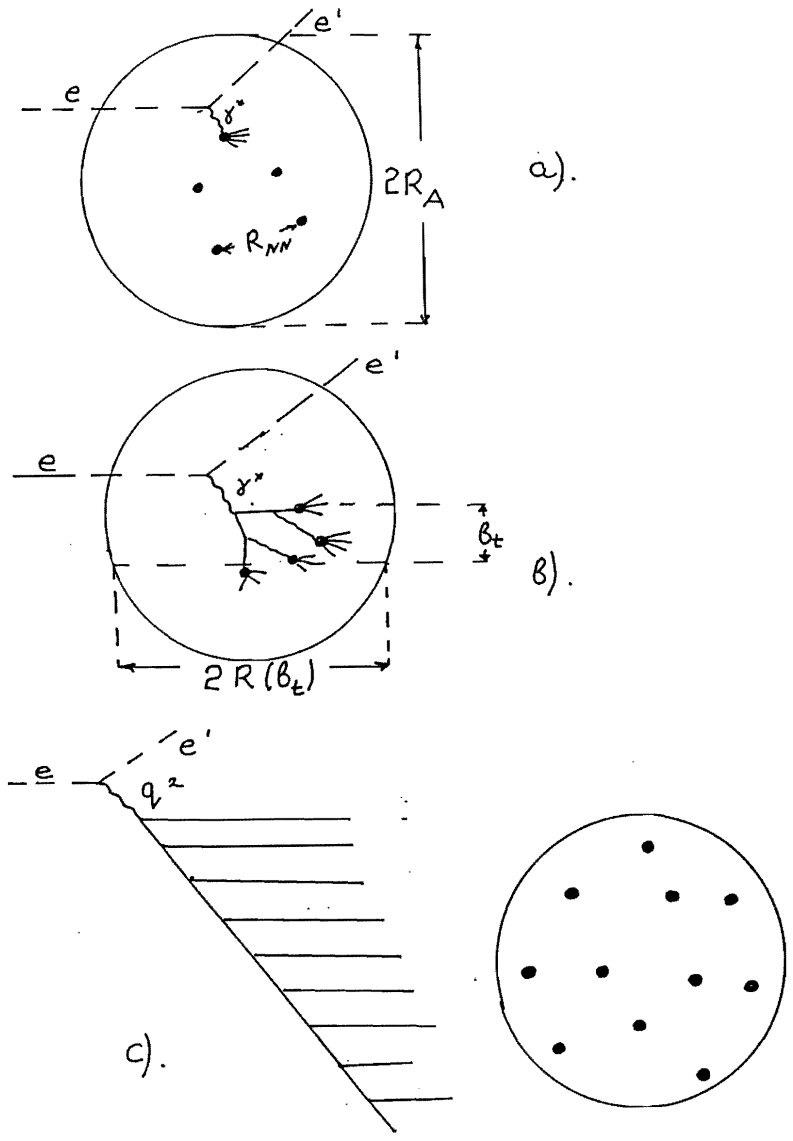

Figure 22

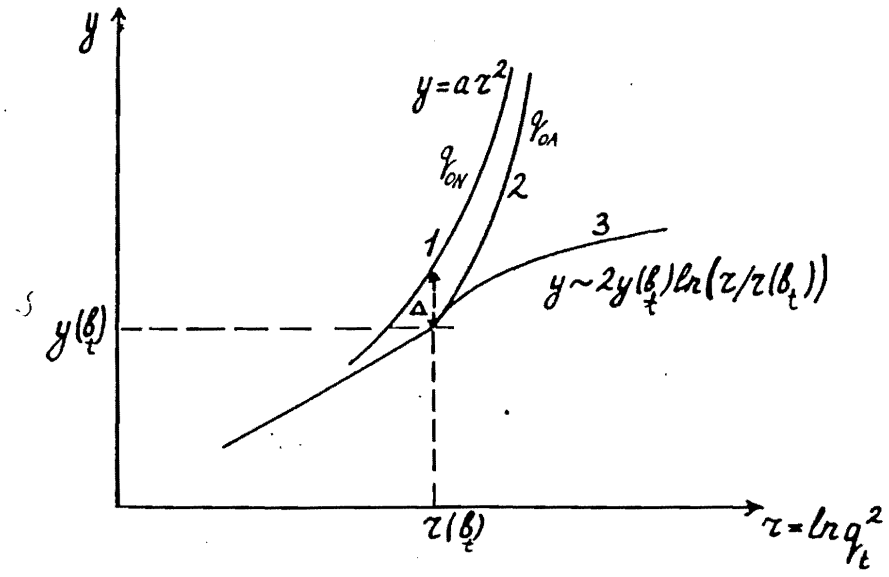

Figure 24a

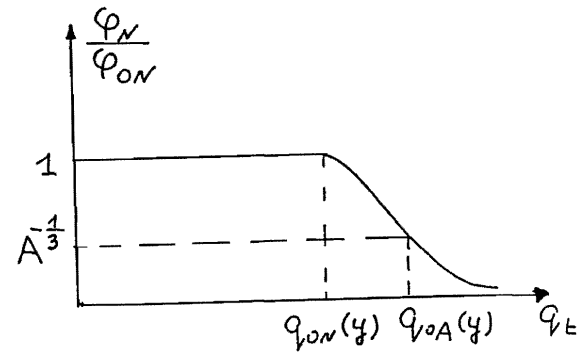

Figure 24b

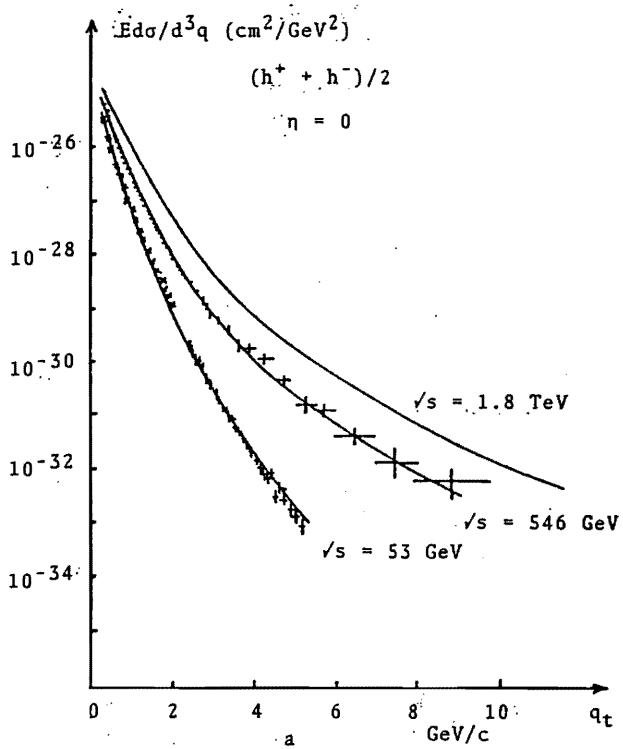

a

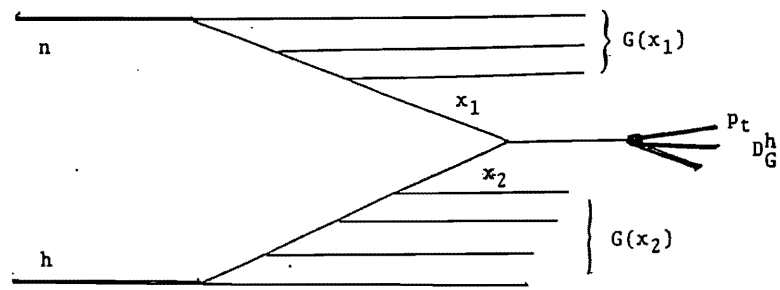

Figure 24c

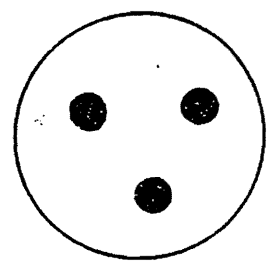

Figure 25b

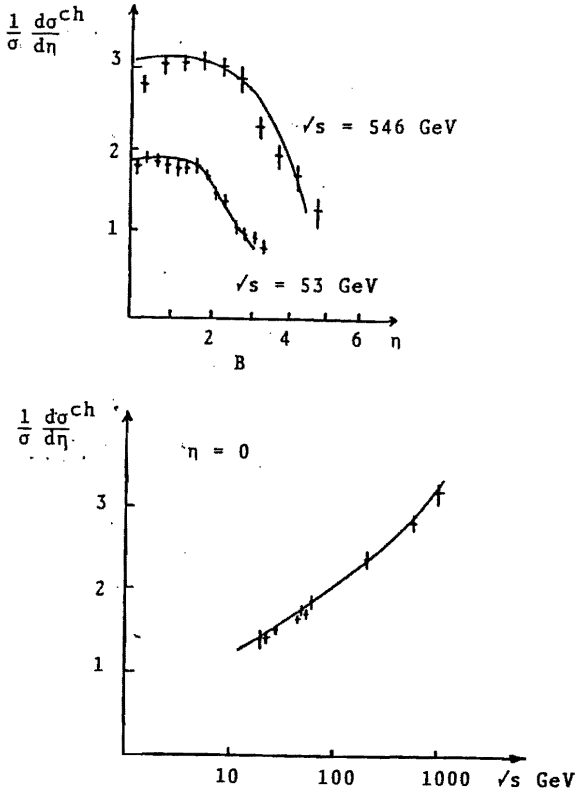

Figure 25a

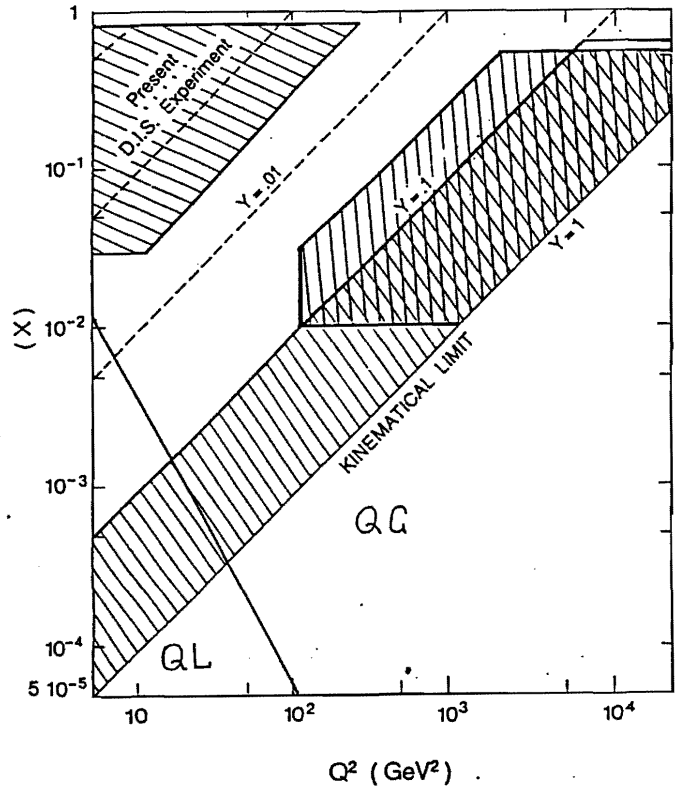

Figure 26a

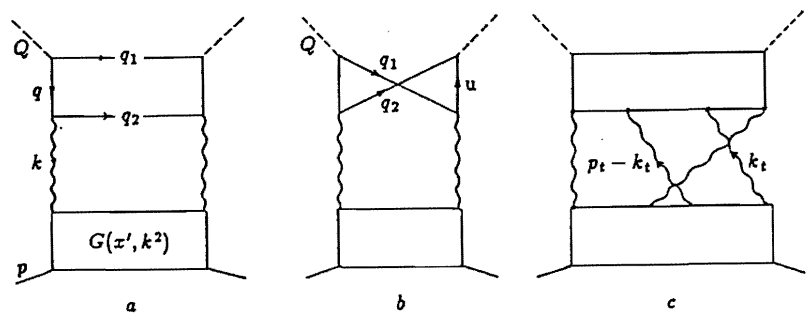

Figure 26b

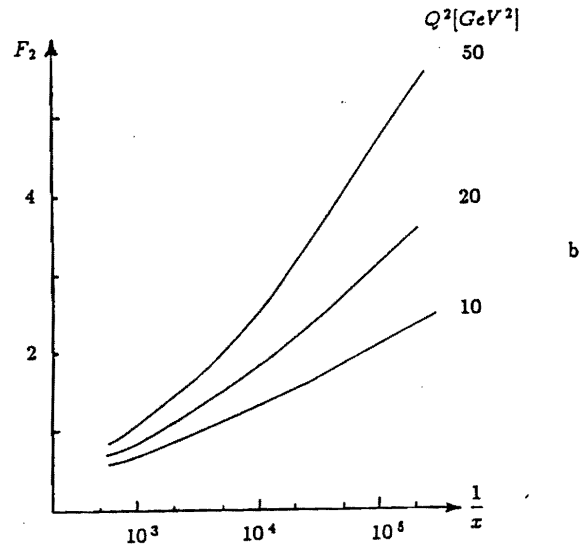

Figure 26c

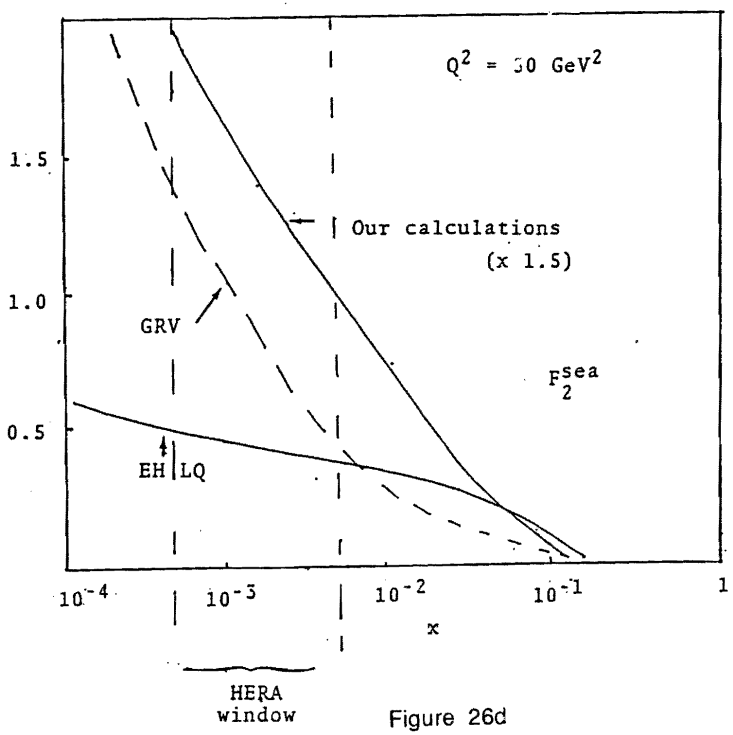

Figure 26d

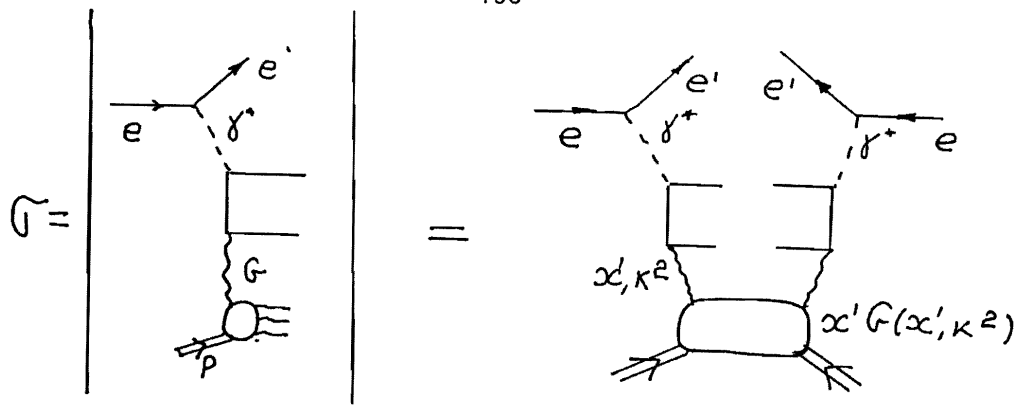

Figure 27a

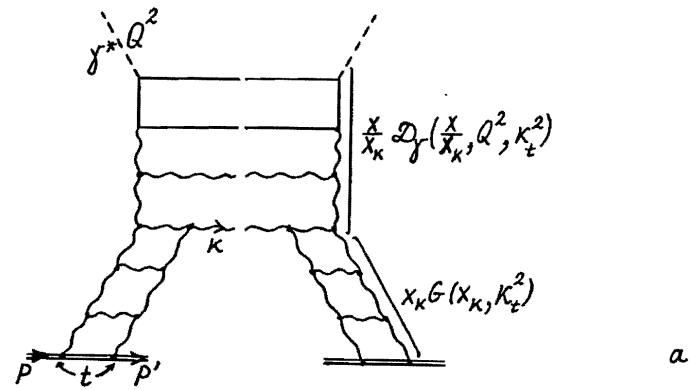

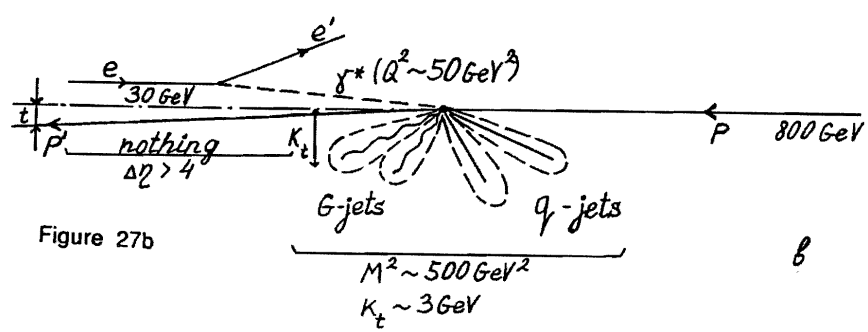

Figure 27b

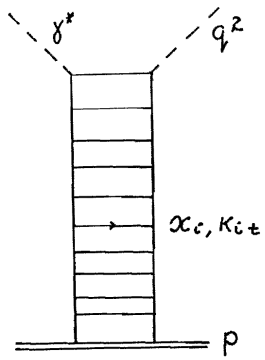

Figure 28a

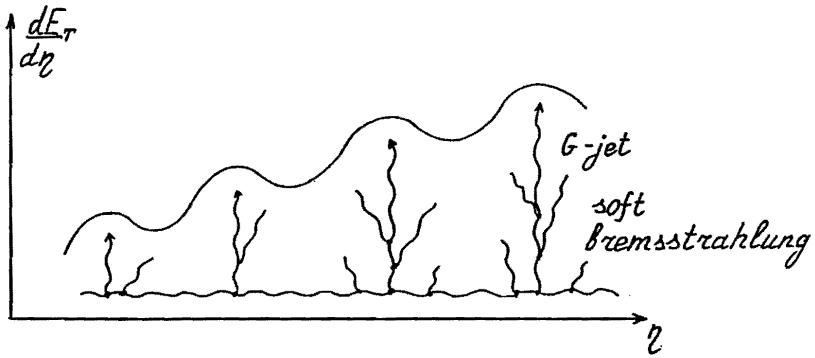

Figure 28b

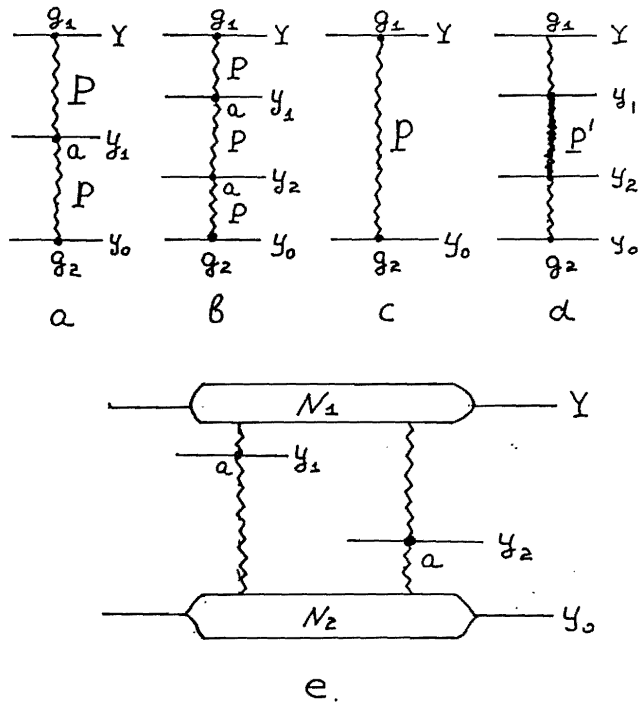

Figure 29

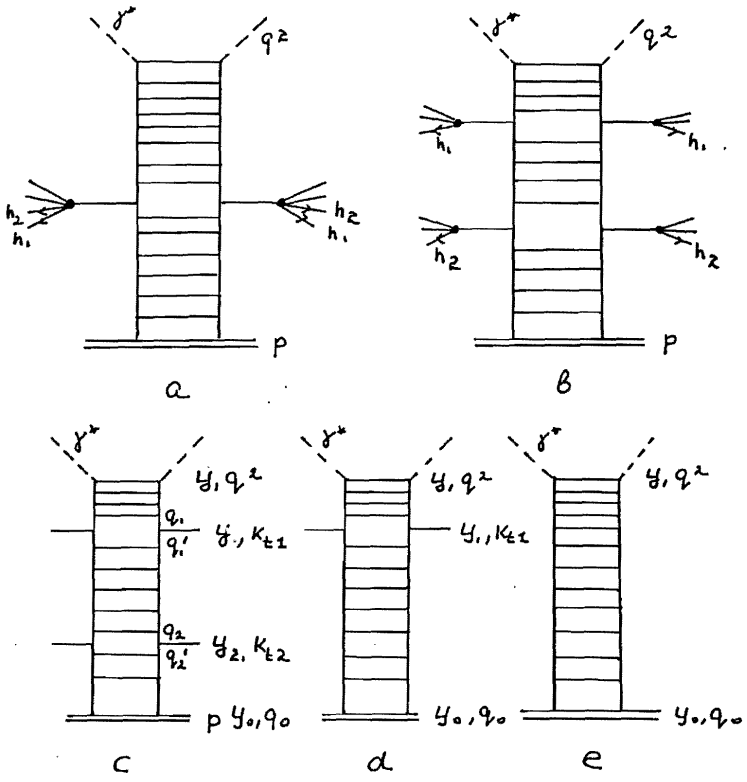

Figure 30

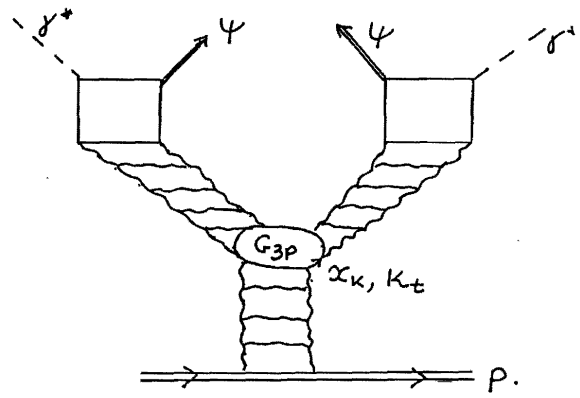

Figure 31